Prepared in cooperation with the Minnesota Pollution Control Agency and the Minnesota Department of Natural Resources

Application of Dimensionless Sediment Rating Curves to Predict Suspended-Sediment Concentrations, Bedload, and Annual Sediment Loads for Rivers in Minnesota

Scientific Investigations Report 2016–5146

U.S. Department of the Interior
U.S. Geological Survey

Cover. Sucker River near Palmers, Minnesota, during spring runoff just prior to collection of an equal-width-increment suspended-sediment concentration water sample. This site was recently fitted with a bank-operated cableway, because the road, which had provided the sampling platform for previous samples to be collected, had been destroyed during record flooding in June 2012. Photograph by Jerry Storey, U.S. Geological Survey, taken on May 3, 2013.

Application of Dimensionless Sediment Rating Curves to Predict Suspended-Sediment Concentrations, Bedload, and Annual Sediment Loads for Rivers in Minnesota

By Christopher A. Ellison, Joel T. Groten, David L. Lorenz, and Karl S. Koller

Prepared in cooperation with the Minnesota Pollution Control Agency and the Minnesota Department of Natural Resources

Scientific Investigations Report 2016–5146

U.S. Department of the Interior
U.S. Geological Survey

U.S. Department of the Interior
SALLY JEWELL, Secretary

U.S. Geological Survey
Suzette M. Kimball, Director

U.S. Geological Survey, Reston, Virginia: 2016

For more information on the USGS—the Federal source for science about the Earth, its natural and living resources, natural hazards, and the environment—visit http://www.usgs.gov or call 1–888–ASK–USGS.

For an overview of USGS information products, including maps, imagery, and publications, visit http://store.usgs.gov.

Any use of trade, firm, or product names is for descriptive purposes only and does not imply endorsement by the U.S. Government.

Although this information product, for the most part, is in the public domain, it also may contain copyrighted materials as noted in the text. Permission to reproduce copyrighted items must be secured from the copyright owner.

Suggested citation:
Ellison, C.A., Groten, J.T., Lorenz, D.L., and Koller, K.S., 2016, Application of dimensionless sediment rating curves to predict suspended-sediment concentrations, bedload, and annual sediment loads for rivers in Minnesota: U.S. Geological Survey Scientific Investigations Report 2016–5146, 68 p., http://dx.doi.org/10.3133/sir20165146.

ISSN 2328-0328 (online)

Acknowledgments

This report presents a compilation of information supplied by many agencies and individuals. The authors would like to thank the Minnesota Pollution Control Agency and the Minnesota Department of Natural Resources for their assistance with this study. Dave Rosgen from Wildland Hydrology, Ian Chisholm and Nick Proulx from the Minnesota Department of Natural Resources, and Nolan Baratono from the Minnesota Pollution Control Agency provided technical assistance and offered valuable insight.

Brett Savage, Kristen Kieta, Mike Roberts, Jerry Storey, Will Lund, and Molly McCool of the U.S. Geological Survey are acknowledged for assistance with office and field aspects of the study. Tim Straub and Brenda Densmore of the U.S. Geological Survey are acknowledged for their technical reviews of the report.

Contents

Acknowledgments iii
Abstract 1
Introduction 2
Background Information on Dimensionless Sediment Rating Curves 3
Purpose and Scope 6
Description of Study Area 6
Methods of Data Collection and Analysis 11
Suspended-Sediment Concentrations 11
Bedload 11
Streamflow Data 15
Bankfull Streamflow Determination 16
Pfankuch Stability Rating 16
Determining Suspended-Sediment Concentration and Bedload at Bankfull Streamflow 16
Data Analysis 19
Streamflow, Suspended-Sediment Concentrations, Bedload, and Particle-Size Fractions 22
Suspended-Sediment Concentrations 31
Bedload 31
Particle-Size Fractions 32
Relations among Suspended-Sediment Concentration and Bedload with Streamflow 32
Dimensionless Sediment Rating Curves 39
Regression Trendlines 39
Suspended-Sediment Concentrations 50
Bedload 50
Nash-Sutcliffe Model Efficiencies 51
Suspended-Sediment Concentrations 51
Bedload 51
Model Biases and Limitations 51
Annual Sediment Loads 54
Suspended-Sediment Loads 54
Bedload 59
Implications of the Model Assessments 59
Summary and Conclusions 62
References Cited 63
Appendixes 68

Figures

1. Map showing major Hydrologic Unit Code 4 Basins and locations of sediment sampling sites....4
2. Map showing generalized soil types and locations of sediment sampling sites....8
3. Map showing landscape relief and locations of sediment sampling sites....9
4. Map showing generalized land cover and locations of sediment sampling sites....10
5. Photographs showing configurations for collection of suspended-sediment concentrations at select sites....14
6. Pfankuch (1975) stream channel stability rating assessment for Pomme De Terre River at Appleton, Minnesota, U.S. Geological Survey station number 05294000....18
7. Hydrographs and dates of suspended-sediment samples for selected sites in Minnesota, 2007 through 2013....24
8. Flow-duration curves and corresponding values associated with suspended-sediment concentration samples for selected sites in Minnesota, 2007 through 2013....26
9. Graphs showing relations between suspended-sediment concentrations and streamflow for selected sites in Minnesota, 2007 through 2013....35
10. Graphs showing relations between bedload and streamflow for selected sites in Minnesota, 2007 through 2013....37
11. Graphs showing Pagosa Springs and Minnesota dimensionless suspended-sediment rating curves and site-specific regression trendlines for Pfankuch stability categories of good/fair for selected rivers in Minnesota, 2007 through 2013....45
12. Graphs showing Pagosa Springs and Minnesota dimensionless suspended-sediment rating curves and site-specific regression trendlines for Pfankuch stability categories of poor for selected rivers in Minnesota, 2007 through 2013....46
13. Graphs showing Pagosa Springs and Minnesota dimensionless bedload rating curves and site-specific regression trendlines for Pfankuch stability categories of good/fair for selected rivers in Minnesota, 2007 through 2013....48
14. Graphs showing Pagosa Springs and Minnesota dimensionless bedload rating curves and site-specific regression trendlines for Pfankuch stability categories of poor for selected rivers in Minnesota, 2007 through 2013....49
15. Graphs showing Nash-Sutcliffe Efficiency values for Pagosa Springs and Minnesota dimensionless rating curves and site-specific models for suspended-sediment concentrations for Pfankuch stability categories of good/fair and poor for selected rivers in Minnesota....52
16. Graphs showing Nash-Sutcliffe Efficiency values for Pagosa Springs and Minnesota dimensionless rating curves and site-specific models for bedload for Pfankuch stability categories of good/fair and poor for selected rivers in Minnesota....53
17. Graphs showing measured annual suspended-sediment loads based on R-LOADEST models (site [measured]) with 95-percent prediction intervals, and estimated loads based on the Pagosa Springs and Minnesota dimensionless sediment rating curve models for good/fair stability sites....56
18. Graphs showing measured annual suspended-sediment loads based on R-LOADEST models (site [measured]) with 95-percent prediction intervals, and estimated loads based on the Pagosa Springs and Minnesota dimensionless sediment rating curve models for poor stability sites for 2012....57

19. Graphs showing measured annual suspended-sediment loads based on R-LOADEST models (site [measured]) with 95-percent prediction intervals, and estimated suspended-sediment loads based on the Pagosa Springs and Minnesota dimensionless sediment rating curve models for poor stability sites for 2013.....58
20. Graphs showing measured annual bedload based on R-LOADEST models (site [measured]) with 95-percent prediction intervals and estimated bedload based on the Pagosa Springs and Minnesota dimensionless sediment rating curve models for good/fair stability sites (sites 8, 11) and poor stability sites (sites 5, 10, 12, 13, 18) for 2012 60
21. Graphs showing measured annual bedload based on R-LOADEST models (site [measured]) with 95-percent prediction intervals and estimated bedload based on the Pagosa Springs and Minnesota dimensionless sediment rating curve models for good/fair stability sites (sites 8, 11) and poor stability sites (sites 5, 10, 12, 13, 18) for 2013 61

Tables

1. Sediment sampling sites in selected basins in Minnesota 12
2. Bankfull streamflow, Pfankuch stability rating, and Rosgen stream classifications for sediment sampling sites in Minnesota.....17
3. Determination of ratio estimator and suspended-sediment concentration at bankfull streamflow for the Big Fork River near Craigsville, Minnesota.....19
4. Determination of partial estimates, pseudo values, and final jackknife estimate of suspended-sediment concentration at bankfull streamflow for the Big Fork River near Craigsville, Minnesota 19
5. Range of streamflow, suspended-sediment concentrations and bedload in samples collected from selected sites in Minnesota.....23
6. Summary statistics for streamflow, suspended-sediment concentrations, suspended particle-size fractions, and bedload collected from selected sites in Minnesota, 2007 through 2013.....28
7. Kendall's rank correlation tau statistics for relating total suspended-sediment concentration and bedload to streamflow 33
8. Suspended-sediment concentration at bankfull streamflow estimated using ratio estimators and jackknife resampling statistic for selected sites in Minnesota, 2007 through 2013 40
9. Bedload at bankfull streamflow estimated using ratio estimators and jackknife resampling statistic for selected sites in Minnesota, 2007 through 2013.....41
10. Sites in Minnesota used to develop dimensionless sediment rating curves 42
11. Determination of dimensionless and corresponding dimensional values of streamflow and suspended-sediment concentration using Minnesota dimensionless sediment rating curves for the North Fork Whitewater River near Elba, Minnesota 44
12. Model biases for suspended-sediment concentration and bedload transport for Pagosa Springs and Minnesota dimensionless sediment rating curve models and site-specific models 55

Appendix Tables

1–1. Pfankuch stream stability surveys for study sites in Minnesota 68
1–2. Streamflow, suspended-sediment concentrations, bedload particle-size fractions, bedload, and suspended particle-size fractions collected from selected sites in Minnesota, 2007 through 2013 68
1–3. Summary of site-specific simple linear regression models for suspended-sediment concentrations and bedload transport for selected sites in Minnesota, 2007 through 2013 68

Conversion Factors

U.S. customary units to International System of Units

Multiply	By	To obtain
	Length	
inch (in.)	25.4	millimeter (mm)
foot (ft)	0.3048	meter (m)
mile (mi)	1.609	kilometer (km)
	Area	
square mile (mi^2)	2.590	square kilometer (km^2)
	Volume	
pint (pt)	0.4732	liter (L)
quart (qt)	0.9464	liter (L)
cubic foot (ft^3)	0.02832	cubic meter (m^3)
	Flow rate	
cubic foot per second (ft^3/s)	0.02832	cubic meter per second (m^3/s)
	Mass	
ton, short (2,000 lb)	0.9072	megagram (Mg)
ton per day (ton/d)	0.9072	metric ton per day
ton per day (ton/d)	0.9072	megagram per day (Mg/d)

Temperature in degrees Celsius (°C) may be converted to degrees Fahrenheit (°F) as follows:

$$°F = (1.8 \times °C) + 32$$

Temperature in degrees Fahrenheit (°F) may be converted to degrees Celsius (°C) as follows:

$$°C = (°F - 32) / 1.8$$

International System of Units to U.S. customary units (used for particle-size determinations and sampling devices and containers)

Multiply	By	To obtain
	Length	
millimeter (mm)	0.03937	inch (in.)
	Volume	
liter (L)	2.113	pint (pt)

Datum

Vertical coordinate information is referenced to the North American Vertical Datum of 1988 (NAVD 88).

Horizontal coordinate information is referenced to the North American Datum of 1983 (NAD 83).

Elevation, as used in this report, refers to distance above the vertical datum.

Supplemental Information

Concentrations of chemical constituents in water are given in either milligrams per liter (mg/L) or micrograms per liter (µg/L).

Water year is defined as the 12-month period from October 1 through September 30 and is designated by the calendar year in which it ends.

Abbreviations

BCF	bias-correction factor
BOC	bank-operated cableway
DSRC	dimensionless sediment rating curve
HUC	hydrologic unit code
LMRWD	Lower Minnesota River Watershed District
log 10	base-10 logarithm
MNDNR	Minnesota Department of Natural Resources
MOVE-1	maintenance of variance extension, type 1
MPCA	Minnesota Pollution Control Agency
NSE	Nash-Sutcliffe Efficiency
PRS	Pfankuch rating system
R^2	coefficient of determination
SLR	simple linear regression
SSC	suspended-sediment concentration
SSL	suspended-sediment load
TMDL	total maximum daily load
TSS	total suspended solids
USACE	U.S. Army Corps of Engineers
USGS	U.S. Geological Survey
®	registered trademark

Application of Dimensionless Sediment Rating Curves to Predict Suspended-Sediment Concentrations, Bedload, and Annual Sediment Loads for Rivers in Minnesota

By Christopher A. Ellison,[1] Joel T. Groten,[1] David L. Lorenz,[1] and Karl S. Koller[2]

Abstract

Consistent and reliable sediment data are needed by Federal, State, and local government agencies responsible for monitoring water quality, planning river restoration, quantifying sediment budgets, and evaluating the effectiveness of sediment reduction strategies. Heightened concerns about excessive sediment in rivers and the challenge to reduce costs and eliminate data gaps has guided Federal and State interests in pursuing alternative methods for measuring suspended and bedload sediment. Simple and dependable data collection and estimation techniques are needed to generate hydraulic and water-quality information for areas where data are unavailable or difficult to collect.

The U.S. Geological Survey, in cooperation with the Minnesota Pollution Control Agency and the Minnesota Department of Natural Resources, completed a study to evaluate the use of dimensionless sediment rating curves (DSRCs) to accurately predict suspended-sediment concentrations (SSCs), bedload, and annual sediment loads for selected rivers and streams in Minnesota based on data collected during 2007 through 2013. This study included the application of DSRC models developed for a small group of streams located in the San Juan River Basin near Pagosa Springs in southwestern Colorado to rivers in Minnesota. Regionally based DSRC models for Minnesota also were developed and compared to DSRC models from Pagosa Springs, Colorado, to evaluate which model provided more accurate predictions of SSCs and bedload in Minnesota.

Multiple measures of goodness-of-fit were developed to assess the effectiveness of DSRC models in predicting SSC and bedload for rivers in Minnesota. More than 600 dimensionless ratio values of SSC, bedload, and streamflow were evaluated and delineated according to Pfankuch stream stability categories of “good/fair” and “poor” to develop four Minnesota-based DSRC models. The basis for Pagosa Springs and Minnesota DSRC model effectiveness was founded on measures of goodness-of-fit that included proximity of the model(s) fitted line to the 95-percent confidence intervals of the site-specific model, Nash-Sutcliffe Efficiency values, model biases, and deviation of annual sediment loads from each model to the annual sediment loads calculated from measured data.

Composite plots comparing Pagosa Springs DSRCs, Minnesota DSRCs, site-specific regression models, and measured data indicated that regionally developed DSRCs (Minnesota DSRC models) more closely approximated measured data for nearly every site. Pagosa Springs DSRC models had markedly larger exponents (slopes) when compared to the Minnesota DSRC models and the site-specific regression models, and over-represent SSC and bedload at streamflows exceeding bankfull. The Nash-Sutcliffe Efficiency values for the Minnesota DSRC model for suspended-sediment concentrations closely matched Nash-Sutcliffe Efficiency values of the site-specific regression models for 12 out of 16 sites. Nash-Sutcliffe Efficiency values associated with Minnesota DSRCs were greater than those associated with Pagosa Springs DSRCs for every site except the Whitewater River near Beaver, Minnesota site. Pagosa Springs DSRC models were less accurate than the mean of the measured data at predicting SSC values for one-half of the sites for good/fair stability sites and one-half of the sites for poor stability sites. Relative model biases were calculated and determined to be substantial (greater than 5 percent) for Pagosa Springs and Minnesota models, with Minnesota models having a lower mean model bias. For predicted annual suspended-sediment loads (SSL), the Minnesota DSRC models for good/fair and poor stream stability sites more closely approximated the annual SSLs calculated from the measured data as compared to the Pagosa Springs DSRC model.

Results of data analyses indicate that DSRC models developed using data collected in Minnesota were more effective at compensating for differences in individual stream characteristics across a variety of basin sizes and flow regimes than DSRC models developed using data collected for Pagosa Springs, Colorado. Minnesota DSRC models retained a substantial portion of the unique sediment signatures for most rivers, although deviations were observed for streams with

[1]U.S. Geological Survey.

[2]Minnesota Department of Natural Resources.

limited sediment supply and for rivers in southeastern Minnesota, which had markedly larger regression exponents. Compared to Pagosa Springs DSRC models, Minnesota DSRC models had regression slopes that more closely matched the slopes of site-specific regression models, had greater Nash-Sutcliffe Efficiency values, had lower model biases, and approximated measured annual sediment loads more closely. The results presented in this report indicate that regionally based DSRCs can be used to estimate reasonably accurate values of SSC and bedload.

Practitioners are cautioned that DSRC reliability is dependent on representative measures of bankfull streamflow, SSC, and bedload. It is, therefore, important that samples of SSC and bedload, which will be used for estimating SSC and bedload at the bankfull streamflow, are collected over a range of conditions that includes the ascending and descending limbs of the event hydrograph. The use of DSRC models may have substantial limitations for certain conditions. For example, DSRC models should not be used to predict SSC and sediment loads for extreme streamflows, such as those that exceed twice the bankfull streamflow value because this constitutes conditions beyond the realm of current (2016) empirical modeling capability. Also, if relations between SSC and streamflow and between bedload and streamflow are not statistically significant, DSRC models should not be used to predict SSC or bedload, as this could result in large errors. For streams that do not violate these conditions, DSRC estimates of SSC and bedload can be used for stream restoration planning and design, and for estimating annual sediment loads for streams where little or no sediment data are available.

Introduction

Historically, the U.S. Environmental Protection Agency has listed sediment as one of the leading causes of impairment in the Nation's rivers and streams (U.S. Environmental Protection Agency, 1990, 1992, 1995, 1998, 2000, 2002, 2007). Excessive sediment in rivers degrades water quality, exacerbates flooding, fills in reservoirs and lakes, causes loss of channel navigability, harms aquatic habitat, and transports detrimental contaminants (Baker, 1980; U.S. Army Corps of Engineers, 2003; Minnesota Pollution Control Agency, 2009). The Minnesota Pollution Control Agency (MPCA) lists turbidity as the top water-quality impairment affecting more than 6,000 miles (mi) of streams throughout Minnesota (Minnesota Pollution Control Agency, 2009; U.S. Environmental Protection Agency, 2012). Heightened concerns about sediment-laden rivers have bolstered efforts by the MPCA and the Minnesota Department of Natural Resources (MNDNR) to investigate new strategies for monitoring sediment transport and reducing excess sediment in rivers.

Beginning in 2007, the U.S. Geological Survey (USGS), in collaboration with the MPCA, established a network of sites across Minnesota and began collecting water samples for analyses of suspended-sediment concentrations (SSCs), turbidity, and total suspended-solids (TSS) to improve understanding of fluvial sediment relations and transport processes. In 2012, the USGS, in cooperation with the U.S. Army Corps of Engineers (USACE), the MNDNR, and the Lower Minnesota River Watershed District (LMRWD), expanded sediment sampling from 8 to 22 sites. In addition to collecting SSC samples, the USGS began collecting bedload samples to quantify the contribution of bedload to total sediment loads. During this time, hundreds of streamflow measurements and SSC, turbidity, TSS, and bedload samples were collected to develop statistical relations among these constituents (U.S. Geological Survey National Water Information System, http://dx.doi.org/10.5066/F7P55KJN; Ellison and others, 2014). Data collected from the sites contributed to the decision by the MPCA to transition from a total maximum daily load (TMDL) turbidity standard to a TSS water-quality standard (Greg Johnson, Minnesota Pollution Control Agency, oral commun., various dates). Similarly, the MNDNR and USACE have used SSC-streamflow and bedload-streamflow relations developed by the USGS to improve sediment budgets and to guide various scale river restoration projects throughout the State.

Previous studies led by the USGS described regional sediment-related characteristics for rivers in Minnesota and developed statistical relations among streamflow, SSC, turbidity, and TSS (Tornes, 1986; Tornes and others, 1997; Ellison and others, 2014). These data indicated that rivers in Minnesota demonstrated site-specific sediment signatures with high variability in the relation between SSC and streamflow; in fact, statistical relations between SSC and streamflow were not significant (that is, p-values greater than 0.05) or were weakly significant (that is, p-values less than 0.05 with corresponding coefficient of determination [R^2] values less than 0.25) at approximately one-half of the sampling locations. Variability in the strength of the relation between SSC and streamflow is attributed to variability in the rate of sediment supply, which is affected by factors including sediment availability, season, basin size, and source location within the basin. Considerable variability in SSCs also may be the result of a hysteresis effect with streamflow. Clockwise hysteresis (higher sediment concentration on the rising limb of the hydrograph) is common in smaller basins because of increased shear stress on the rising limb of the hydrograph (Julien, 2002) and because sediment sources are closer to the stream channel. Counterclockwise hysteresis (higher sediment concentration on the falling limb of the hydrograph) may happen in large basins where upstream sources continue to supply the bulk of the load after the streamflow peaks (Knighton, 1998). Seasonal differences contribute to the variability in SSCs because sediment transport typically is greatest in the spring during snowmelt runoff. The availability of sediment at the source location also affects how SSCs vary with streamflow at a particular location. Because of these and other factors, the variability and range of SSCs during any runoff event may differ from the concentrations during other periods, even though streamflow may be identical or similar (Porterfield, 1972).

Mandates to reduce costs, eliminate data gaps, and improve data accuracy have guided Federal and State interests in pursuing alternative methods of measuring and estimating SSCs and bedload. Physically collected samples for analysis of SSCs and bedload remain the most accurate and reliable means for determining sediment loads; however, the specialized equipment, training, and labor required to collect samples are time consuming, expensive, and hazardous in certain conditions. Reliable and consistent sediment data are needed by Federal, State, and local government agencies for establishing and monitoring water-quality standards, planning river restoration, quantifying sediment budgets, and evaluating the effectiveness of sediment reduction strategies. More data, however, are needed to improve understanding of sediment transport relations for rivers with sparse or no available sediment data.

One alternative to collecting physical sediment samples is to use theoretical sediment prediction models. The availability of modeling software and the benefit of evaluating a variety of scenario simulations make models an attractive alternative to data collection; however, studies indicate that theoretical model results commonly differ markedly from measured loads, causing a high level of uncertainty about the ability of models to accurately predict loads (Lopes and others, 2001; Barry and others, 2008; Rosgen, 2010). Methods using surrogate technologies have become available to provide real-time, continuous monitoring of sediment concentrations. The new methods involve the use of continuous turbidity monitoring and hydroacoustic technology (Rasmussen and others, 2009; Wood, 2014). Continuous turbidity monitoring uses scattered light to provide real-time SSC monitoring (Rasmussen and others, 2009), whereas hydroacoustic technology uses sound waves to measure SSCs (Wood, 2014). Although these surrogate methods are promising, they are not applicable in all conditions and entail expensive and complex equipment installations. Furthermore, surrogate measurements must be calibrated from physically collected sediment samples, require extensive analyses, and the associated surrogate equipment requires recurring maintenance and monitoring to ensure reliability of the data.

Another alternative to collecting physical sediment samples is the use of dimensionless sediment rating curves (DSRCs) to reduce costs and improve the accuracy of predicting sediment transport (Troendle and others, 2001; Barry and others, 2008; Rosgen, 2006, 2010). Dimensionless rating curves have demonstrated potential to predict constituents of interest by scaling existing data at several regionally representative sites and applying the curves at sites where data are sparse or nonexistent. Previous studies demonstrated that dimensionless relations can be used to help understand naturally occurring relations among hydraulic and water-quality properties. For example, Leopold and others (1964) used dimensionless curves to express the stage-discharge relation for streamgages in the eastern United States. Padmanabhan and Johnson (2010) developed regional dimensionless rating curves to estimate streamflow and stream stages in the Red River Basin of Minnesota (fig. 1) and in North Dakota for use in bridge design and floodplain management. Dietrich and others (1989) normalized bedload transport rates to relate bedload particle coarsening to imbalances in sediment transport-supply ratios. Additionally, Troendle and others (2001) used DSRCs to determine departure from river stability and to predict supply of sediment to rivers.

The U.S. Geological Survey, in cooperation with the Minnesota Pollution Control Agency and the Minnesota Department of Natural Resources, completed a study to evaluate the use of DSRCs to accurately predict SSCs, bedload, and annual sediment loads for selected rivers and streams in Minnesota based on data collected during 2007 through 2013. This study included the application of DSRCs developed for a small group of streams located in the San Juan River Basin (not shown) near Pagosa Springs in southwestern Colorado to rivers in Minnesota. Regionally based DSRC models also were developed and compared to DSRCs from Pagosa Springs, Colorado, to evaluate which model provided more accurate predictions of SSCs and bedload in Minnesota.

Background Information on Dimensionless Sediment Rating Curves

The DSRC method relies on the intrinsic relations among streamflow, SSC, and bedload. Rosgen (2006, 2007, and 2010) continued work by Barry and others (2004) and Troendle and others (2001) by expanding the application of dimensionless relations to improve predictions of suspended sediment and bedload in rivers. Rosgen's objectives for developing DSRC models were to provide a tool for river restoration planning and design, reduce the error from theoretical sediment prediction models, and help identify rivers that depart from known reference conditions. The Rosgen method (Rosgen, 2010) involves developing dimensionless relations between SSC and streamflow and between bedload and streamflow, and uses bankfull streamflow as a normalization parameter to develop the DSRC models.

In most streams, bankfull streamflow is associated with the flow that just fills the channel to the top of its banks where the water begins to overflow onto a floodplain (Leopold and others, 1964). Dunne and Leopold (1978) described bankfull stage as "the point on the streambank that corresponds to the discharge at which channel maintenance is the most effective, that is, the discharge at which moving sediment, forming or removing bars, forming or changing bends and meanders, and generally doing work that results in the mean morphologic characteristics of channels." Although channel geomorphic processes such as migration, aggradation, incision, avulsion, and other significant morphological changes may be active during extreme flood events, it is generally accepted that bankfull streamflow transports the greatest quantity of sediment material throughout time, because of the higher frequency of occurrence (Wolman and Miller, 1960; Leopold and others, 1964). These channel morphology characteristics associated with bankfull streamflow were the basis for the use of bankfull streamflow as a logical reference index for the development of DSRCs.

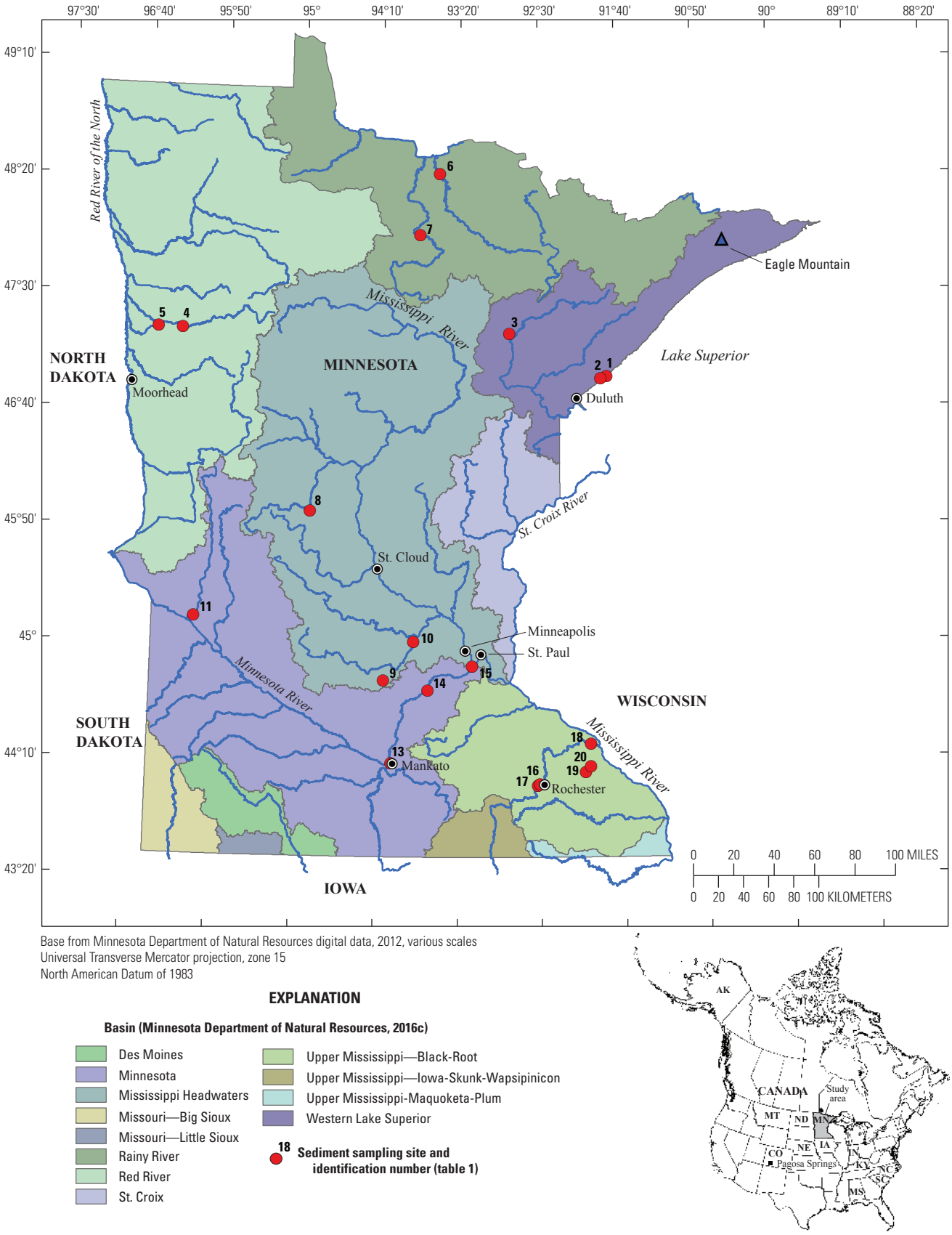

Base from Minnesota Department of Natural Resources digital data, 2012, various scales
Universal Transverse Mercator projection, zone 15
North American Datum of 1983

EXPLANATION

Basin (Minnesota Department of Natural Resources, 2016c)

- Des Moines
- Minnesota
- Mississippi Headwaters
- Missouri—Big Sioux
- Missouri—Little Sioux
- Rainy River
- Red River
- St. Croix
- Upper Mississippi—Black-Root
- Upper Mississippi—Iowa-Skunk-Wapsipinicon
- Upper Mississippi-Maquoketa-Plum
- Western Lake Superior

18 **Sediment sampling site and identification number (table 1)**

Figure 1. Major Hydrologic Unit Code 4 Basins and locations of sediment sampling sites.

Bankfull stage is not always easily identifiable in the field, and a combination of methods may be needed to determine the bankfull streamflow of a stream. For example, flood plains, which are useful for identifying the point where streamflow tops the banks, can be small and indistinct under certain conditions or disconnected from the main-stem channel, making a visual determination of bankfull stage difficult. For conditions when bankfull stage is not easily identifiable, bankfull stage may be determined by using a combination of indicators such as substantial change in slope on the streambank, changes in particle sizes or color, or changes in vegetation density located along the boundary of the active channel (Leopold and others, 1964; Rosgen, 2007). In general, bankfull streamflow is a momentary flow that has a mean recurrence interval ranging from 1.05 to 1.8 years with an interval of 1.5 years commonly used (Dunne and Leopold, 1978). For highly developed urban basins, Rosgen (1996) determined that the return period of bankfull streamflow was closer to 1.1 years.

Collecting SSC and bedload data during bankfull stage can be difficult because of the inherent unpredictability of the timing of flow magnitudes and physical constraints typical during bankfull streamflow conditions. Moreover, there is a marked level of uncertainty regarding the representativeness of samples collected at or near bankfull streamflow during any single event because of the variability in SSCs and bedload from effects of hysteresis, antecedent conditions, and random pulses of sediment inputs (Porterfield, 1972; Knighton, 1998; Edwards and Glysson, 1999). It is, therefore, important to collect samples across a wide range of conditions (such as snowmelt runoff and precipitation events in summer and fall) and during the ascending and descending limb of the event hydrograph to accurately estimate SSC and bedload at bankfull streamflow. The consequence of relying on values that under- or over-represent SSC and bedload may be large inaccuracies in sediment load computations and subsequent interpretations.

The bankfull stage conditions of streamflow, SSC, and bedload are normalized across a range of flows to predict dimensional SSC, bedload, and annual sediment loads (Rosgen, 2010). Dimensionless values of SSC and bedload are determined from ratios of measured values of SSC and bedload, and calculated values of SSC and bedload at the bankfull streamflow. Corresponding streamflows also are made dimensionless as the ratio of measured or calculated streamflow to the calculated bankfull streamflow. Dimensionless ratio values of SSC and bedload are plotted against dimensionless ratio streamflows to create predictive relations (Rosgen, 2010). After the DSRC models are developed, a minimum number of samples (typically four to six) of SSC and bedload acquired over a range of conditions near bankfull streamflow may be collected at sites where sediment data are needed. These samples are used to determine site-specific SSC and bedload at bankfull streamflow and are applied as multiplicative discrete values with DSRC models to calculate dimensional SSCs and bedload. Representative measures of bankfull streamflow, SSCs, and bedload collected over a range of conditions are crucial for DSRC model development and reliability in predicted values.

In addition to using bankfull streamflow as a normalization parameter, Rosgen (2010) incorporated the link between sediment transport and channel stability to improve the prediction efficiency of DSRC models. A stable channel consists of a set of characteristics within which riparian and aquatic habitat is optimized resulting in a more diverse and stable biological community (Asmus, 2011). In contrast, channel instability is linked to an imbalance between sediment production and sediment transport capacity (Lane, 1955; Rosgen, 1996; Montgomery and Buffington, 1998; Watson and others, 2002). Lane (1955) described channel stability as “the dynamic equilibrium that exists between stream power and the discharge of bed material sediment.” Rosgen (1996) described stream channel stability as “the ability of the stream to maintain, over time, its dimension, pattern, and profile in such a manner that it is neither aggrading nor degrading and is able to transport without adverse consequence the flows and detritus of its watershed.” Watson and others (2002) described channel stability as a function of sediment continuity for which an even balance exists between sediment supply and sediment transport capacity.

Pfankuch (1975) developed a rating system to evaluate relative channel stability for the U.S. Forest Service by estimating potential changes in sediment supply from channel geomorphic characteristics. This rating system is known as the Pfankuch rating system (PRS) and is used to assign stability ratings of excellent, good, fair, and poor to stream reaches by evaluating stream channel characteristics that include bed and bank scour, bank slope, degree of mass wasting, substrate mobility and size, deposition and sand bar production, and vegetative bank cover. The PRS has been used by academia, Federal, State, and local governments to relate channel stability to aquatic biota (Rounick and Winterbourn 1982; Death and Winterbourn, 1994, 1995; Duncan and others, 1999; Robertson and Milner, 1999). The PRS was modified by Rosgen (1996) for use with his widely adopted stream classification system.

Results from Rosgen (2010) indicate that DSRCs developed from a small group of streams located in the San Juan River Basin near Pagosa Springs in southwestern Colorado (fig. 1) may be used to estimate sediment transport for geographically far-removed streams with different flow regimes, geology, and climate. Rosgen (2010) developed four reference DSRC model equations delineated by Pfankuch (1975) stream stability categories using data collected from the streams in Colorado. Using the Pagosa Springs DSRCs, Rosgen (2010) completed a verification study and observed close agreements between the Pagosa Springs DSRC predicted values of SSC and bedload with measured values from streams in Canada, Alaska, Montana, Colorado, North Carolina, South Carolina, Indiana, Kentucky, Mississippi, and Nebraska. The four DSRC equations developed by Rosgen (2010) for good/fair and poor stability ratings for the Pagosa Springs DSRC models follow:

Suspended DSRC (good/fair stability):

$$SSC = 0.0636 + 0.9326Q^{2.4085} \quad (1)$$

Bedload DSRC (good/fair stability):

$$Q_b = -0.0113 + 1.0139Q^{2.1929} \quad (2)$$

Suspended DSRC (poor stability):

$$SSC = 0.0989 + 0.9213Q^{3.659} \quad (3)$$

Bedload DSRC (poor stability):

$$Q_b = 0.07176 + 1.02176Q^{2.3772} \quad (4)$$

where

SSC is a dimensionless ratio value of suspended-sediment concentration,

Q is a dimensionless ratio value of streamflow, and

Q_b is a dimensionless ratio value of bedload.

Rosgen identified three limitations associated with the application of DSRC models (Dave Rosgen, Wildland Hydrology, oral commun., various dates). First, DSRC models should not be used to predict SSC and loads for extreme streamflows, such as those that exceed twice the bankfull value. Streamflows that exceed twice the bankfull value constitute conditions beyond the realm of current (2016) empirical modeling capability (Dave Rosgen, Wildland Hydrology, oral commun., various dates). Second, if relations based on measured data between SSCs and streamflow or between bedload and streamflow in a particular region substantially deviate from Pagosa Springs DSRC models, then regionally specific DSRCs should be developed following a similar approach used to develop the Pagosa Springs DSRC models (Rosgen, 2006). Third, DSRC models assume a statistically significant relation (p-value less than 0.05) exists between SSC and streamflow, and between bedload and streamflow. If relations are not statistically significant (p-values greater than 0.05), DSRCs are not applicable and should not be used to predict SSC or bedload, as this could result in large errors (that is, DSRC predicted loads deviate substantially from measured loads). Rivers with low sediment supply because of cohesive soils or low gradient may likely violate this assumption. For rivers that violate the third limitation-assumption, the mean value of SSC and bedload samples collected across a range of conditions could be used for quantifying sediment loads.

Although previous studies (Tornes, 1986; Tornes and others, 1997; Blanchard and others, 2011; Ellison and others, 2014) have documented that nearly every stream in Minnesota has a unique sediment transport signature, the dimensionless rating curve method presented by Rosgen (2010) demonstrated the potential to compensate for differences in streams across a variety of basin sizes, streamflow regimes, and climate types. Anticipated benefits of developing a curve model for SSCs and bedload include (1) improved sediment budgets, (2) reduced costs associated with extensive sediment data collection, (3) ability to identify streams that depart from reference conditions, (4) access to a tool for restoration prioritization, and (5) access to important information for planning river restoration activities.

Purpose and Scope

This report describes the application and evaluation of the effectiveness of DSRCs to predict SSCs, bedload, and annual sediment loads for rivers in Minnesota. Specifically, this report describes the following:

1. SSCs, bedload, streamflow, and particle-size fractions for selected rivers across major basins in Minnesota from 2007 through 2013;
2. Development and evaluation of relations among streamflow, SSCs, and bedload for selected rivers stratified by Pfankuch stability categories of “good/fair” and “poor”; and
3. The application and evaluation of DSRCs developed using data from Colorado and Minnesota to approximate measured SSCs and bedload for rivers in Minnesota, including DSRC model limitations.

Description of Study Area

Minnesota encompasses 86,939 square miles (mi^2) in the upper midwestern United States (Minnesota Department of Natural Resources, 2016a). Land surface elevations range from 601 feet, (ft) along the shoreline of Lake Superior to about 2,302 ft above the North American Vertical Datum of 1988 (NAVD 88) at Eagle Mountain, which is only 13 mi away from the lowest elevation at the Lake Superior shoreline (fig. 1; Minnesota Department of Natural Resources, 2016a). Minnesota is in a transition zone between the moist eastern United States and the Great Plains (not shown) and has a continental climate with cold winters and warm to hot summers (Minnesota Department of Natural Resources, 2016b). Winter is characterized by below-freezing temperatures with snow as the main form of precipitation. High humidity and warm temperatures are common during the summer months in southern regions of the State, whereas northern regions of Minnesota report more moderate humidity and cooler temperatures. Mean annual precipitation across the State ranges from 35 inches (in) in the southeast to 20 in. in the northwest (Minnesota Department of Natural Resources, 2016b). The six hydrologic unit code (HUC) HUC–level 4 basins (Rainy River, Red River, Western Lake Superior, Mississippi Headwaters, Minnesota, and Upper Mississippi – Black-Root [Minnesota Department of Natural Resources, 2016c; Minnesota Geospatial Information Office, 2016]) selected for this study represent a cross section of basin characteristics present in Minnesota (fig. 1).

Familiarity with the geologic history of Minnesota (Sims and Morey, 1972; Ojakangas and Matsch, 1982; Minnesota Department of Natural Resources, 2016d), specifically of advancing and retreating glaciers, is fundamental to understanding regional vulnerability to erosion and extent of sediment supply and transport. The Wisconsinan glaciation, which occurred from 85,000 to 11,000 years ago, left deep layers of rock, sand, and clay, known as glacial till, across much of the State and contributed to the development of the general soil types (fig. 2) and topographic relief (fig. 3) present today (2016) (Lusardi, 1997; Minnesota Department of Natural Resources, 2016d). In northeastern Minnesota, Precambrian bedrock that formed from volcanic activity (4,000–541 million years ago) remains close to the surface. Volcanic bedrock was more resistant to glacial erosion than other rock types, resulting in less glacial till in the northeastern part of the State compared to other parts of the State. Today (2016), most of the northeastern part of the State remains forested, but has some open pasture and sparse cultivated crops (fig. 4; Minnesota Department of Natural Resources, 2016a; 2016f).

Northwestern Minnesota lies in the dried lakebed of glacial Lake Agassiz (not shown), which was formed from meltwaters following the Wisconsinan glaciation (Sims and Morey, 1972; Ojakangas and Matsch, 1982). In northwestern Minnesota, bedrock formed during the Archean period (4,000–2,500 million years ago) and was covered by clay-rich glacial drift during the Wisconsinan glaciation period (Minnesota Department of Natural Resources, 2016d). The area is flat, except for beach ridges at the borders of glacial Lake Agassiz. Fine-grained glacial lake deposits and decayed organic material reaching depths of about 160 ft formed rich soils that are ideal for agriculture (Lusardi, 1997).

Much of southwestern Minnesota sits in the channel of glacial River Warren (not shown), an enormous flood torrent that drained Lake Agassiz between 11,700 and 9,400 years ago and formed the present day Minnesota River Basin (fig. 1; Minnesota Department of Natural Resources, 2016d). The region contains the Coteau des Prairies (not shown), a plateau that extends into Minnesota, South Dakota, and Iowa (Minnesota Department of Natural Resources, 2016d). The plateau consists of thick glacial deposits and divides southwestern Minnesota into the Minnesota and Missouri River Basins (Missouri River Basin not shown). Wetlands known as prairie potholes were once abundant in southwestern Minnesota but most (90 percent) have been drained for agriculture (Minnesota Department of Natural Resources, 2016d).

The southeastern corner of the State is the only region of Minnesota to escape the Wisconsinan glaciation, although evidence exists that it was subject to earlier glaciations (Minnesota Department of Natural Resources, 2016d). This region is referred to as the driftless region because of the lack of Wisconsinan glacial till, or drift. Paleozoic bedrock exposures in southeastern Minnesota are covered with large deposits of unconsolidated sand that were transported by glacial winds from the nearby ice sheet. Topsoils in southeastern Minnesota are more shallow and poorer than those to the west (Minnesota Department of Natural Resources, 2016d). Rivers in southeastern Minnesota have developed more extensive geomorphic processes like lateral migration and downcutting compared to areas affected by the Wisconsinan glaciation period and have cut deep valleys into the underlying bedrock, resulting in more efficient drainage systems and more advanced erosion (Minnesota Department of Natural Resources, 2016d). The transition region in central Minnesota (land use changes from predominately agriculture to forested) lies in a mixture of cultivated crops, pasture, and forests (Minnesota Department of Natural Resources, 2016a). Urban (developed) areas, which contain three study sites, are scattered throughout the State, but the largest is the Minneapolis-St. Paul metropolitan area.

Precipitation amounts varied across the State from 2007 through 2013. For example, precipitation was greater than the historical mean for the State in 2007 and for most of the State in 2008, with the exception of south-central and lower east-central regions, which had less than the historical mean precipitation (Minnesota Department of Natural Resources, 2016d). For 2009, most of the State had precipitation that approximated the historical mean amounts, whereas small regions in north-central, east-central, and southwest regions had less than historical mean precipitation. Precipitation alternated from markedly greater than the historical mean precipitation for most of the State during 2010 to markedly less than mean precipitation for most of the State during 2011. For 2012, precipitation amounts were less than the historical mean in the southeast, southwest, and northwest regions of the State and markedly greater than the historical mean in the northeast and east-central regions of the State. In 2013, nearly all of the State had precipitation greater than the historical mean, with the exception of the southeast region, which had precipitation that was less than the historical mean (Minnesota Department of Natural Resources, 2016e).

Similarly, streamflow also varied across the State during the study period. For the northeast region, streamflow overall was greater than historical median streamflow during 2007, 2008, 2010, 2011, and 2013, and less than the historical median streamflow during 2009 and 2012, with the exception of May and June in 2012, which had record streamflow in the Duluth, Minnesota, area (U.S. Geological Survey, 2016; Czuba and others, 2012). For the northwest region, streamflow was greater than historical median streamflow during 2008 through 2011, and 2013, and was less than historical median streamflow in 2012. In the central region of the State, streamflow was similar to historical median streamflow during 2008 and 2010, less than historical median streamflow during 2009, and greater than historical median streamflow during 2011 through 2013. For the southwest region, streamflow was similar to historical median streamflow during 2008 and 2013, with the exception of July 2013, which had streamflow that was greater than historical median streamflow. Also for the southwest region, streamflow was less than the historical median streamflow during 2009, and was greater than historical median streamflow during 2010. In 2012, streamflow was less than historical median streamflow from January through

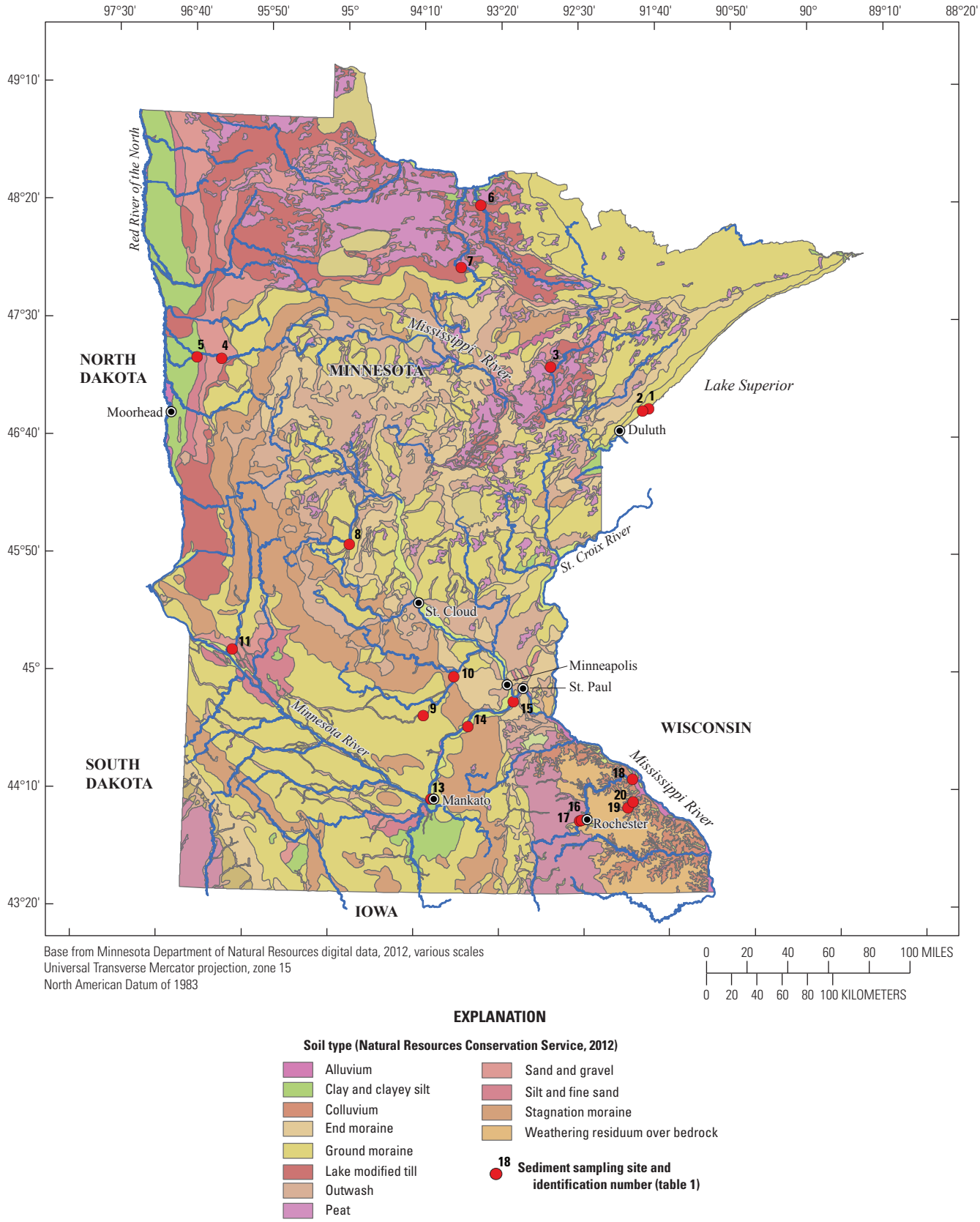

Figure 2. Generalized soil types and locations of sediment sampling sites.

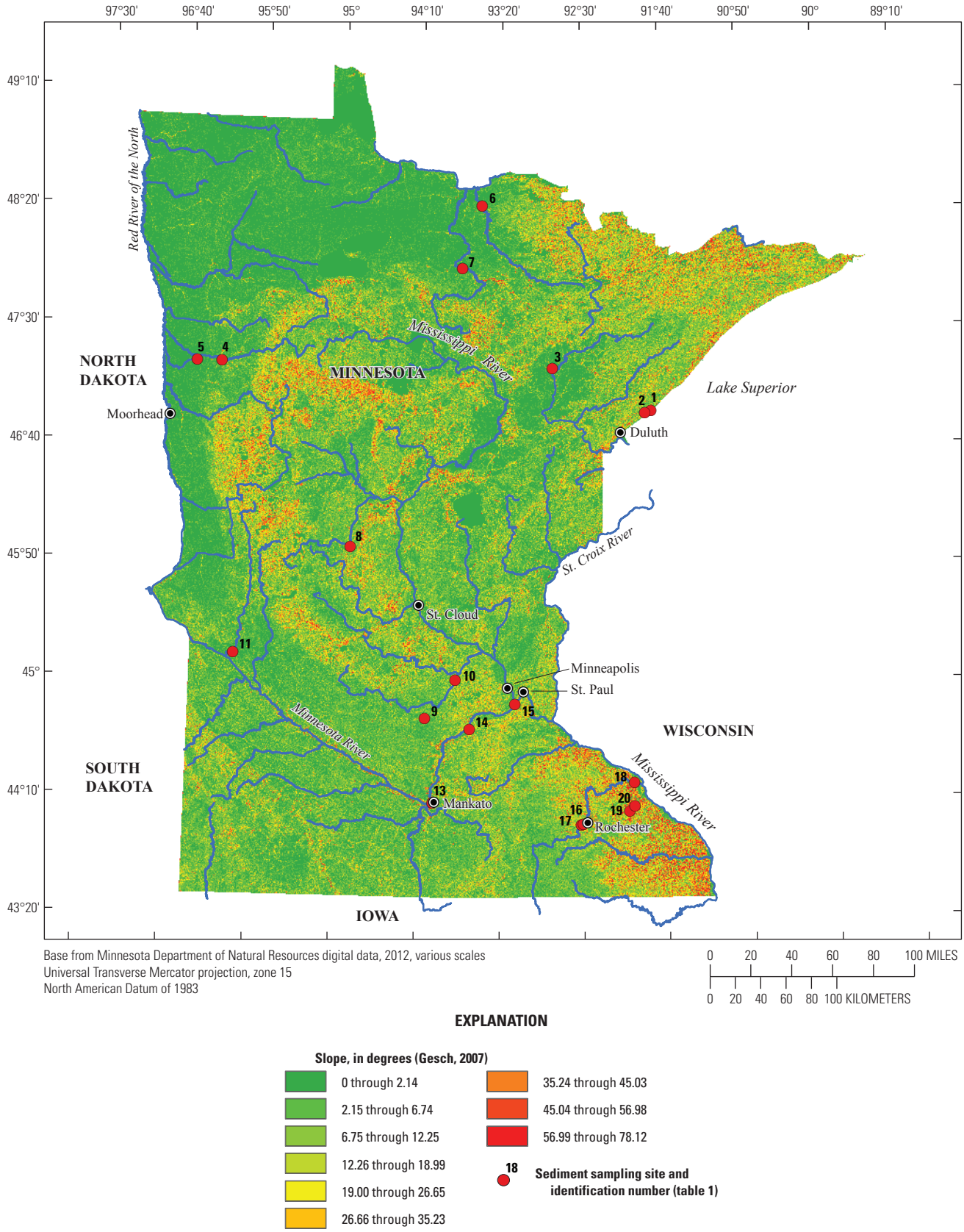

Figure 3. Landscape relief and locations of sediment sampling sites.

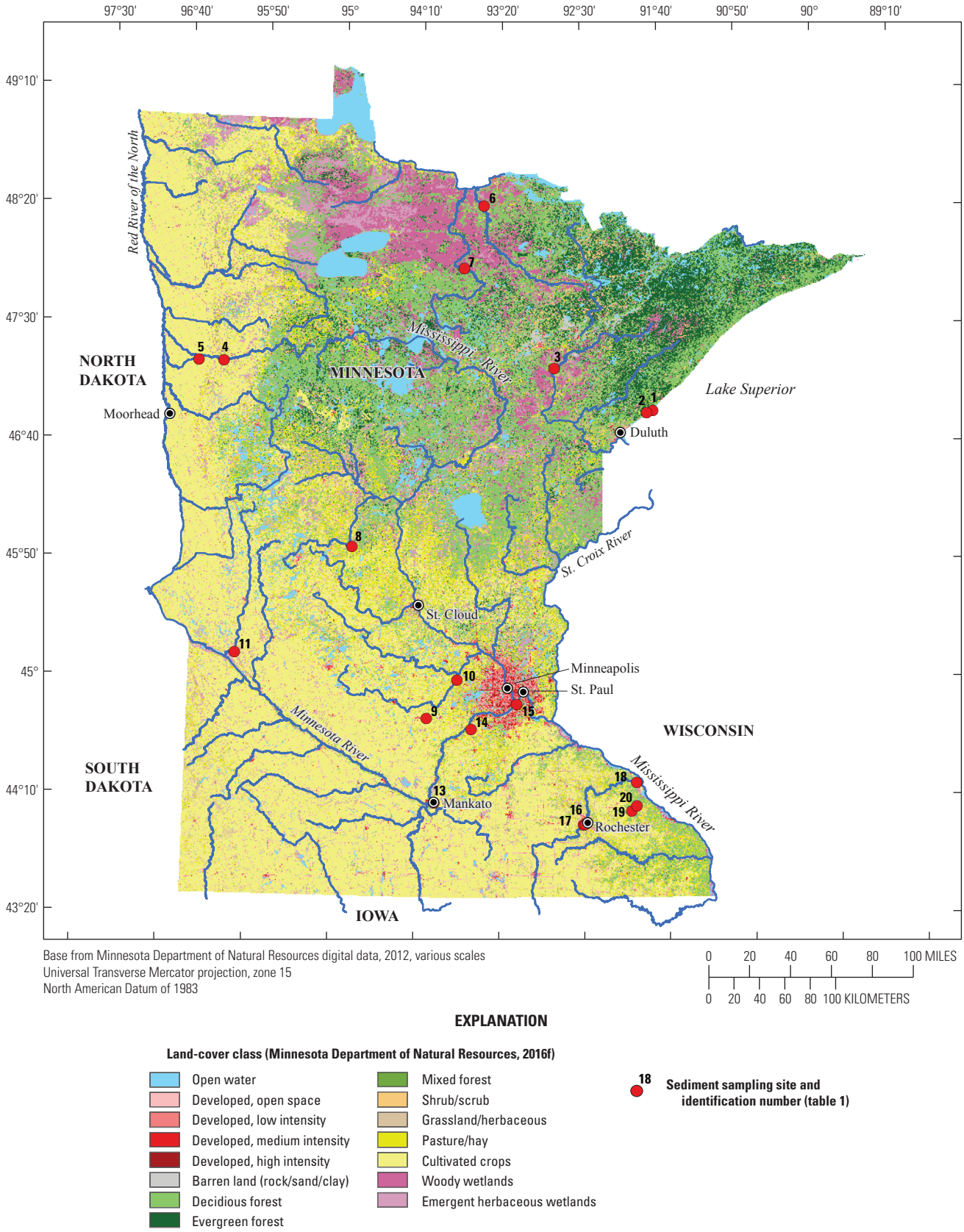

Figure 4. Generalized land cover and locations of sediment sampling sites.

April, greater than historical median streamflow in May and June, and similar to historical median streamflow for the remainder of the year (U.S. Geological Survey, 2016).

Methods of Data Collection and Analysis

This section describes methods used for the collection of sediment samples, measurement of streamflow, analysis of Pagosa Springs DSRCs, and the development of Minnesota DSRCs. A total of 20 sites (table 1) were sampled from 2007 through 2013, with most of the samples collected in 2012 and 2013. Sites were collocated at established USGS or MNDNR streamgages with the exception of three sites (sites 16, 17, and 19; table 1), and were sampled 5 to 14 times per year during the open-water season (March through November; table 1). Few samples (4 total) were collected during the winter because a previous study (Tornes, 1986) indicated that less than 4 percent of annual sediment loads in rivers of Minnesota are transported during the winter months. In Minnesota, it is likely that transport of sediment is minimal during the winter because streamflow is generally at its lowest, is contained under ice, and little sediment is contributed from the surrounding landscape or from the streambed and adjacent banks.

Data from 15 of the 20 sites were selected specifically for this study using samples collected from March 2012 through November 2013. Five additional sites were incorporated in the study using available SSC and bedload data collected beginning in February 2007 as part of USGS collaborative studies with the MPCA, USACE, and the LMRWD. For the five additional sites, two sites are part of an ongoing collaborative study between the USGS, USACE, and the LMRWD to quantify sediment transport in the lower part of the Minnesota River Basin (sites 14 and 15; table 1; fig. 1); these two sites were sampled from March 2011 through November 2013 (U.S. Army Corps of Engineers, 2003; Lower Minnesota River Watershed District, 2009). Three of the five additional sites are part of an ongoing collaborative study between the USGS and MPCA (sites 1, 13, and 18; table 1), and were sampled from 2007 through 2013 (Ellison and others, 2014). The remaining 15 sites directly support the evaluation from this study of DSRCs for use in rivers in Minnesota.

Water samples were collected at all sites for analysis of SSC and particle-size fractions less than 0.0625 millimeters (mm; categorized as fines). Particles equal to or greater than 0.0625 mm are categorized as sands. Bedload sampling began in 2012 for this study with the exception of site 15 (Minnesota River at Fort Snelling State Park, Minn.). For this site, bedload samples were collected beginning in 2011 to support the USGS collaborative study with the USACE and LMRWD. Streamflow data were obtained from existing USGS or MNDNR streamgages (U.S. Geological Survey, 2016; Minnesota Department of Natural Resources, 2014) with the exception of three sites (sites 16, 17, and 19; table 1) where no streamgage was available.

Suspended-Sediment Concentrations

Depth-integrated suspended-sediment samples were collected at equal-width intervals across stream transects using isokinetic samplers according to procedures by Edwards and Glysson (1999). For collection of suspended-sediment samples, the total stream width at each site was divided into 10 equal-widths, and individual depth-integrated samples were collected at the centroid of each increment. Individual samples from each centroid were kept primarily in 1-pint glass bottles, with each vertical increment generally contained within a single bottle. Under certain conditions, 1-quart glass bottles, or 1 or 3-liter (L) plastic bags may have been used to collect the samples according to procedures by Edwards and Glysson (1999). Care was taken not to overfill the sample bottle. If a bottle inadvertently was overfilled, the contents were discarded and the vertical increment was resampled. Typically, ten 1-pint bottles were collected for each suspended-sediment sample, although in some cases, two or more vertical increments composed a single bottle following methods described by Edwards and Glysson (1999). Following collection, samples were transported to the USGS sediment laboratory in Iowa City, Iowa, where they were composited into a single sample and analyzed for SSC and particle-size fraction according to Guy (1969).

Most SSC samples were collected using a D–74 rigid bottle sampler suspended from a bridge during nonwadeable flows or a DH–48 hand-held sampler during wadeable flows. When river depths exceeded 15 ft, a D–96 collapsible-bag sampler was used to collect the sample (Davis, 2005). Two sites (16 and 17) initially could not be sampled during high flows because culverts constricted streamflow and forced the sampler into the culvert. Sites 16 and 17 were configured with a cable-pulley system (fig. 5A) to allow sampling during high flows. For site 2 in northeastern Minnesota, the road crossing used to collect samples was washed out during record flooding in June 2012 (Czuba and others, 2012), so the site was configured with a Tacoma bank-operated cableway (BOC) (Rickly Hydrological Co., Inc., 2015) (fig. 5*B*). Tacoma BOC systems facilitate deployment of heavy samplers in the absence of a sampling platform (for example, bridges).

Bedload

The lower 4 in. of the sampled water column near the streambed commonly are referred to as the unsampled zone (Edwards and Glysson, 1999) because isokinetic samplers (Davis, 2005) are designed to prevent sampling near the streambed. The unsampled zone is where larger particles move by rolling, sliding, or bouncing along the streambed. The material in the unsampled zone, called bedload, is rarely sampled because of the difficulty and uncertainty associated with collecting representative samples. For this report, the term “bedload” refers to the collection of suspended particles in the unsampled zone and also is used to describe the

Table 1. Sediment sampling sites in selected basins in Minnesota.

[USGS, U.S. Geological Survey; NAD 83, North American Datum of 1983; mi², square mile; Minn.,Minnesota; C, continuous streamflow available; P, partial streamflow available; Ave., avenue; SW, southwest; --, no streamgage available; NW, northwest; NGVD 29, National Geodetic Vertical Datum of 1929; NAVD 88, North American Vertical Datum of 1988]

Site number (figs. 1–4)	USGS station number	Station name	Latitude (north) (NAD 83)	Longitude (west) (NAD 83)	Gage elevation above vertical datum (feet)	Drainage area (mi²)	Sampling period	Type of streamflow record	Number of suspended-sediment samples	Number of bedload samples
1	04015330[a]	Knife River near Two Harbors, Minn.	46°56′49″	91°47′32″	640[c]	84	05/2007–09/2013	C	52	9
2	04015340[b]	Sucker River near Palmers, Minn.	46°55′50″	91°51′29″	10[c]	39	05/2012–09/2013	C	21	7
3	04020000[b]	Swan River near Toivola, Minn.	47°15′01″	92°48′38″	35[c]	239	08/2012–09/2013	P	21	4
4	05062500[a]	Wild Rice River at Twin Valley, Minn.	47°16′00″	96°14′40″	1,008.2[d]	934	02/2007–08/2013	C	50	15
5	05063000[b]	Wild Rice River near Ada, Minn.	47°15′50″	96°30′00″	890.1[c]	1,100	03/2007–08/2013	C	48	20
6	05131500[a]	Little Fork River at Littlefork, Minn.	48°23′45″	93°32′57″	1,083.6[c]	1,680	05/2007–08/2013	C	55	16
7	05131870[b]	Big Fork River near Craigsville, Minn.	47°57′13″	93°45′16″	30.0[c]	1,020	03/2012–08/2013	P	22	16
8	05245100[a]	Long Prairie River at Long Prairie, Minn.	45°58′30″	94°51′56″	1,281.7[d]	434	03/2012–08/2013	C	22	20
9	05278930[b]	Buffalo Creek near Glencoe, Minn.	44°45′50″	94°05′27″	971.0[c]	373	05/2007–07/2013	P	66	18
10	05279400[b]	South Fork Crow River at Delano, Minn.	45°02′31″	93°47′22″	900.8[c]	1,269	05/2012–08/2013	C	22	20
11	05294000[a]	Pomme De Terre River at Appleton, Minn.	45°12′10″	96°01′20″	978.6[c]	905	03/2012–07/2013	C	21	19
12	05320500[a]	Le Sueur River near Rapidan, Minn.	41°06′35″	94°02′30″	775.8[d]	1,110	03/2012–06/2013	C	27	21
13	05325000[a]	Minnesota River at Mankato, Minn.	44°10′08″	94°00′11″	747.9[d]	14,900	01/2007–08/2013	C	53	21
14	05330000[a]	Minnesota River near Jordan, Minn.	44°41′35″	93°38′30″	690.0[d]	16,200	03/2012–11/2013	C	17	13
15	05330920[a]	Minnesota River at Fort Snelling State Park, Minn.	45°52′13″	93°11′32″	0[c]	16,900	03/2011–11/2013	C	24	11

Table 1. Sediment sampling sites in selected basins in Minnesota.—Continued

[USGS, U.S. Geological Survey; NAD 83, North American Datum of 1983; mi², square mile; Minn.,Minnesota; C, continuous streamflow available; P, partial streamflow available; Ave., avenue; SW, southwest; --, no streamgage available; NW, northwest; NGVD 29, National Geodetic Vertical Datum of 1929; NAVD 88, North American Vertical Datum of 1988]

Site number (figs. 1–4)	USGS station number	Station name	Latitude (north) (NAD 83)	Longitude (west) (NAD 83)	Gage elevation above vertical datum (feet)	Drainage area (mi²)	Sampling period	Type of stream-flow record	Number of suspended-sediment samples	Number of bedload samples
16	05372983	Cascade Creek at 45th Ave. SW in Rochester, Minn.	44°01′02″	92°31′56″	15.0[c]	18	03/2012–07/2013	--	22	23
17	0537298550	Cascade Creek at 35th Ave. NW in Rochester, Minn.	44°01′18″	92°30′57″	15.0[c]	19	03/2012–07/2013	--	22	13
18	05374900[b]	Zumbro River at Kellogg, Minn.	44°18′43″	92°00′14″	669.5[d]	1,400	05/2007–08/2013	C	56	21
19	05376000	North Fork Whitewater River near Elba, Minn.	44°06′34″	92°03′20″	15.0[c]	15	03/2012–08/2013	--	21	11
20	05376800[b]	Whitewater River near Beaver, Minn.	44°09′03″	92°00′18″	694.0[d]	694	03/2012–08/2013	C	20	22

[a]U.S. Geological Survey streamgage.

[b]Minnesota Department of Natural Resources streamgage.

[c]Vertical datum is assumed, NGVD 29 or NAVD 88 datum elevation not established.

[d]Vertical datum in NGVD 29.

[e]Vertical datum in NAVD 88.

Figure 5. Configurations for collection of suspended-sediment concentrations at select sites. *A*, Cable-pulley deployment system at Cascade Creek at 45th Ave SW in Rochester, Minnesota (site 16), and *B*, Tacoma bank-operated-cableway at Sucker River near Palmers, Minnesota (site 2).

magnitude of annual sediment loads, in tons per year, attributed to the movement of suspended particles in the unsampled zone. In Minnesota, little information exists regarding bedload and bedload contribution to total sediment loads. A study completed in Wisconsin determined that 50 to 60 percent of the total sediment load being discharged into the Mississippi River from the Chippewa River (not shown) was composed of bedload (Rose, 1992). The Chippewa River is a sand-dominated channel and is representative of many rivers in southeastern Minnesota; however, the channel bed material composition of the Chippewa River is markedly different than rivers outside southeastern Minnesota, which vary in material composition from boulder, cobble, sand, silt, and clay-rich systems.

Most bedload samples were collected in 2012 and 2013; however, some bedload samples were collected before 2012 as part of other sediment studies. For example, bedload samples were collected beginning in 2011 at site 15 in the lower Minnesota River Basin (fig. 1). Two types of USGS-approved pressure-differential bag samplers, the Helley-Smith and the BL-84 sampler (Davis, 2005), were used to collect bedload samples. Mesh pore sizes of bags used to collect bedload samples varied from 0.112 to 0.5 mm depending on site conditions. The single equal-width-increment method of collecting bedload samples according to Edwards and Glysson (1999) was used at all sites and bedload samples were collected concurrently with suspended-sediment samples. Collection of bedload samples entailed starting at one bank and collecting one sample at 20 evenly spaced vertical increments in the stream transect. Bag samples were transferred into 3-L plastic rigid containers and composited for analysis. Bedload samples were analyzed for nine particle-size distributions (ranging from 0.0625 to 16 mm) using the dry-sieve method (Guy, 1969) at the University of Minnesota Civil Engineering Department by USGS Minnesota Water Science Center (WSC) staff. The general procedure for bedload particle-size distribution analysis consisted of (1) air or oven drying the collected bedload sample(s) at 80° C, (2) weighing the total sample, (3) nesting the desired number of sediment sieves and adding the sediment material to the top sieve, (4) placing the nested sieves and sediment material in a Ro-tap sieve shaker and shaking the sample for 20 minutes, (5) disassembling the nested sieves and weighing each sieve to determine the individual size-fraction weights, (6) calculating the percentages of each size-class from the ratio of individual size-class weights to total sample weight, and (7) comparing the difference in weights of the total sample with the sum of the individual size-class weights to determine sample loss or gain during the analysis. Quality-control measures included (1) reanalyzing a sample if there was more than a 3-percent difference between the initial and final weight of the sample and (2) reanalyzing one sample in 20 to ensure less than 5-percent difference in weight in any size class is being achieved (Julie Nason, U.S. Geological Survey, Iowa Sediment Laboratory, oral commun., various dates).

No specific sampler or bag worked mutually well for all sites. Despite numerous attempts to collect bedload samples at site 20 in southeastern Minnesota using bags of varying pore sizes, bedload samplers were unable to collect representative samples of bedload when streamflows exceeded approximately 500 cubic feet per second (ft^3/s). The authors for this study hypothesized that high concentrations of silt- and sand-sized particles blocked the pores and prevented water from flowing through the bag. This hypothesis is supported by onsite observations of water exiting the orifice of the bedload sampler upon extraction of the sampler at the water surface during high streamflows.

Streamflow Data

Instantaneous and daily mean streamflow data were obtained from existing USGS or MNDNR streamgages to determine bankfull streamflow, develop relations between SSC and streamflow and between bedload and streamflow, and calculate annual sediment loads. The USGS and MNDNR determine streamflows at streamgages by use of the rating-curve method (the relation between streamgage height and streamflow) outlined in Rantz and others (1982). Rating curves at streamgages are developed by relating gage height to streamflow for a range of measured streamflows. For sites used in this study (table 1), nine were USGS continuous-record streamgages (sites 1, 4, 6, 8, 11–15) and eight (sites 2, 3, 5, 7, 9, 10, 18, and 20) were MNDNR streamgages. Five MNDNR streamgages (sites 2, 5, 10, 18, and 20) were year-round continuous streamgages and three (sites 3, 7, and 9) were decommissioned during the winter months (Lisa Pearson, Minnesota Department of Natural Resources, oral commun., various dates) and provided partial records during the open water season. Real-time data for continuous-record streamgages are updated hourly and preliminary data are available at http://waterdata.usgs.gov/nwis/current for USGS streamgages (U.S. Geological Survey, 2016) or at http://www.dnr.state.mn.us/waters/csg/index.html for MNDNR streamgages (Minnesota Department of Natural Resources, 2014). The data are finalized and published following the end of the water year (September 30) for USGS streamgages (U.S. Geological Survey, 2016) and calendar year (December 31) for MNDNR streamgages (Minnesota Department of Natural Resources, 2014).

For site 7 in northern Minnesota, gaps in the streamflow record were estimated by extending streamflow from a nearby USGS streamgage 05132000 (Big Fork River at Big Falls, Minn., not shown) using the MOVE-1 (maintenance of variance extension, type 1) package developed by Hirsch (1982) for S-plus statistical software (TIBCO® Software Inc., 2010). The MOVE-1 method improves streamflow estimates at partial-record sites by accounting for the loss of variance associated with ordinary least squares regression (Hirsch, 1982). The correlation between the partial record and the USGS continuous-record streamgage for site 7 had a coefficient of

determination (R^2) of 0.99 and was used to generate daily mean streamflows during the time period for which streamflow data were not available. For sites 3 and 9, a partial streamflow record was available; however, a nearby year-round continuous-record streamgage was not available for computing daily mean streamflows at the partial-record site using the MOVE-1 method. For sites 16, 17, and 19, streamgages were not available onsite. For site 19 in southeastern Minnesota, the MNDNR had decommissioned the streamgage in 2012 for a programmed redeployment of the streamgage downstream. For sites with no streamflow records, instantaneous streamflow for the time the sediment samples were collected was estimated using rating curves developed from periodic onsite measured streamflows and measurements of water levels from an established point with an assumed vertical datum (table 1).

Bankfull Streamflow Determination

Bankfull elevations were determined using methods outlined by Leopold and others (1964) and Rosgen (1994, 1996). A combination of field elevation surveys and bankfull field indicators, such as change in slope, changes in vegetation, stain lines, top of point bars, changes in bank material, or bank undercuts along streambanks were used to establish the point on the bank for bankfull stage at each site. For sites with continuous-record streamgages, bankfull elevations were extrapolated to the wire-weight gage height. Wire-weight gages are used to measure the elevation of the water-level surface (Sauer and Turnipseed, 2010). The relation between water-surface elevation (gage height) and streamflow was used to determine bankfull streamflow. Recurrence intervals were retrieved from USGS StreamStats program (U.S. Geological Survey, 2015) to confirm that the bankfull streamflow approximated the 1.5-year recurrence interval. For sites where recurrence intervals could not be computed because of sparse streamflow data (that is, sites 16 and 17), field indicators of bankfull stage were extrapolated to water levels measured from an established point, and bankfull streamflow was estimated using the developed rating curve. Bankfull streamflows for each site are presented in table 2.

Pfankuch Stability Rating

Pfankuch stream channel stability surveys (Pfankuch, 1975) were completed at each site by MNDNR or USGS field staff using the Rosgen (2007) modified Pfankuch stability rating assessment form. Pfankuch stability ratings of good/fair and poor were used to delineate data for DSRC model development. The Pfankuch stability rating form completed for site 11 is presented in figure 6 as an example, and Pfankuch stability ratings are available for all sites in appendix table 1–1.

Determining Suspended-Sediment Concentration and Bedload at Bankfull Streamflow

The number of samples used to determine SSC and bedload at bankfull streamflow ranged from 2 samples at site 3 to 16 samples at site 12. Samples selected to determine SSC and bedload at bankfull streamflow were limited to samples collected within the range of one-half to 2 times bankfull streamflow. Samples within this range of streamflow were collected during snowmelt runoff or summer precipitation events and included bankfull stage for at least one sampling event at each site. Based on availability, equal numbers of samples on the ascending and descending limb of the hydrograph were used to minimize disproportionate effects of individual samples from the effects of hysteresis. Once the samples were selected, SSC and bedload were paired with their corresponding instantaneous streamflows, and the mean values of SSC, bedload, and streamflow were calculated. Ratio estimators for SSC and bedload at bankfull streamflow were calculated for each site by dividing each mean SSC and bedload value by the corresponding mean instantaneous streamflow. Site-specific SSC and bedload values at bankfull streamflow were determined by multiplying the ratio estimator and the bankfull streamflow at that site. Determination of the ratio estimator and subsequent determination of SSC at bankfull streamflow using six samples at the Big Fork River near Craigsville, Minn. (site 7), in northern Minnesota is shown in table 3.

Following the initial determination of SSC and bedload at the bankfull streamflow, an additional step was incorporated to remove bias from the estimates using the Jackknife statistic (Quenouille, 1956; Hinkley, 1983; Tukey, 1986; Abdi and Williams, 2010). The Jackknife statistic is a resampling procedure (also referred to as "leave one out procedure") used as a cross-validation tool to estimate and remove bias from estimators. For this process, the estimators are the values of SSC and bedload at bankfull streamflow. The jackknife procedure uses discrete estimates of SSC and bedload and iteratively drops out one sample at a time from the total number of samples and calculates a new mean for each iteration. The new mean of the "leave one out" discrete samples is referred to as a partial estimate. The number of partial estimates is equal to the number of samples used in the calculation of SSC or bedload at bankfull streamflow. Using the partial estimates, a new value, called a pseudo value, is calculated by subtracting the individual partial estimates from the whole sample estimate. The equation (Hinkley, 1983) for computing the pseudo values is

$$T_n = NT - (N - 1)\, T_p \qquad (5)$$

where

T_n is the pseudo value in milligrams per liter or tons per day,

N is the number of samples,

T is whole sample estimate of SSC in milligrams per liter, or bedload in tons per day, obtained from the ratio estimator, and

T_p is the partial estimate.

The jackknife estimate is then calculated as the mean of the pseudo values using the following equation (Hinkley, 1983):

$$T_j = \frac{1}{n}\sum_{i=1}^{n} T_n, i \qquad (6)$$

where

T_j is the jackknife bias-free estimate of SSC or bedload at bankfull streamflow,

n is the number of samples, and

T_n is the pseudo value for each iteration i.

Determination of partial estimates, pseudo values, and the final jackknife bias-free estimate for site 7 in northern Minnesota are shown in table 4.

Table 2. Bankfull streamflow, Pfankuch stability rating, and Rosgen stream classifications for sediment sampling sites in Minnesota.

[USGS, U.S. Geological Survey; ft³/s; cubic foot per second; Minn., Minnesota; Ave., avenue; SW, southwest; NW, northwest; NGVD 29, National Geodetic Vertical Datum of 1929; NAVD 88, North American Vertical Datum of 1988]

Site number (figs. 1–4)	USGS station number	Station name	Bankfull streamflow (ft³/s)	Pfankuch[a] stability rating	Rosgen[b] Stream Classification
1	04015330[c]	Knife River near Two Harbors, Minn.	1,880	Fair	B2
2	04015340[d]	Sucker River near Palmers, Minn.	380	Poor	B2
3	04020000[d]	Swan River near Toivola, Minn.	1,230	Good	C6
4	05062500[c]	Wild Rice River at Twin Valley, Minn.	1,000	Fair	C5
5	05063000[d]	Wild Rice River near Ada, Minn.	1,560	Poor	F5
6	05131500[c]	Little Fork River at Littlefork, Minn.	6,900	Fair	F3
7	05131870[d]	Big Fork River near Craigsville, Minn.	1,970	Good	C6
8	05245100[c]	Long Prairie River at Long Prairie, Minn.	530	Fair	E5
9	05278930[d]	Buffalo Creek near Glencoe, Minn.	500	Fair	C4
10	05279400[d]	South Fork Crow River at Delano, Minn.	2,360	Poor	C5
11	05294000[c]	Pomme De Terre River at Appleton, Minn.	550	Good	C4
12	05320500[c]	Le Sueur River near Rapidan, Minn.	3,100	Poor	F4
13	05325000[c]	Minnesota River at Mankato, Minn.	12,330	Poor	F5
14	05330000[c]	Minnesota River near Jordan, Minn.	14,600	Poor	F4
15	05330920[c]	Minnesota River at Fort Snelling State Park, Minn.	28,500	Fair	C5
16	05372983[e]	Cascade Creek at 45th Ave. SW in Rochester, Minn.	150	Poor	F5
17	0537298550[e]	Cascade Creek at 35th Ave. NW in Rochester, Minn.	155	Poor	C4
18	05374900[d]	Zumbro River at Kellogg, Minn.	5,300	Poor	F5
19	05376000[e]	North Fork Whitewater River near Elba, Minn.	670	Good	C4
20	05376800[d]	Whitewater River near Beaver, Minn.	1,600	Poor	C5

[a]From Pfankuch, 1975.

[b]From Rosgen, 1994.

[c]U.S. Geological Survey streamgage.

[d]Minnesota Department of Natural Resources streamgage.

[e]Vertical datum is assumed, NGVD 29 or NAVD 1988 datum elevation not established.

USGS ID: 05294000

Worksheet 5-7. Pfankuch (1975) stream channel stability rating procedure, as modified by Rosgen (1996, 2001b).

Stream: Pomme De Terre River **Location:** Appleton, MN **Valley Type:** **Observers:** CAE/JTG **Date:** 9/29/14

Location	Key	Category	Excellent Description	Excellent Rating	Good Description	Good Rating	Fair Description	Fair Rating	Poor Description	Poor Rating
Upper banks	1	Landform slope	Bank slope gradient <30%.	2	Bank slope gradient 30–40%.	4	Bank slope gradient 40–60%.	6	Bank slope gradient > 60%.	8
	2	Mass erosion	No evidence of past or future mass erosion.	3	Infrequent. Mostly healed over. Low future potential.	6	Frequent or large, causing sediment nearly yearlong.	9	Frequent or large, causing sediment nearly yearlong OR imminent danger of same.	12
	3	Debris jam potential	Essentially absent from immediate channel area.	2	Present, but mostly small twigs and limbs.	4	Moderate to heavy amounts, mostly larger sizes.	6	Moderate to heavy amounts, predominantly larger sizes.	8
	4	Vegetative bank protection	> 90% plant density. Vigor and variety suggest a deep, dense soil-binding root mass.	3	70–90% density. Fewer species or less vigor suggest less dense or deep root mass.	6	50–70% density. Lower vigor and fewer species from a shallow, discontinuous root mass.	9	<50% density plus fewer species & less vigor indicating poor, discontinuous and shallow root mass.	12
Lower banks	5	Channel capacity	Bank heights sufficient to contain the bankfull stage. Width/depth ratio departure from reference width/depth ratio = 1.0. Bank-Height Ratio (BHR) = 1.0.	1	Bankfull stage is contained within banks. Width/depth ratio departure from reference width/depth ratio = 1.0–1.2. Bank-Height Ratio (BHR) = 1.0–1.1.	2	Bankfull stage is not contained. Width/depth ratio departure from reference width/depth ratio = 1.2–1.4. Bank-Height Ratio (BHR) = 1.1–1.3.	3	Bankfull stage is not contained; over-bank flows are common with flows less than bankfull. Width/depth ratio departure from reference width/depth ratio > 1.4. Bank-Height Ratio (BHR) > 1.3.	4
	6	Bank rock content	> 65% with large angular boulders. 12"+ common.	2	40–65%. Mostly boulders and small cobbles 6–12".	4	20–40%. Most in the 3–6" diameter class.	6	<20% rock fragments of gravel sizes, 1–3" or less.	8
	7	Obstructions to flow	Rocks and logs firmly imbedded. Flow pattern w/o cutting or deposition. Stable bed.	2	Some present causing erosive cross currents and minor pool filling. Obstructions fewer and less firm.	4	Moderately frequent, unstable obstructions move with high flows causing bank cutting and pool filling.	6	Frequent obstructions and deflectors cause bank erosion yearlong. Sediment traps full, channel migration occurring.	8
	8	Cutting	Little or none. Infrequent raw banks <6".	4	Some, intermittently at outcurves and constrictions. Raw banks may be up to 12".	8	Significant. Cuts 12–24" high. Root mat overhangs and sloughing evident.	12	Almost continuous cuts, some over 24" high. Failure of overhangs frequent.	16
	9	Deposition	Little or no enlargement of channel or point bars.	4	Some new bar increase, mostly from coarse gravel.	8	Moderate deposition of new gravel and coarse sand on old and some new bars.	12	Extensive deposit of predominantly fine particles. Accelerated bar development.	16
Bottom	10	Rock angularity	Sharp edges and corners. Plane surfaces rough.	1	Rounded corners and edges. Surfaces smooth and flat.	2	Corners and edges well rounded in 2 dimensions.	3	Well rounded in all dimensions, surfaces smooth.	4
	11	Brightness	Surfaces dull, dark or stained. Generally not bright.	1	Mostly dull, but may have <35% bright surfaces.	2	Mixture dull and bright, i.e., 35–65% mixture range.	3	Predominantly bright, > 65%, exposed or scoured surfaces.	4
	12	Consolidation of particles	Assorted sizes tightly packed or overlapping.	2	Moderately packed with some overlapping.	4	Mostly loose assortment with no apparent overlap.	8	No packing evident. Loose assortment, easily moved.	8
	13	Bottom size distribution	No size change evident. Stable material 60–100%.	4	Distribution shift light. Stable material 50–80%.	8	Moderate change in sizes. Stable materials 20–50%.	12	Marked distribution change. Stable materials 0–20%.	16
	14	Scouring and deposition	<5% of bottom affected by scour or deposition.	8	5–30% affected. Scour at constrictions and where grades steepen. Some deposition in pools.	12	30–50% affected. Deposits and scour at obstructions, constrictions and bends. Some filling of pools.	18	More than 50% of the bottom in a state of flux or change nearly yearlong.	24
	15	Aquatic vegetation	Abundant growth moss-like, dark green perennial. In swift water, too.	1	Common. Algae forms in low velocity and pool areas. Moss here, too.	2	Present but spotty, mostly in backwater. Seasonal algae growth makes rocks slick.	3	Perennial types scarce or absent. Yellow-green, short-term bloom may be present.	4
			Excellent total =	25	**Good total =**	24	**Fair total =**	3	**Poor total =**	0

Stream type	A1	A2	A3	A4	A5	A6	B1	B2	B3	B4	B5	B6	C1	C2	C3	C4	C5	C6	D3	D4	D5	D6
Good (Stable)	38-43	38-43	54-90	60-96	60-96	50-80	38-45	38-45	40-60	40-64	48-68	40-60	38-50	38-50	60-85	70-90	70-90	60-85	85-107	85-107	85-107	67-9
Fair (Mod. unstable)	44-47	44-47	91-129	96-132	96-142	81-110	46-56	46-56	61-78	65-84	69-88	61-78	51-61	51-61	86-105	91-110	91-110	86-105	108-132	108-132	108-132	99-12
Poor (Unstable)	48+	48+	130+	133+	143+	111+	59+	59+	79+	85+	89+	79+	62+	62+	106+	111+	111+	106+	133+	133+	133+	126

Stream type	DA3	DA4	DA5	DA6	E3	E4	E5	E6	F1	F2	F3	F4	F5	F6	G1	G2	G3	G4	G5	G6
Good (Stable)	40-63	40-63	40-63	40-63	40-63	50-75	50-75	40-63	60-85	60-85	85-110	85-110	90-115	80-95	40-60	40-60	85-107	85-107	90-112	85-107
Fair (Mod. unstable)	64-86	64-86	64-86	64-86	64-86	76-96	76-96	64-86	86-105	86-105	111-125	111-125	116-130	96-110	61-78	61-78	108-120	108-120	113-125	108-120
Poor (Unstable)	87+	87+	87+	87+	87+	97+	97+	87+	106+	106+	126+	126+	131+	111+	79+	79+	121+	121+	126+	121+

*Rating should be adjusted to potential stream type, not existing.

Grand total =	52
Existing stream type =	C3
***Potential stream type =**	
Modified channel stability rating =	Good

Copyright © 2006 Wildland Hydrology

WARSSS page 5-46

Figure 6. Pfankuch (1975) stream channel stability rating assessment for Pomme De Terre River at Appleton, Minnesota, U.S. Geological Survey station number 05294000. (Form used with permission from Wildland Hydrology.)

Table 3. Determination of ratio estimator and suspended-sediment concentration at bankfull streamflow for the Big Fork River near Craigsville, Minnesota (site 7; U.S. Geological Survey station number 05131870).

[SSC, suspended-sediment concentration; mg/L, milligram per liter; ft^3/s, cubic foot per second; Minn., Minesota]

Date	Hydrograph position	SSC (mg/L)	Streamflow (ft^3/s)
Big Fork River near Craigsville, Minn., U.S. Geological Survey station number 05131870			
4/19/2012	rising	74	2,420
4/19/2012	rising	59	2,410
4/27/2012	falling	21	1,980
5/17/2013	falling	21	1,800
4/18/2012	rising	41	1,780
5/3/2012	falling	19	1,310
	Mean	**39.2**	**1,950**
		Ratio estimator	**0.0201**
		Bankfull streamflow	**1,970 ft^3/s**
		SSC at bankfull	**40 mg/L**

Table 4. Determination of partial estimates, pseudo values, and final jackknife estimate of suspended-sediment concentration at bankfull streamflow for the Big Fork River near Craigsville, Minnesota (site 7; U.S. Geological Survey station number 05131870).

[ft^3/s, cubic foot per second; SSC, suspended-sediment concentration; mg/L, milligram per liter]

Bankfull steamflow (ft^3/s)	Measured SSC (mg/L)	Instantaneous streamflow (ft^3/s)	Partial SSC estimate (mg/L)	Pseudo SSC value (mg/L)	Jackknife bias-free SSC estimate (mg/L)	Jackknife estimate of bias (mg/L)
1,970	74	2,419	34	67	39	0.25
	59	2,410	37	51		
	21	1,981	43	21		
	21	1,806	43	21		
	41	1,782	39	45		
	19	1,310	41	33		
Mean	**39**	**1,951**	**40**	**39**		

Data Analysis

Suspended-sediment concentrations, bedload, and instantaneous and daily mean streamflows were formatted for analysis using S-plus statistical software (TIBCO® Software Inc., 2010) and the R statistical environment (R Development Core Team, 2011). Summary statistics, Kendall's tau analysis, Nash-Sutcliffe Efficiencies (NSE), weighted nonlinear regression analyses, simple linear regression analyses, model biases, and R-LOADEST (Runkel and others, 2004; Cohn and others, 1989; R Development Core Team, 2011) load estimates composed the analyses. Summary statistics included the minimum, maximum, mean, median, total numbers of samples, and standard deviation. The Pagosa Springs and Minnesota DSRC models were evaluated using multiple measures of goodness-of-fit that included the following: (1) proximity of the model(s) fitted line to the 95-percent confidence intervals of the site-specific model, (2) NSE values, (3) estimates of model biases, and (4) deviations between modeled (predicted) and measured annual sediment loads.

Kendall's tau analyses (Kendall, 1938, 1975) were used to test for significance and measure the strength of the relations between SSC and streamflow and between bedload and streamflow at each site; p-values less than 0.05 indicated

statistically significant monotonic relations. Data from sites without significant relations among variables (*p*-values of 0.05 or greater) were not used to develop models. Kendall's tau measures the strength of nonlinear relations (Helsel and Hirsch, 2002). Nonlinear relations are characterized by response variable(s) increasing (or decreasing) at a nonlinear rate as the explanatory variable increases. In this study, SSC and bedload are response variables, and streamflow is the explanatory variable.

Kendall's tau correlation analysis is applicable for water-quality data like SSC and bedload, which rarely follows a linear relation. Unlike parametric statistical analyses, Kendall's tau does not require the assumption that data are normally distributed; therefore, Kendall's tau works well with SSC and bedload data, which rarely are normally distributed. Furthermore, Kendall's tau is a rank-based procedure that is resistant to the effects of small numbers of unusual values (Helsel and Hirsch, 2002). The measure of strength is scaled to be in the range of -1 to 1, and a value close to 0 indicates that no relation exists between the two variables. A positive tau correlation value indicates that the response variable is increasing as the explanatory variable increases, whereas a negative tau correlation value indicates that the response variable is decreasing as the explanatory variable increases. Tau correlation values approaching values of 1 or -1 indicate a strong monotonic relation between the two variables. Information from the Kendall's tau analysis such as the *p*-value and the tau correlation value were used to select data from sites with significant relations for use in DSRC model development.

Data collected from rivers in Minnesota were used to develop DSRCs similar to methods described in Rosgen (2010) using data collected in Colorado. Minnesota DSRC model prediction efficiency was optimized using a weighted parameter method. More than 600 dimensionless ratio values were calculated using available SSCs, bedload, and streamflow data. Dimensionless ratio values were evaluated and delineated according to Pfankuch stream stability categories of good/fair and poor (Pfankuch, 1975), and selected dimensionless ratio values were used to develop four Minnesota-based DSRC models. Data from sites identified through the Kendall's tau correlation analyses with no relation (that is, *p*-values of 0.05 or greater) between SSC and streamflow or between bedload and streamflow were not used in the development of Minnesota DSRC models.

A weighted nonlinear least squares regression approach (nls function) was used for the analyses in the R statistical environment (R Development Core Team, 2011). Weighted least squares were used to generate estimates of model parameters that account for observed heteroscedastic variance of the residuals (residuals increasing as streamflow increased) (Chaterjee and others, 2000). Weights were estimated using ordinary nonlinear least squares (nls function without weights), and the R statistical environment computed the relational slopes (B_2) between response (SSC and bedload) and explanatory (streamflow) variables. Weights were calculated using the following equation:

$$Wi = 1 / Qi^{B_2} \tag{7}$$

where

W_i is the weight applied to each measured value,
Q_i is streamflow in cubic feet per second, and
B_2 is the estimated slope between response and explanatory variables.

Weights are used to assign each sample a proportional effect on parameter estimates (Chaterjee and others, 2000). Using weighted least squares, samples with less error (smaller residuals) are assigned more weight than samples with greater error (larger residuals). Using ordinary nonlinear least squares regression (without weights) for this dataset would treat all data equally, giving samples with greater error disproportionate effect and giving samples with less error too little effect. As part of model development, a framework was incorporated so that the values of the model coefficients (B_1) and numerical constant ($1 - B_1$) ensured that the fitted trendline of the model would pass through the point of interception of the calculated values of SSC and bedload at bankfull with bankfull streamflow. The proposed form of DSRC models for Minnesota was

$$y_i = (1 - B_1) + B_1 X_i^{B_2} + \varepsilon_i \tag{8}$$

where

y_i is a dimensionless ratio value of SSC or bedload,
$(1 - B_1)$ is the intercept determined from the data,
B_1 is a coefficient determined from the data,
X_i is a dimensionless ratio value of streamflow,
B_2 is the slope determined from the data, and
ε_i is the random error representing the discrepancy in the approximation accounting for the failure of the model to fit the data exactly.

The intercept, $(1 - B_1)$ and coefficient, B_1, are constructed so that when the model(s) dimensionless output value is back transformed into dimensional form, the predicted value of SSC or bedload at the corresponding bankfull streamflow using the model will closely match the estimated SSC and bedload at bankfull streamflow.

The site-specific regression models represent the relations between SSC and streamflow and between bedload and streamflow and may be linear, nonlinear, and subject to transformation (for example, log normal or log 10) to make the data normally distributed before developing the models. Site-specific simple linear regression (SLR) models were developed for each site for SSC and bedload for use in evaluating the goodness-of-fit of Minnesota and Pagosa Springs DSRC models. For this study, SSC and bedload were the response variables, and streamflow was the explanatory variable. The site-specific SLR models were used to construct reference trendlines from which to evaluate the goodness-of-fit

of the Minnesota and Pagosa Springs DSRC models. The SLR method was used because it minimizes the sum of squared vertical distances (residuals) between the observed values of the response variable and the calculated (fitted values) values from the linear approximation. For SLR to produce a usable model, assumptions are that the two variables are related linearly, that the variance of the residuals are constant (homoscedastic), and that the residuals are distributed normally (Helsel and Hirsch, 2002). These assumptions usually are violated by measured water data, so the data typically are transformed to logarithmic values to satisfy these assumptions. For this study, the data indicated that the residuals for SSCs were not distributed normally; therefore, the data were transformed using a logarithmic base 10 transformation. Conversely, the bedload data did not indicate non-normality in the distribution of the residuals, or did not indicate improvement in the model results from transforming the data; thus, bedload data were not transformed prior to model development. The SLR model predicts values of a response variable, SSC, in milligrams per liter, or bedload, in tons per day, based on a single explanatory variable of streamflow using the following form of the model:

$$y_i = B_0 + B_1 x_1 + \varepsilon_i , \qquad i = 1, 2, \ldots . n \tag{9}$$

where

- y_i is the *i*th observation of the response variable, SSC in milligrams per liter, or bedload in tons per day;
- x_i is the *i*th observation of the explanatory variable, streamflow in cubic feet per second;
- B_0 is the y-intercept;
- B_1 is the slope;
- ε_i is the random error or residual for the *i*th observation; and
- n is the sample size.

For simple linear regression models for SSCs, the model results were corrected for bias introduced (because of the logarithmic transformations) using the Duan (1983) bias-correction factor (BCF). Regression-computed SSC values used to develop the reference trendlines were corrected for bias by multiplying the retransformed SSC value by the BCF (Duan, 1983). For SLR models for bedload, the model results did not require a BCF correction because the bedload data were not transformed prior to model development.

Nash-Sutcliffe Efficiency values (Nash and Sutcliffe, 1970) were used to evaluate the effectiveness of Pagosa Springs and Minnesota DSRC models to approximate measured SSCs and bedload values. The NSE value is calculated using the measured values of the sampled data, modeled values, and the mean of the measured values according to the following equation:

$$NSE = 1 - \frac{\sum_{i=1}^{T} \left(Xo,i - Xm,i \right)^2}{\sum_{i=1}^{T} \left(Xo,i - Xmean \right)^2} \tag{10}$$

where

- NSE is the Nash-Sutcliffe Efficiency value,
- T is the number of observations used,
- Xo,i is the measured (observed) value for each observation *i* (SSC in milligrams per liter or bedload, in tons per day),
- Xm,i is the modeled value for each observation *i* (SSC in milligrams per liter or bedload in tons per day), and
- $Xmean$ is the mean of the measured values (SSC in milligrams per liter or bedload in tons per day).

Nash-Sutcliffe Efficiency values can range from negative infinity to 1. An NSE value of 1 indicates that the model matches the observed values exactly, an NSE value of 0 indicates that the model is predicting values that are no better than the mean of the measured values, and negative values of NSE indicates that the mean of the measured values is better than the model at approximating individual measured values. In general, models are considered to be predictive if the NSE value is greater than 0.20 (Jenkins, 2015).

Potential sources of systematic and random errors should be identified when developing models (McCuen and others, 2006). Systematic errors introduce biases in the data, whereas random errors may be associated with unusually high or low values (sample outliers). Positive systematic biases cause models to overestimate measured values, and negative systematic biases cause models to underestimate measured values. Biases are estimated using the mean error, where the error is the difference between the predicted and measured values. Model bias ($\bar{e}$) has the same units as the sampled data and is computed using the following equation:

$$\bar{e} = \frac{1}{n} \Sigma_{i=1}^{n} \left(\hat{Y}_i - Y_i \right) \tag{11}$$

where

- $\bar{e}$ is model bias in the same units as the sampled data,
- n is the sample size,
- $\hat{Y}_i$ is the predicted value, and
- Y_i is the measured value.

Bias typically is reported in relative terms (R_b), which is the ratio of the bias to the mean of the measured values and is computed by

$$R_b = 100 \frac{\bar{e}}{\bar{y}} \tag{12}$$

where

R_b is relative bias in percent,

$\bar{e}$ is model bias in the same units as the sampled data, and

$\bar{y}$ is the mean value of the measured values.

A relative bias greater than 5 percent is considered to be substantial (McCuen and others, 2006). Relative biases were computed to assess how model biases affected the ability of the models to approximate measured values. Outliers represent random errors and may result from mistakes associated with data collection or natural anomalies that do not match the rest of the collected data. In this study, a total of 18 outliers out of 664 SSC and bedload samples were identified and removed during development of DSRC models because of unusually high percentages of sand (for SSC samples) or because of unusually high mass (for bedload samples) in the sample.

Annual sediment loads of SSC and bedload calculated from the measured data were compared to loads estimated using Pagosa Springs and Minnesota DSRCs. A rating-curve model using the R-LOADEST package (available at: https://github.com/USGS-R/rloadest), which is an R implementation of the LOAD ESTimator (LOADEST) program of Runkel and others (2004), was used to compute annual suspended-sediment load (SSL), annual bedload, and 95-percent prediction intervals for the measured data using the R statistical environment. R-LOADEST is based on the rating-curve method (Runkel and others, 2004; Cohn and others, 1989; Cohn and others, 1992; Crawford, 1991) that uses regression analysis to estimate constituent loads in relation to explanatory variables; typical explanatory variables include streamflow, time, and a seasonal component. Development of the rating-curve model for SSC and streamflow followed methods described in Ellison and others (2014). For this report, annual SSL and annual bedload calculated from the measured (observed) data, using R-LOADEST package, are referred to as measured annual SSL and measured annual bedload. In this study, streamflow was the only explanatory variable used in the regression functions developed to compare annual sediment loads. Output from R-LOADEST does not represent the total annual sediment load at each site because this study's evaluation of DSRC models required that streamflow values be restricted to not exceed twice the bankfull streamflow. For the Pagosa Springs and Minnesota DSRC models, daily values of SSC were computed and SSLs were estimated using the following equation (Porterfield, 1972):

$$Q_s = Q_w \times C_s \times K \tag{13}$$

where

Q_s is the suspended-sediment load, in tons (English short tons) per day,

Q_w is the daily mean streamflow, in cubic feet per second,

C_s is SSC, in milligrams per liter, and

K is a coefficient (0.0027) to convert the units of measurement of streamflow and SSC into tons per day and assumes a specific gravity of 2.65 for sediment.

Annual sediment loads using the Pagosa Springs and Minnesota DSRC models for 2012 and 2013 were estimated by summing daily sediment loads for streamflow values as large as twice the bankfull streamflow value. Sites with only partial streamflow records could not be used to compare annual SSL and bedload among DSRC models.

Streamflow, Suspended-Sediment Concentrations, Bedload, and Particle-Size Fractions

This section describes streamflow, SSCs, bedload, and particle-size fractions for sites selected in this study (fig. 1). Suspended sediment and bedload samples were collected during a wide range of streamflow conditions (table 5). The frequency, timing, and magnitudes of streamflow and the timing of sediment sampling during the study period are illustrated in figure 7. Samples encompassed a full range of streamflows and included bankfull streamflow for at least one sampling event at each site. Flow-duration curves that show the percentage of time that streamflow was equaled or exceeded at each site, along with corresponding streamflow values associated with SSC samples, are shown in figure 8. The SSC, bedload, and streamflow data are available in the USGS National Water Information System at http://dx.doi.org/10.5066/F7P55KJN and appendix table 1–2.

In addition, summary statistics for streamflow, SSCs, suspended particle-size fractions, and bedload are presented for all 20 sites in table 6.

Table 5. Range of streamflow, suspended-sediment concentrations and bedload in samples collected from selected sites in Minnesota.

[ft^3/s, cubic foot per second; mg/L, milligram per liter; tons/day; tons per day; mm, millimeter; D100 is the largest particle, in mm, collected in the sample; Minn.; Minnesota; Ave., avenue; SW, southwest; NW, northwest]

Site number (figs. 1–4)	Station name	USGS station number	Range of streamflow sampled (ft^3/s)	Range of suspended-sediment concentration (mg/L)	Range of suspended-sediment concentration less than 0.0625 millimeters (percent)	Range of bedload discharge (tons/day)	D100 particle size (mm)
1	Knife River near Two Harbors, Minn.	04015330	4–11,100	2–926	31–99	0.03–556	11–68
2	Sucker River near Palmers, Minn.	04015340	3–400	1–94	66–93	0–73	2–137
3	Swan River near Toivola, Minn.	04020000	14–1,823	10–177	71–99	0.1–0.5	< 0.0625
4	Wild Rice River at Twin Valley, Minn.	05062500	26–4,920	3–775	21–98	1.6–65.2	4–18
5	Wild Rice River near Ada, Minn.	05063000	16–2,731	6–1,140	16–96	1.2–505	2–18
6	Little Fork River at Littlefork, Minn.	05131500	38–9,710	9–375	25–100	6.7–143	6–18
7	Big Fork River near Craigsville, Minn.	05131870	109–2,924	5–74	38–93	0.4–25.6	5–18
8	Long Prairie River at Long Prairie, Minn.	05245100	126–691	2–107	41–99	0.3–84.4	4–17
9	Buffalo Creek near Glencoe, Minn.	05278930	1–3,500	5–307	13–99	0.02–181.4	2–23
10	South Fork Crow River at Delano, Minn.	05279400	103–5,312	27–446	5–98	1.2–392.5	4–15
11	Pomme De Terre River at Appleton, Minn.	05294000	128–695	41–267	71–98	0.04–15.7	2–15
12	Le Sueur River near Rapidan, Minn.	05320500	43–8,150	34–1,843	32–98	1.6–490.3	5–65
13	Minnesota River at Mankato, Minn.	05325000	324–77,470	27–927	15–98	0.4–1,169.9	2–34
14	Minnesota River near Jordan, Minn.	05330000	900–18,300	33–794	68–91	0.1–13.1	3–10
15	Minnesota River at Fort Snelling State Park, Minn.	05330920	937–67,600	26–1,010	61–98	1.3–57.3	3–16
16	Cascade Creek at 45th Ave. SW in Rochester, Minn.	05372983	2–204	12–907	54–99	0.0–21.8	3–33
17	Cascade Creek at 35th Ave. NW in Rochester, Minn.	0537298550	1–175	28–808	57–100	0.0–4.0	5–6
18	Zumbro River at Kellogg, Minn.	05374900	420–7,035	17–1,250	2–96	50.2–1,183.6	6–23
19	North Fork Whitewater River near Elba, Minn.	05376000	37–975	11–640	23–97	0.1–102.5	2–30
20	Whitewater River near Beaver, Minn.	05376800	129–6,529	29–4,820	7–93	7.2–545.2	2–14

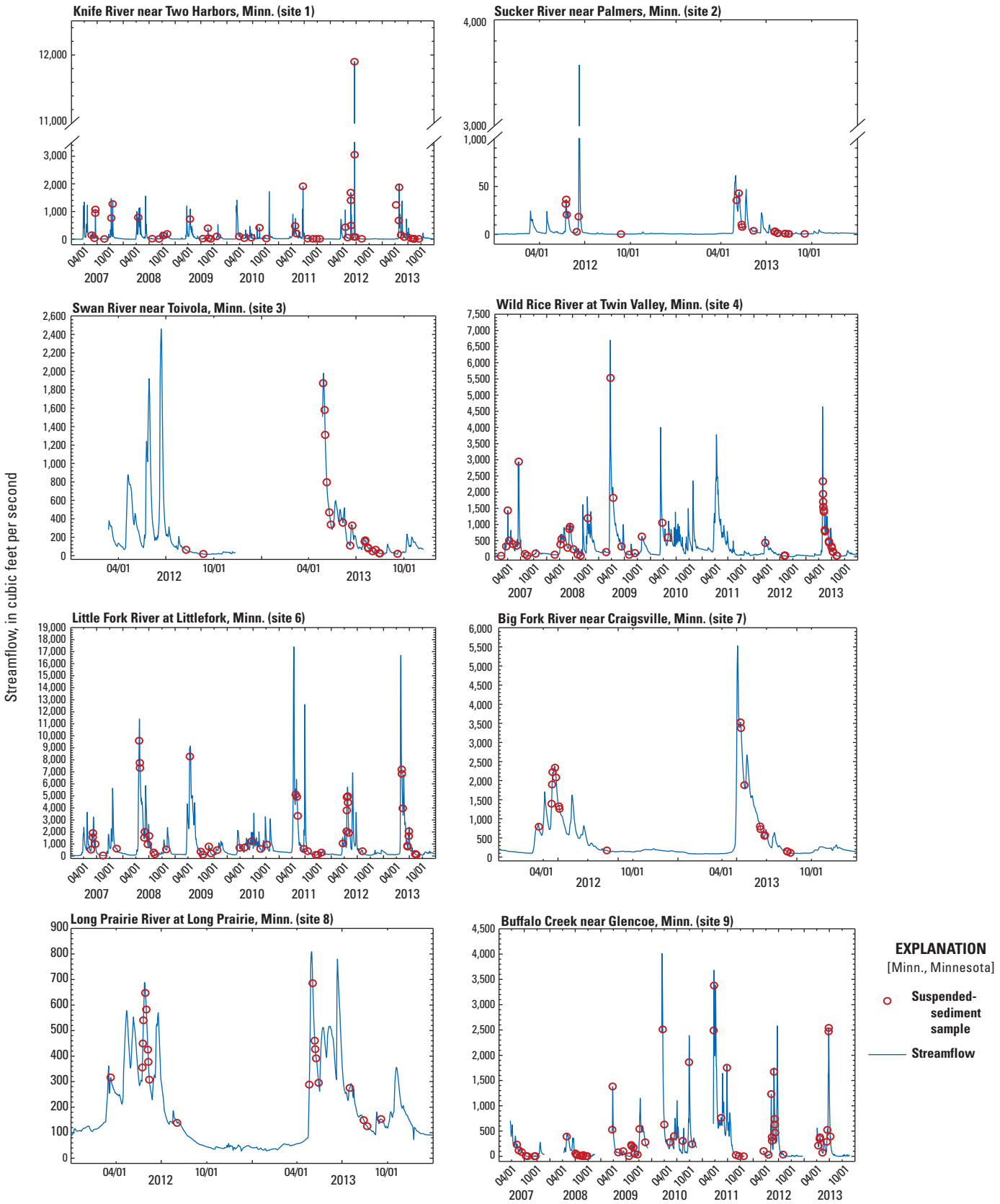

Figure 7. Hydrographs and dates of suspended-sediment samples for selected sites in Minnesota, 2007 through 2013.

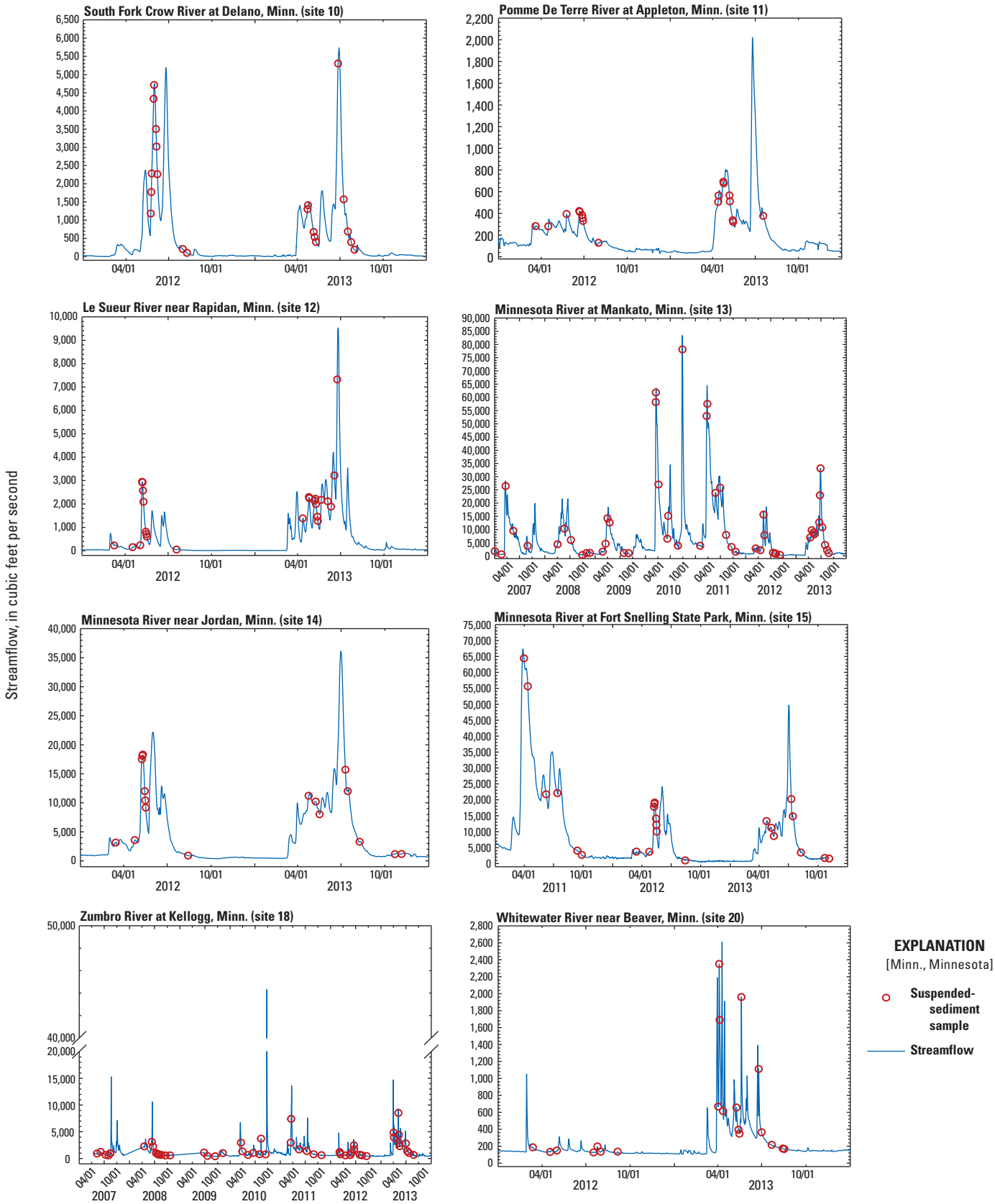

Figure 7. Hydrographs and dates of suspended-sediment samples for selected sites in Minnesota, 2007 through 2013.—Continued

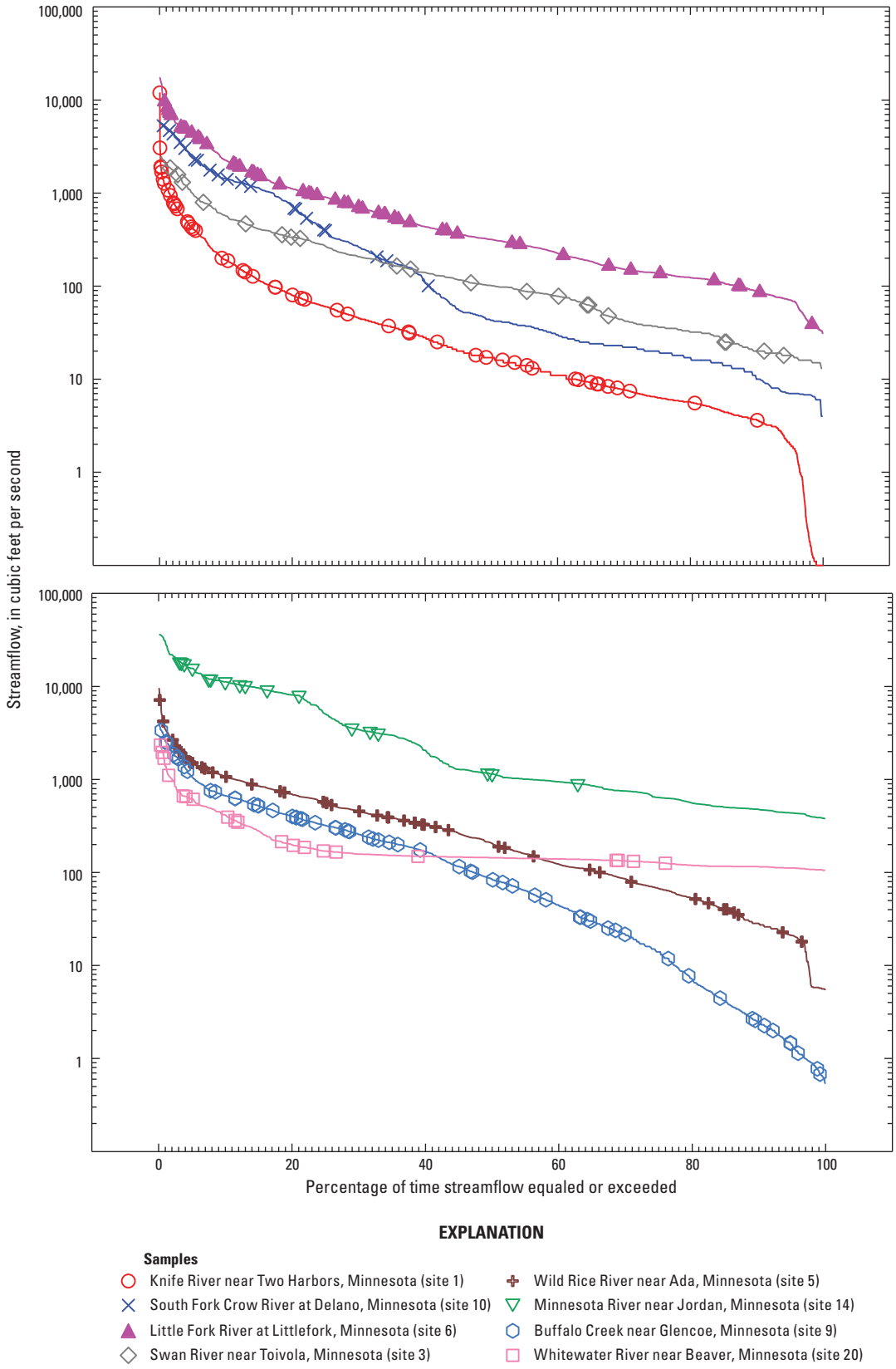

Figure 8. Flow-duration curves and corresponding values associated with suspended-sediment concentration samples for selected sites in Minnesota, 2007 through 2013.

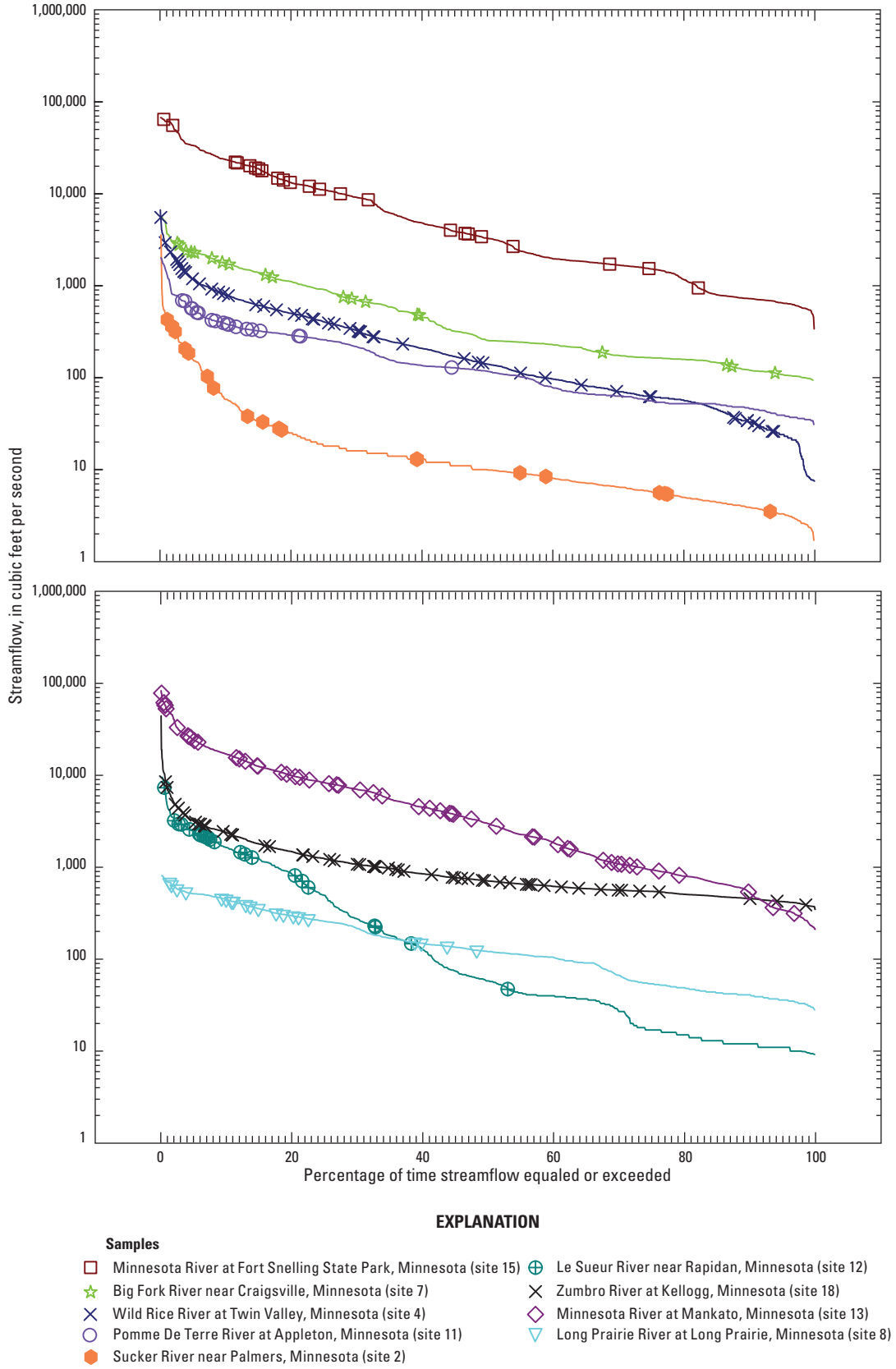

Figure 8. Flow-duration curves and corresponding values associated with suspended-sediment concentration samples for selected sites in Minnesota, 2007 through 2013.—Continued

Table 6. Summary statistics for streamflow, suspended-sediment concentrations, suspended particle-size fractions, and bedload collected from selected sites in Minnesota, 2007 through 2013.

[*N*, number of samples; StdDev, standard deviation; Minn., Minnesota; ft³/s, cubic foot per second; mg/L, milligram per liter; mm, millimeter; ton/d, tons per day; D100 is largest particle, in mm, in the sample; <, less than; --, not computed; Ave., avenue; SW, southwest; NW, northwest]

Constituent	Minimum	Mean	Median	Maximum	Total *N*	StdDev
Knife River near Two Harbors, Minn. (site 1)						
Streamflow, instantaneous (ft³/s)	4	844	136	11,100	65	1,890
Suspended-sediment concentration (mg/L)	2	100	12	926	52	206
Suspended-sediment concentration less than 0.0625 mm (percent)	31	80	84	99	48	17.1
Bedload transport (tons/day)	0.03	154	98	556	9	180
D100 particle size (mm)	11	40	34	68	8	18.7
Sucker River near Palmers, Minn. (site 2)						
Streamflow, instantaneous (ft³/s)	3	145	62	400	26	154
Suspended-sediment concentration (mg/L)	1	23	9	94	19	30.1
Suspended-sediment concentration less than 0.0625 mm (percent)	52	82	83	93	19	9.82
Bedload transport (tons/day)	0.00	14.1	1.08	76.2	7	28.2
D100 particle size (mm)	2	39	17	137	7	49.9
Swan River near Toivola, Minn. (site 3)						
Streamflow, instantaneous (ft³/s)	14	511	161	1,770	25	619.4
Suspended-sediment concentration (mg/L)	10	43	26	177	21	46.1
Suspended-sediment concentration less than 0.0625 mm (percent)	71	89	92	99	21	8.1
Bedload transport (tons/day)	0.07	0.29	0.27	0.53	4	0.20
D100 particle size (mm)	< 1	< 1	< 1	< 1	4	--
Wild Rice River at Twin Valley, Minn. (site 4)						
Streamflow, instantaneous (ft³/s)	26	757	434	4,920	64	869
Suspended-sediment concentration (mg/L)	3	108	42	775	49	146
Suspended-sediment concentration less than 0.0625 mm (percent)	43	83	88	98	46	13.6
Bedload transport (tons/day)	1.55	22.7	16.2	65.2	15	20.3
D100 particle size (mm)	4	10	10	18	15	4.10
Wild Rice River near Ada, Minn. (site 5)						
Streamflow, instantaneous (ft³/s)	16	740	415	2,700	67	736
Suspended-sediment concentration (mg/L)	6	173	70	1,100	46	234
Suspended-sediment concentration less than 0.0625 mm (percent)	26	71	72	96	42	18.4
Bedload transport (tons/day)	1.22	110	58.2	383	20	130
D100 particle size (mm)	2	11	10	18	20	4.70
Little Fork River at Littlefork, Minn. (site 6)						
Streamflow, instantaneous (ft³/s)	38	2,320	1,550	9,700	72	2,500
Suspended-sediment concentration (mg/L)	9	52	27	375	56	64.5
Suspended-sediment concentration less than 0.0625 mm (percent)	25	87	92	100	55	15.2
Bedload transport (tons/day)	6.48	45.4	34.6	144	16	34.2
D100 particle size (mm)	6	10	9	18	16	3.09

Table 6. Summary statistics for streamflow, suspended-sediment concentrations, suspended particle-size fractions, and bedload collected from selected sites in Minnesota, 2007 through 2013.—Continued

[*N*, number of samples; StdDev, standard deviation; Minn., Minnesota; ft³/s, cubic foot per second; mg/L, milligram per liter; mm, millimeter; ton/d, tons per day; D100 is largest particle, in mm, in the sample; <, less than; --, not computed; Ave., avenue; SW, southwest; NW, northwest]

Constituent	Minimum	Mean	Median	Maximum	Total *N*	StdDev
Big Fork River near Craigsville, Minn (site 7)						
Streamflow, instantaneous (ft³/s)	109	1,470	1,500	2,900	36	933
Suspended-sediment concentration (mg/L)	5	25	21	74	20	18.7
Suspended-sediment concentration less than 0.0625 mm (percent)	61	83	85	93	20	9.16
Bedload transport (tons/day)	0.41	7.90	4.09	25.6	16	8.16
D100 particle size (mm)	5	8	7	18	15	3.46
Long Prairie River at Long Prairie, Minn. (site 8)						
Streamflow, instantaneous (ft³/s)	126	362	374	691	43	166
Suspended-sediment concentration (mg/L)	2	32	22	107	22	29.7
Suspended-sediment concentration less than 0.0625 mm (percent)	41	66	68	93	22	15.7
Bedload transport (tons/day)	0.33	20.8	16.7	73.9	21	19.1
D100 particle size (mm)	4	6	5	17	20	3.59
Buffalo Creek near Glencoe, Minn. (site 9)						
Streamflow, instantaneous (ft³/s)	1	583	287	3,500	83	832
Suspended-sediment concentration (mg/L)	5	59	44	298	65	55.0
Suspended-sediment concentration less than 0.0625 mm (percent)	15	79	87	99	58	20.0
Bedload transport (tons/day)	0.02	53.8	25.7	181	18	60.8
D100 particle size (mm)	2	10	9	23	17	5.58
South Fork Crow River at Delano, Minn. (site 10)						
Streamflow, instantaneous (ft³/s)	103	1,840	1,310	5,290	41	1,680
Suspended-sediment concentration (mg/L)	27	87	54	446	20	95.1
Suspended-sediment concentration less than 0.0625 mm (percent)	5	79	92	98	20	29.7
Bedload transport (tons/day)	1.19	93.9	46.5	364	21	110
D100 particle size (mm)	4	8	8	15	21	2.74
Pomme De Terre River at Appleton, Minn. (site 11)						
Streamflow, instantaneous (ft³/s)	128	420	390	695	40	136
Suspended-sediment concentration (mg/L)	41	129	93	267	21	73.9
Suspended-sediment concentration less than 0.0625 mm (percent)	71	87	91	98	21	8.19
Bedload transport (tons/day)	0.04	3.17	1.37	15.3	19	4.16
D100 particle size (mm)	2	6	6	15	17	3.02
Le Sueur River near Rapidan, Minn. (site 12)						
Streamflow, instantaneous (ft³/s)	43	2,000	2,010	8,150	51	1,600
Suspended-sediment concentration (mg/L)	34	450	419	1,840	29	401
Suspended-sediment concentration less than 0.0625 mm (percent)	32	64	66	98	29	18.4
Bedload transport (tons/day)	0.27	217	198	490	22	136
D100 particle size (mm)	5	25	22	65	22	13.2

Table 6. Summary statistics for streamflow, suspended-sediment concentrations, suspended particle-size fractions, and bedload collected from selected sites in Minnesota, 2007 through 2013.—Continued

[*N*, number of samples; StdDev, standard deviation; Minn., Minnesota; ft³/s, cubic foot per second; mg/L, milligram per liter; mm, millimeter; ton/d, tons per day; D100 is largest particle, in mm, in the sample; <, less than; --, not computed; Ave., avenue; SW, southwest; NW, northwest]

Constituent	Minimum	Mean	Median	Maximum	Total *N*	StdDev
Minnesota River at Mankato, Minn. (site 13)						
Streamflow, instantaneous (ft³/s)	324	11,800	6,450	77,500	75	15,900
Suspended-sediment concentration (mg/L)	27	207	141	927	53	192
Suspended-sediment concentration less than 0.0625 mm (percent)	15	80	84	98	36	16.1
Bedload transport (tons/day)	0.39	288	137	1,140	21	369
D100 particle size (mm)	2	12	13	34	21	8.26
Minnesota River near Jordan, Minn. (site 14)						
Streamflow, instantaneous (ft³/s)	900	10,400	10,400	18,300	29	5,590
Suspended-sediment concentration (mg/L)	33	262	243	794	16	204
Suspended-sediment concentration less than 0.0625 mm (percent)	68	85	86	91	16	6.44
Bedload transport (tons/day)	0.07	3.57	2.70	12.8	13	4.09
D100 particle size (mm)	3	7	7	10	8	2.67
Minnesota River at Fort Snelling State Park, Minn. (site 15)						
Streamflow, instantaneous (ft³/s)	1,320.0	16,040	12,800	67,600	40	16,900
Suspended-sediment concentration (mg/L)	26	225	114	1,010	24	273
Suspended-sediment concentration less than 0.0625 mm (percent)	61	87	89	98	24	9.00
Bedload transport (tons/day)	1.31	30.3	15.7	165	17	39.1
D100 particle size (mm)	3	8	7	16	9	4.15
Cascade Creek at 45th Ave. SW in Rochester, Minn. (site 16)						
Streamflow, instantaneous (ft³/s)	2	50	29	204	45	55.0
Suspended-sediment concentration (mg/L)	12	197	67	907	22	258
Suspended-sediment concentration less than 0.0625 mm (percent)	54	81	86	99	22	15.8
Bedload transport (tons/day)	0.00	2.94	0.57	21.8	23	5.63
D100 particle size (mm)	3	12	8	33	17	8.98
Cascade Creek at 35th Ave. NW in Rochester, Minn. (site 17)						
Streamflow, instantaneous (ft³/s)	2	53	36	217	34	55.4
Suspended-sediment concentration (mg/L)	28	226	115	808	21	239
Suspended-sediment concentration less than 0.0625 mm (percent)	57	85	88	100	21	14.2
Bedload transport (tons/day)	0.00	0.63	0.06	3.96	13	1.33
D100 particle size (mm)	5	6	6	6	2	0.99
Zumbro River at Kellogg, Minn. (site 18)						
Streamflow, instantaneous (ft³/s)	420	1650	1,007	7,040	75	1,500
Suspended-sediment concentration (mg/L)	17	221	121	1,250	54	267
Suspended-sediment concentration less than 0.0625 mm (percent)	2	67	71	96	54	20.8
Bedload transport (tons/day)	50.2	339	303	1,024	21	293
D100 particle size (mm)	6	10	9	23	21	4.84

Table 6. Summary statistics for streamflow, suspended-sediment concentrations, suspended particle-size fractions, and bedload collected from selected sites in Minnesota, 2007 through 2013.—Continued

[*N*, number of samples; StdDev, standard deviation; Minn., Minnesota; ft³/s, cubic foot per second; mg/L, milligram per liter; mm, millimeter; ton/d, tons per day; D100 is largest particle, in mm, in the sample; <, less than; --, not computed; Ave., avenue; SW, southwest; NW, northwest]

Constituent	Minimum	Mean	Median	Maximum	Total *N*	StdDev
North Fork Whitewater River near Elba, Minn. (site 19)						
Streamflow, instantaneous (ft³/s)	29	173	114	797	31	190
Suspended-sediment concentration (mg/L)	11	94	37	640	21	153
Suspended-sediment concentration less than 0.0625 mm (percent)	23	65	62	97	21	23.6
Bedload transport (tons/day)	0.04	19.9	0.45	113	10	37.8
D100 particle size (mm)	2	10	9	30	9	10.1
Whitewater River near Beaver, Minn. (site 20)						
Streamflow, instantaneous (ft³/s)	129	815	360	6,520	41	1,320
Suspended-sediment concentration (mg/L)	29	1,000	145	4,820	18	1,620
Suspended-sediment concentration less than 0.0625 mm (percent)	28	59	56	93	18	16.7
Bedload transport (tons/day)[1]	--	--	--	--	22	--
D100 particle size (mm)	2	8	7	14	22	3.43

[1]Bedload samples collected but results were rated poor/nonrepresentative; statistics not computed.

Suspended-Sediment Concentrations

The raw SSC and streamflow data used for this study are available in the U.S. Geological Survey National Water Information System at http://dx.doi.org/10.5066/F7P55KJN, and also are provided in appendix table 1-2. Sites in southeastern Minnesota and the lower Minnesota River Basin had the highest mean SSC during the study period. Site 20 in southeastern Minnesota had the highest mean SSC (1,000 mg/L) followed by sites 12, 14, 17, and 18 with 450, 262, 226, and 221 mg/L, respectively (table 6). Although the Minnesota River Basin has low relief in the valley, the edges of the river valley are lined with steep erodible bluffs and ravines. Tributaries in the Minnesota River Basin such as the LeSueur River (not shown) cut through the valley walls and contribute large volumes of sediment into the Minnesota River. Site 20 in southeastern Minnesota produced the single highest SSC of 4,820 mg/L at a streamflow of 1,739 ft³/s during a summer rainfall event in June 2013 (appendix table 1–2).

Measured SSCs varied across regions of Minnesota. For northwestern Minnesota, sites 4 and 5 (table 6) had higher mean SSC than sites in the central and northeastern parts of the State; however, the proximity of sites 4 and 5 to the beach ridge of glacial Lake Agassiz represent higher sediment- producing reaches for the northwestern region (Blanchard and others, 2011; Ellison and others, 2014). The lowest mean SSCs were measured in the northeast, north-central, and central regions of the State at sites 2, 7, and 8 with 23, 25, and 32 mg/L, respectively.

Northeastern Minnesota near Lake Superior is composed of glacial till in the headwater reaches that transitions to bedrock outcrops where stream gradients increase quickly and become sediment transport zones (Fitzpatrick and others, 2006). Low gradient headwaters contain forests and wetlands that are resistant to erosion; however, stream reaches near transition zones between the headwaters and the bedrock outcrops are vulnerable to erosion and may contribute large amounts of sediment into Lake Superior (Fitzpatrick and others, 2006). For example, high SSCs were measured at site 1 in northeastern Minnesota during high streamflows associated with spring runoff and summer precipitation (Ellison and others, 2014). Among sites in northeastern Minnesota, the Knife River near Two Harbors, Minn. (site 1) had the highest mean SSC of 100 mg/L with a maximum SSC of 926 mg/L measured during record flooding on June 20, 2012.

Bedload

Bedload samples were collected concurrently with SSC samples, and bedload data had spatial patterns similar to SSC patterns (table 6). The highest mean bedload of 339 tons per day (ton/d) was measured at site 18 in southeastern Minnesota followed by sites 13, 12, 1, and 5 with 288, 217, 154, and 110 ton/d, respectively. Each of the aforementioned sites have sediment sources in the landscape that contribute to the high observed bedload. For example, the Le Sueur River at site 12 cuts through valley walls of the Minnesota River Basin, and the Wild Rice River at site 5 cuts through beach ridges of

glacial Lake Agassiz. The Zumbro River at site 18, the Knife River at site 1, and the Minnesota River at site 13 are actively down-cutting through thick layers of glacial till.

Unrestricted supplies of unconsolidated sands, medium to steep stream gradients, and the highest precipitation rates in the State (Minnesota Department of Natural Resources, 2016a, 2016b, 2016c, 2016d) likely contribute to large bedload rates in southeastern Minnesota. The Whitewater River near Beaver, Minn. (site 20) likely discharges the largest amount of bedload of all sites in this study; however, bedload rates could not be computed for site 20 because of sample collection limitations at higher flows. Alternative assessment methods, such as the Bureau of Reclamation Automated Modified Einstein Procedure (BORAMEP) (Bureau of Reclamation, 2010) will be needed to estimate bedload for future studies at site 20.

Cohesive soils, low stream gradient, and higher percentage of wetlands and lakes contribute to smaller bedload rates at sites 8 through 11 in central Minnesota. Also, sites 14 and 15 in the lower Minnesota River Basin had markedly smaller mean bedload rates (3.57 and 30.3 ton/d, respectively) than site 13 (288 ton/d), which is located farther upstream in the Minnesota River. Low stream gradients in the lower Minnesota River Basin likely contributed substantially to the observed decrease in bedload in the lower reach.

With the exception of site 1, some of the smallest bedload rates were measured in north-central and northeastern Minnesota. The Swan River near Toivola, Minn. (site 3) in northeastern Minnesota is a low gradient site (fig. 3); the nearby upstream soils primarily consist of consolidated silt and fine sand (fig. 2) and bedload rates were less than 0.5 ton/d (table 6). Similarly, estimated bedload rates at the Sucker River near Palmers, Minn. (site 2) in the northeastern part of the State and the Big Fork River near Craigsville, Minn. (site 7) in the north-central part of the State produced relatively smaller mean bedload rates of 14.1 and 7.90 ton/d, respectively. Low bedload rates measured at these rivers are attributed in part to cobbles and boulder-sized particles that are ubiquitous in the river channels; these large particles only move during extreme streamflow events. This report provides first-ever measurements of bedload at each of the study sites, and offers important information and insight regarding the contribution of bedload to total sediment loads.

Particle-Size Fractions

Suspended-sediment concentrations for fines (particle sizes less than 0.0625 mm) were measured in markedly higher percentages than suspended-sands (particle sizes equal to or greater than 0.0625 mm) concentrations at all sites as evidenced by percentages for suspended-sediment concentrations less than 0.0625 mm (hereafter referred to as suspended-fines concentrations) that were greater than 50 percent at all study sites (table 6). Total suspended-sediment concentration for this study is equal to the sum of suspended-fines concentrations and suspended-sands concentrations (for example, a reported value of 65 percent suspended-fines concentrations indicates that the percent of suspended-sands concentrations is equal to 35 percent). Rivers with large percentages of suspended fines transport most of the sediment load to receiving reaches, where low gradient conditions result in deposition and temporary storage.

The largest mean percentage of suspended-fines concentrations was at site 3 in northeastern Minnesota where 89 percent of suspended material consisted of fines. Sites 6, 11, and 15 have mean percentages of suspended-fines concentrations of 87 percent (table 6). Although suspended-fines concentrations composed most of the total suspended sediment, the percentage of suspended-sands concentrations was appreciable at many sites. Overall, percentages of suspended-sands concentrations were higher in southeastern Minnesota when compared to other regions of the State. Suspended sands can affect aquatic habitat by filling in pools, causing aggradation of the channel, and can limit availability of channel substrate for macroinvertebrates (Cummins and Lauff, 1969; Minshall, 1984). Channel aggradation can cause the formation of mid channel bars that redirects streamflow and may accelerate bank failure, lateral migration, and stream widening (Leopold and others, 1964; Knighton, 1998; Rosgen, 2007). The largest mean percentages of suspended-sands concentrations were at sites 20, 12, and 19 with 41, 36, and 35 percent, respectively, of material in suspension being sand-sized (table 6). Other notable percentages of suspended-sands concentrations were at sites 8, 18, and 5 with 34, 33, and 29 percent of material in suspension being sand-sized.

Relations among Suspended-Sediment Concentration and Bedload with Streamflow

Kendall's tau correlation analyses were used to measure the strength of the monotonic relation between SSC and streamflow and between bedload and streamflow at each site. Tau statistics for relating total SSC (composite of suspended fines and sands) and bedload to streamflow are presented in table 7, and the relations between SSC and streamflow and between bedload and streamflow are presented in figures 9 and 10, respectively. Results of Kendall's tau analyses were used to select sites for use in the development of Minnesota DSRC models (for example, sites with no significant relation between SSC streamflow and between bedload and streamflow, p-value greater than 0.05, were excluded in model development). Significant relations between SSC and streamflow were observed at 16 out of the 20 sites and significant relations between bedload and streamflow were observed at 15 out of the 20 sites (table 7).

Strengths of the relations between SSC and streamflow varied among sites (table 7). The strongest relations were observed at sites 20, 1, and 12 with tau values of 0.85, 0.79, and 0.79, respectively. These three sites have ample supplies of sediment, along with favorable topography (for example, steep stream gradients), and unconsolidated soils conducive

Table 7. Kendall's rank correlation tau statistics for relating total suspended-sediment concentration and bedload to streamflow.

[Tau, measure of the strength of nonlinear relations. The measure of strength is scaled to be in the range of -1 to 1, and a value close to 0 indicates that no relation exists between two variables. Tau correlation values approaching values of 1 or -1 indicate a strong monotonic relation between two variables; Normal-*Z*, measure of the number of standard deviations that a value in a normal distribution of data deviates from the mean of the data; *p*-value, statistical probability level; *N*, number of samples; Minn., Minnesota; mg/L, milligram per liter; tons/day, tons per day; <, less than; Ave., avenue; SW, southwest; NW, northwest]

Constituent	Tau	Normal-*Z*	*p*-value	Total *N*
Knife River near Two Harbors, Minn. (site 1)				
Total suspended-sediment concentration (mg/L)	0.79	8.31	<0.01	52
Bedload transport (tons/day)	0.83	3.13	<0.01	9
Sucker River near Palmers, Minn. (site 2)				
Total suspended-sediment concentration (mg/L)	0.55	3.30	<0.01	19
Bedload transport (tons/day)	0.43	1.35	0.177	7
Swan River near Toivola, Minn. (site 3)				
Total suspended-sediment concentration (mg/L)	0.69	4.35	<0.01	21
Bedload transport (tons/day)	-0.33	-0.68	0.497	4
Wild Rice River at Twin Valley, Minn. (site 4)				
Total suspended-sediment concentration (mg/L)	0.70	7.05	<0.01	49
Bedload transport (tons/day)	0.37	1.93	0.054	15
Wild Rice River near Ada, Minn. (site 5)				
Total suspended-sediment concentration (mg/L)	0.66	6.47	<0.01	46
Bedload transport (tons/day)	0.79	4.87	<0.01	20
Little Fork River at Littlefork, Minn. (site 6)				
Total suspended-sediment concentration (mg/L)	0.58	6.30	<0.01	56
Bedload transport (tons/day)	0.15	0.81	0.418	16
Big Fork River near Craigsville, Minn (site 7)				
Total suspended-sediment concentration (mg/L)	0.64	3.94	<0.01	20
Bedload transport (tons/day)	0.26	1.40	0.162	16
Long Prairie River at Long Prairie, Minn. (site 8)				
Total suspended-sediment concentration (mg/L)	0.13	0.85	0.397	22
Bedload transport (tons/day)	0.31	1.99	0.046	21
Buffalo Creek near Glencoe, Minn. (site 9)				
Total suspended-sediment concentration (mg/L)	0.13	1.51	0.130	65
Bedload transport (tons/day)	0.79	4.58	<0.01	18
South Fork Crow River at Delano, Minn. (site 10)				
Total suspended-sediment concentration (mg/L)	0.44	2.70	<0.01	18
Bedload transport (tons/day)	0.69	4.38	<0.01	21
Pomme De Terre River at Appleton, Minn. (site 11)				
Total suspended-sediment concentration (mg/L)	0.18	1.12	0.263	21
Bedload transport (tons/day)	0.37	2.24	0.025	19
Le Sueur River near Rapidan, Minn. (site 12)				
Total suspended-sediment concentration (mg/L)	0.79	5.98	<0.01	29
Bedload transport (tons/day)	0.56	3.64	<0.01	22

Table 7. Kendall's rank correlation tau statistics for relating total suspended-sediment concentration and bedload to streamflow.—Continued

[Tau, measure of the strength of nonlinear relations. The measure of strength is scaled to be in the range of -1 to 1, and a value close to 0 indicates that no relation exists between two variables. Tau correlation values approaching values of 1 or -1 indicate a strong monotonic relation between two variables; Normal-*Z*, measure of the number of standard deviations that a value in a normal distribution of data deviates from the mean of the data; *p*-value, statistical probability level; *N*, number of samples; Minn., Minnesota; mg/L, milligram per liter; tons/day, tons per day; <, less than; Ave., avenue; SW, southwest; NW, northwest]

Constituent	Tau	Normal-*Z*	*p*-value	Total *N*
Minnesota River at Mankato, Minn. (site 13)				
Total suspended-sediment concentration (mg/L)	0.52	5.50	<0.01	53
Bedload transport (tons/day)	0.67	4.26	<0.01	21
Minnesota River near Jordan, Minn. (site 14)				
Total suspended-sediment concentration (mg/L)	0.74	4.01	<0.01	16
Bedload transport (tons/day)	0.54	2.56	0.010	13
Minnesota River at Fort Snelling State Park, Minn. (site 15)				
Total suspended-sediment concentration (mg/L)	0.28	1.94	0.053	24
Bedload transport (tons/day)	0.42	2.25	0.024	17
Cascade Creek at 45th Ave. SW in Rochester, Minn. (site 16)				
Total suspended-sediment concentration (mg/L)	0.57	3.73	<0.01	22
Bedload transport (tons/day)	0.78	5.29	<0.01	23
Cascade Creek at 35th Ave. NW in Rochester, Minn. (site 17)				
Total suspended-sediment concentration (mg/L)	0.48	3.03	<0.01	21
Bedload transport (tons/day)	0.71	3.36	<0.01	13
Zumbro River at Kellogg, Minn. (site 18)				
Total suspended-sediment concentration (mg/L)	0.57	6.07	<0.01	54
Bedload transport (tons/day)	0.68	4.29	<0.01	21
North Fork Whitewater River near Elba, Minn. (site 19)				
Total suspended-sediment concentration (mg/L)	0.60	3.78	<0.01	21
Bedload transport (tons/day)	0.67	2.69	<0.01	10
Whitewater River near Beaver, Minn. (site 20)				
Total suspended-sediment concentration (mg/L)	0.85	4.93	<0.01	18
Bedload transport (tons/day)	0.43	2.82	<0.01	22

to detachment and transport to nearby streams (Minnesota Department of Natural Resources, 2016c). Six out of the 20 sites (sites 14, 4, 3, 5, 7, and 19) had moderately strong tau correlations of 0.74, 0.70, 0.69, 0.66, 0.64, and 0.60, respectively. Seven out of 20 sites had medium tau correlations that ranged from 0.44 to 0.58.

Four of the 20 study sites indicated no significant relation between SSC and streamflow (sites 8, 9, 11, and 15; table 7). Sites with no significant relation between SSC and streamflow tend to have one or more attributes that minimize erosion such as low gradient, cohesive soils, abundance of riparian vegetation, or abundance of lakes and wetlands.

Relations between bedload and streamflow did not always follow the same spatial trend as the relations between SSC and streamflow. The strongest relations were observed at sites 1, 5, 9, 16, and 17 with tau correlations of 0.83, 0.79, 0.79, 0.78, and 0.71, respectively (table 7). Eight sites (table 7) had medium to moderate tau correlations ranging from 0.69 to 0.42, whereas two sites (sites 11 and 8) had significant (*p*-values less than 0.05) but low tau correlations of 0.37 and 0.31, respectively. Five of the 20 sites (sites 2, 3, 4, 6, and 7) did not have significant relations between bedload and streamflow. It is important to note that bedload data collected at site 15 (Minnesota River at Fort Snelling State Park) were not included in model development of the Minnesota bedload DSRC model for good/fair stability sites, even though the relation between bedload and streamflow indicated statistical significance. The data at site 15 were deemed to be

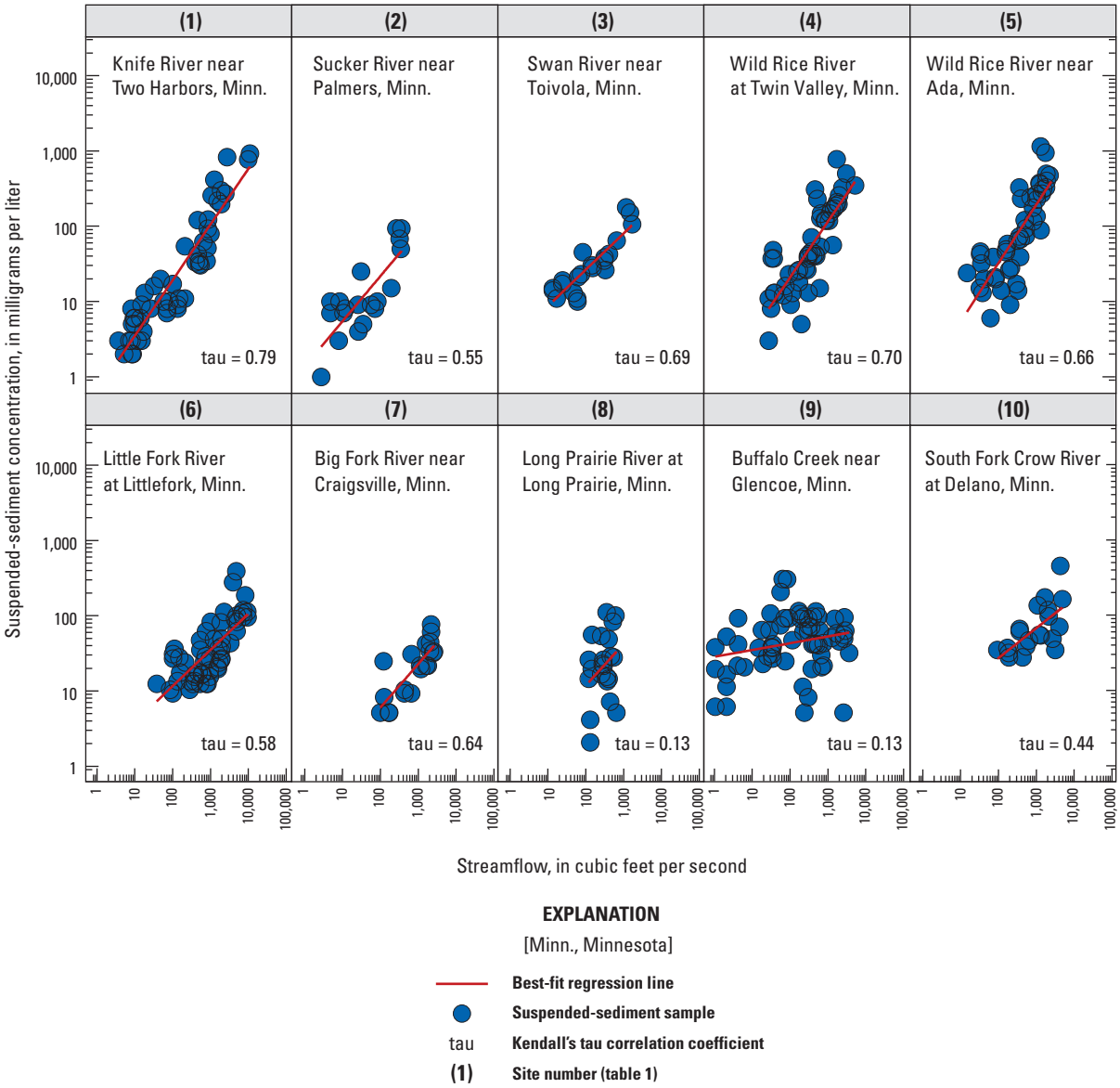

Figure 9. Relations between suspended-sediment concentrations and streamflow for selected sites in Minnesota, 2007 through 2013.

nonrepresentative because samples collected near bankfull streamflow, which were on the falling limb of the hydrograph, indicated disproportionate influence because of the effects of hysteresis.

Interestingly, sites that did not have significant relations between bedload and streamflow but that had significant relations between SSC and streamflow, are all located in northern Minnesota. Factors such as drainage network position, slope, and geologic setting likely contributed to the lack of significant relations between bedload and streamflow. The lack of significance between bedload and streamflow at sites 2, 6, and 7 may in part be attributed to large particles (cobbles and boulders) prevalent in the channel, which require large streamflow events for mobilization, and also in part to the uncertainty associated with the resting position of the sampler on the streambed. It is possible that embedded cobbles may have prevented the sampler from resting on the bed, thus preventing mobilized particles from entering the sampler. For site 3 in northeastern Minnesota, the lack of significance may have resulted from the low gradient and prevalence of fine-sized particles at the site, which would have passed through the larger pore sizes in the sampling bag.

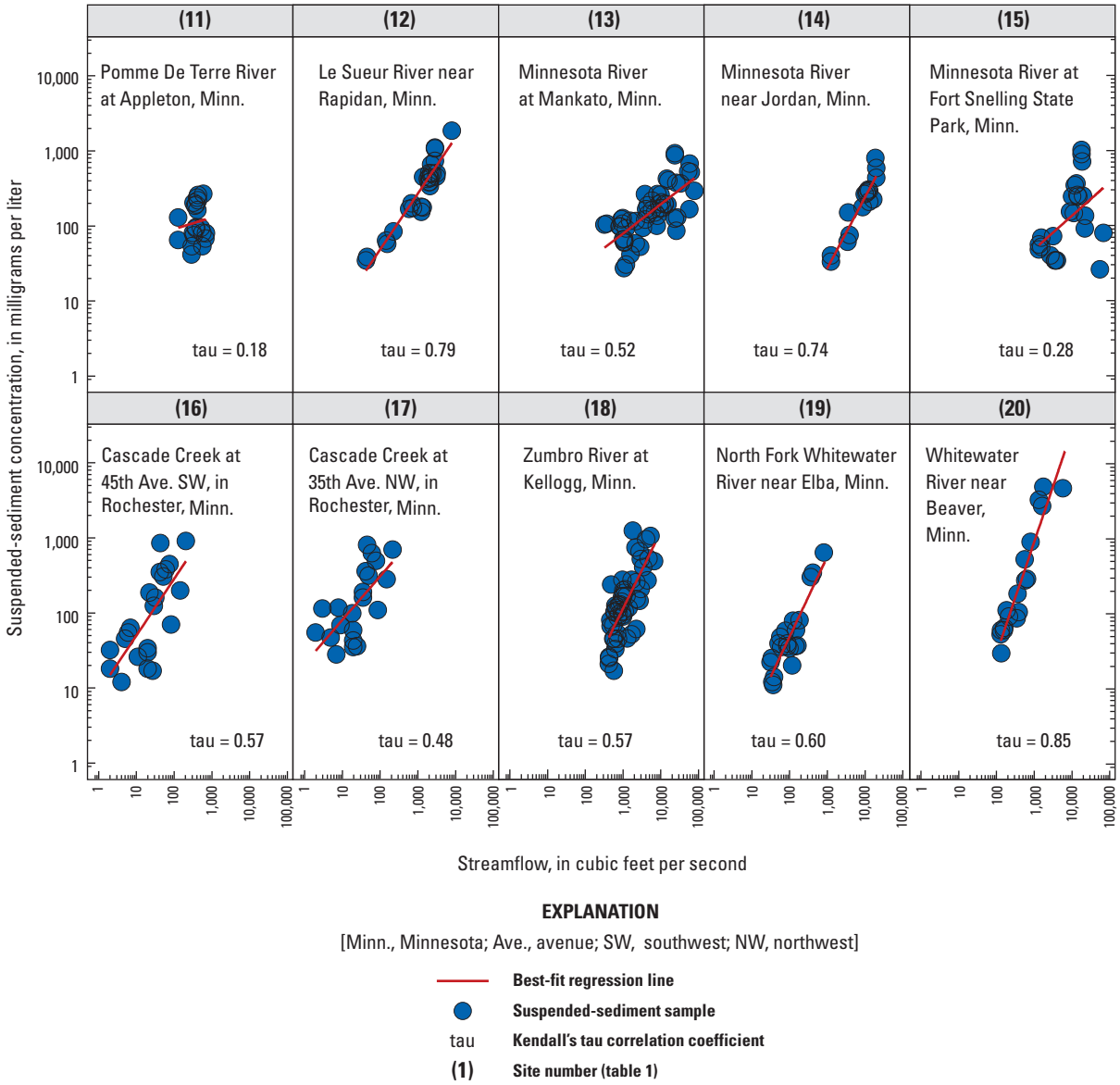

EXPLANATION

[Minn., Minnesota; Ave., avenue; SW, southwest; NW, northwest]

Best-fit regression line

Suspended-sediment sample

tau **Kendall's tau correlation coefficient**

(1) **Site number (table 1)**

Figure 9. Relations between suspended-sediment concentrations and streamflow for selected sites in Minnesota, 2007 through 2013.—Continued

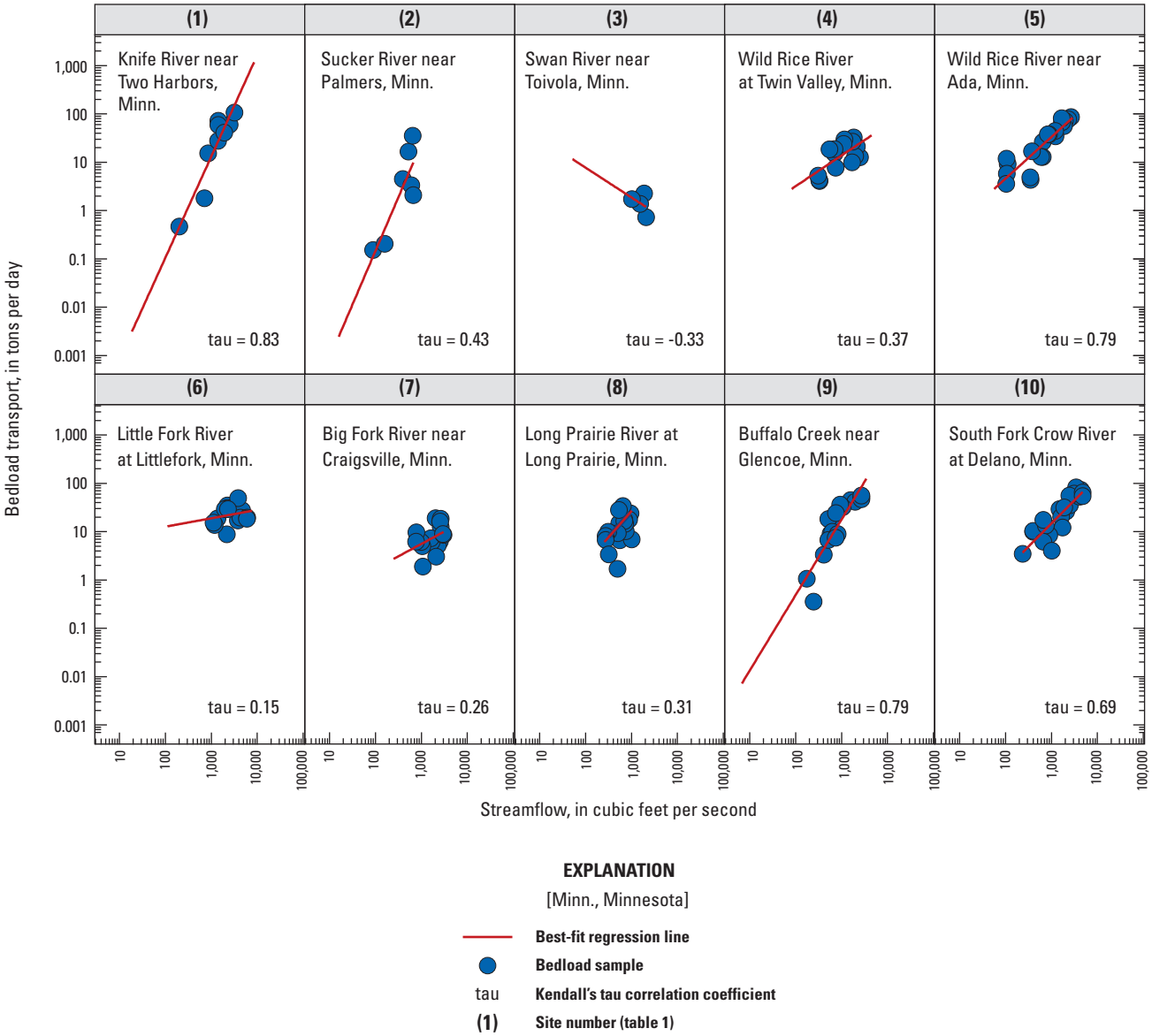

EXPLANATION

[Minn., Minnesota]

Best-fit regression line

Bedload sample

tau **Kendall's tau correlation coefficient**

(1) **Site number (table 1)**

Figure 10. Relations between bedload and streamflow for selected sites in Minnesota, 2007 through 2013.

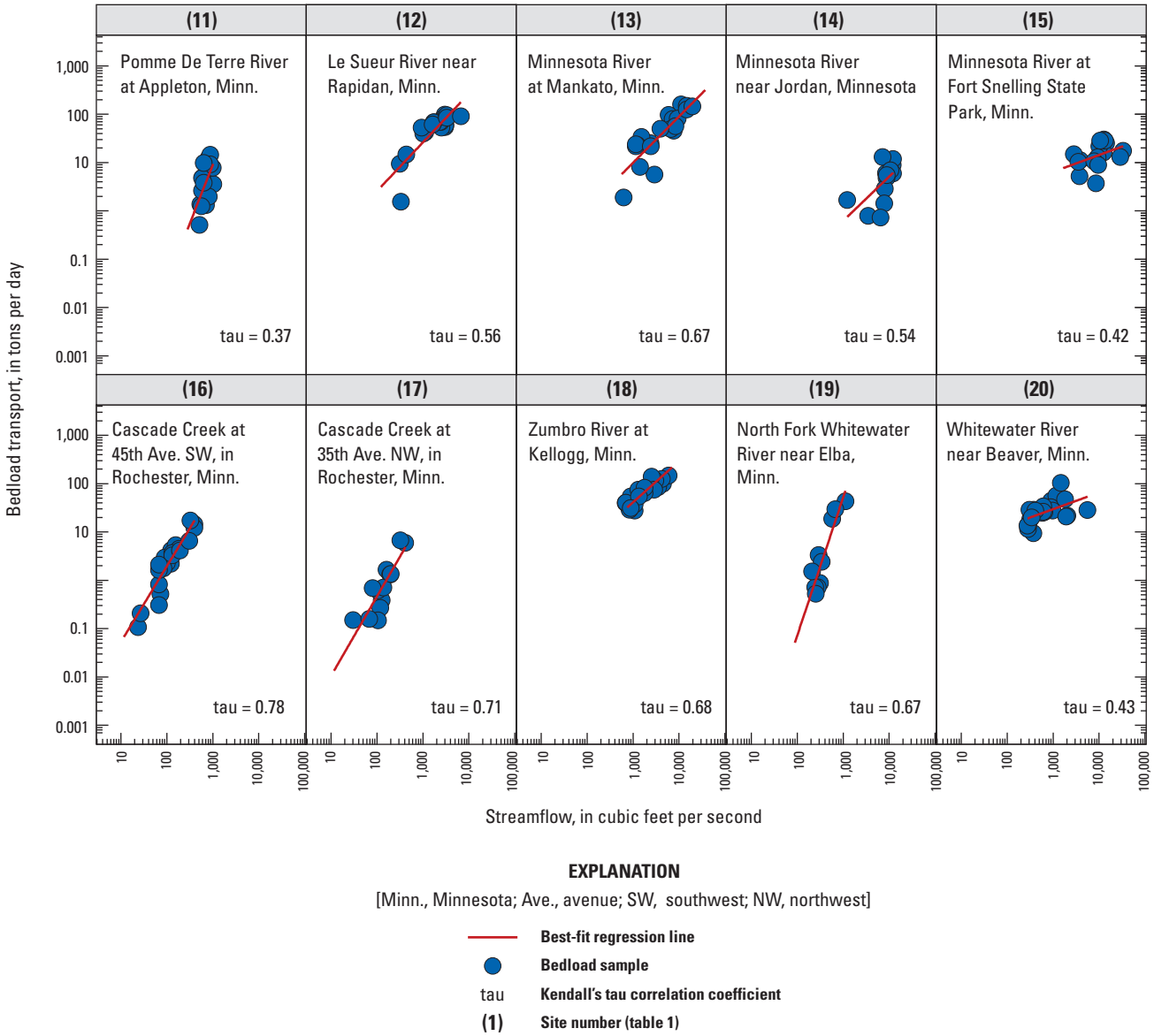

EXPLANATION

[Minn., Minnesota; Ave., avenue; SW, southwest; NW, northwest]

Best-fit regression line

Bedload sample

tau **Kendall's tau correlation coefficient**

(1) **Site number (table 1)**

Figure 10. Relations between bedload and streamflow for selected sites in Minnesota, 2007 through 2013.—Continued

Dimensionless Sediment Rating Curves

This section of the report presents DSRCs developed using data collected in Minnesota, and provides an assessment of the ability of the Pagosa Springs and Minnesota DSRC models to predict SSC and bedload. Evaluations of DSRC models were based on multiple measures of goodness-of-fit that included (1) proximity of the model(s) fitted line to the 95-percent confidence intervals of the site-specific model, (2) Nash-Sutcliffe Efficiency values, (3) estimations of model biases, and (4) deviation of the modeled (predicted) annual sediment loads from the annual sediment loads calculated from the measured data. Estimated SSC and bedload values at bankfull streamflow for each site are presented in tables 8 and 9, respectively. Similarities between ratio-estimated values of SSC and bedload and Jackknife resampling statistic estimates for all sites indicate that biases were not substantial for estimates of SSC and bedload at bankfull streamflow. Sites used to develop DSRC models are presented in table 10.

More than 600 samples were used to develop Minnesota DSRCs for SSC and bedload for good/fair and poor stream stability categories. Four weighted nonlinear regression models were developed according to Pfankuch stream stability categories (appendix table 1–1) using the R statistical environment (nls function; R Development Core Team, 2011). Dimensionless ratio values of streamflow, SSC, and bedload were used to develop the following regression equations:

Suspended DSRC (good/fair stability):

$$SSC = 0.026 + 0.974Q^{0.951} \quad (14)$$

Bedload DSRC (good/fair stability):

$$Q_b = -0.054 + 1.054Q^{1.316} \quad (15)$$

Suspended DSRC (poor stability):

$$SSC = 0.066 + 0.934Q^{1.006} \quad (16)$$

Bedload DSRC (poor stability):

$$Q_b = 0.012 + 0.988Q^{1.306} \quad (17)$$

where

Q is a dimensionless ratio value of streamflow,
Q_b is a dimensionless ratio value of bedload, and
SSC is a dimensionless ratio value of suspended-sediment concentration.

The parameter, Q_b is assumed to be 0 when the dimensionless ratio value of Q is 0.104 or less for equation 15.

Dimensional values of SSC and bedload are derived from dimensionless ratio values of streamflow using the regression equations 14 through 17 (models). This entails converting streamflow to a dimensionless value by dividing streamflow by the known bankfull streamflow at the selected site. This dimensionless streamflow value is used as the input value in one of the dimensionless regression equations (equations 14 through 17) to calculate a dimensionless SSC or bedload value. Finally, the calculated dimensionless SSC or bedload value is multiplied by the known SSC or bedload value at bankfull streamflow from the site of interest to determine the dimensional SSC or bedload value. Table 11 provides an example of calculating dimensionless ratio streamflow and SSC along with corresponding dimensional values at the North Fork Whitewater River near Elba, Minn. (site 19) in southeastern Minnesota.

The Pagosa Springs and Minnesota DSRC models for SSC and bedload were evaluated in comparison to site-specific regression models for model ability to predict suspended-sediment concentrations and bedload. Site-specific regression model equations for SSC and bedload are available in appendix table 1–3. Multiple measures of goodness-of-fit were developed to evaluate the effectiveness of DSRC models in predicting SSC and bedload for rivers in Minnesota. As previously mentioned and described in the following subsections, four methods were used to assess the models: (1) comparison of regression trendlines (proximity of the fitted line of the DSRC model to the 95-percent confidence intervals of the site-specific model), (2) Nash-Sutcliffe Efficiencies, (3) bias estimates, and (4) deviation of annual sediment loads from each model to the annual sediment loads calculated from measured data. Model limitations also are described.

Regression Trendlines

Modeled (predicted) values of SSC and bedload using Pagosa Springs and Minnesota DSRC models were compared to measured values of SSC and bedload by plotting the measured values and the regression trendlines of each of the models on a log-log scale. Site-specific model regression trendlines with 95-percent confidence intervals were included to demonstrate the relations between measured SSC and streamflow and measured bedload and streamflow and to examine the level of agreement between DSRC models and site-specific regression models. Pagosa Springs DSRC models, Minnesota DSRC models, and site-specific regression models are presented for Pfankuch stability ratings of good/fair and poor streams in figures 11 and 12, respectively, for SSC and in figures 13 and 14, respectively, for bedload. Pagosa Springs and Minnesota DSRC models were compared to site-specific regression models to evaluate their effectiveness in predicting SSC and bedload. Site-specific regression models are assumed to provide the most accurate predictions of suspended sediment and bedload across a range of streamflow.

Table 8. Suspended-sediment concentration at bankfull streamflow estimated using ratio estimators and jackknife resampling statistic for selected sites in Minnesota, 2007 through 2013.

[ft³/s, cubic foot per second; SSC, suspended-sediment concentration; mg/L, milligram per liter; *N*, number of samples used in calculation; Minn. ,Minnesota; --, not computed because of large variation in the data; Ave., avenue; SW, southwest; NW, northwest]

Site number (figs. 1–4)	Station name	Bankfull streamflow (ft³/s)	Range of streamflow used in calculation	Mean streamflow (ft³/s)	Ratio estimate of SSC (mg/L)	Jackknife bias-free estimate of SSC (mg/L)	*N*	Standard error (mg/L)	95-percent confidence intervals	
									Upper	Lower
1	Knife River near Two Harbors, Minn.	1,880	1,080–2,760	1,950	361	364	5	87	600	120
2	Sucker River near Palmers, Minn.	380	212–400	330	74	74	5	14	110	40
3	Swan River near Toivola, Minn.	1,230	1,560–1,770	1,670	95	--	2	23	190	0
4	Wild Rice River at Twin Valley, Minn.	1,000	600–1,810	1,120	210	215	6	87	460	0
5	Wild Rice River near Ada, Minn.	1,560	1,100–2,000	1,470	379	381	8	80	570	190
6	Little Fork River at Littlefork, Minn.	6,900	4,880–8,270	5,800	218	213	4	85	480	0
7	Big Fork River near Craigsville, Minn.	1,970	1,310–2,420	1,950	40	39	6	7	60	20
8	Long Prairie River at Long Prairie, Minn.	530	274–547	390	66	66	6	21	120	10
9	Buffalo Creek near Glencoe, Minn.	500	286-525	370	101	101	6	13	130	70
10	South Fork Crow River at Delano, Minn.	2,360	1,200–4,740	2,150	168	172	7	33	260	90
11	Pomme De Terre River at Appleton, Minn.	550	290–694	430	168	--	16	26	230	110
12	Le Sueur River near Rapidan, Minn.	3,100	1,870–2,920	2,270	752	755	10	64	900	610
13	Minnesota River at Mankato, Minn.	12,300	7,000–23,600	12,700	294	298	10	40	390	210
14	Minnesota River near Jordan, Minn.	14,600	9,060–18,300	13,500	427	429	8	51	550	310
15	Minnesota River at Fort Snelling State Park, Minn.	28,500	14,800–22,400	18,600	826	800	6	246	1,400	170
16	Cascade Creek at 45th Ave. SW in Rochester, Minn.	150	75-200	127	455	454	4	143	910	0
17	Cascade Creek at 35th Ave. NW in Rochester, Minn.	155	80-220	135	480	453	4	109	800	0
18	Zumbro River at Kellogg, Minn.	5,300	2,730–5,380	3,900	947	946	6	119	1,300	640
19	North Fork Whitewater River near Elba, Minn.	670	340–750	490	585	582	3	11	630	530
20	Whitewater River near Beaver, Minn.	1,600	810–1,740	1,380	3,357	3,402	4	584	5,300	1,540

Table 9. Bedload at bankfull streamflow estimated using ratio estimators and jackknife resampling statistic for selected sites in Minnesota, 2007 through 2013.

[ft³/s, cubic foot per second; tons/day; tons per day; mg/L, milligram per liter; *N*, number of samples used in calculation; Minn. ,Minnesota; --, not computed because of unreliable samples; Ave., avenue; SW, southwest; NW, northwest]

Site number (figs. 1–4)	Station name	Bankfull stream-flow (ft³/s)	Range of streamflow used in calculation	Mean stream-flow (ft³/s)	Ratio estimate of bedload (tons/day)	Jackknife bias-free estimate of bedload (tons/day)	*N*	Standard error (mg/L)	95-percent confidence intervals	
									Upper	Lower
1	Knife River near Two Harbors, Minn.	1,880	1,060–3,070	1,870	289	290	4	74	527	0.0
2	Sucker River near Palmers, Minn.	380	202–394	320	23	24	5	17	71	0.0
3	Swan River near Toivola, Minn.	1,230	700–1,560	1,160	0.4	0.4	3	0.1	0.7	0.0
4	Wild Rice River at Twin Valley, Minn.	1,000	788–2,300	1,480	23	22	8	7	39	6.1
5	Wild Rice River near Ada, Minn.	1,560	882v2,500	1,530	245	240	8	23	300	190
6	Little Fork River at Littlefork, Minn.	6,900	3,890–6,880	5,170	47	46	4	12	85	8.3
7	Big Fork River near Craigsville, Minn.	1,970	1,310–2,410	1,950	12	12	6	4	23	0.6
8	Long Prairie River at Long Prairie, Minn.	530	276–537	423	27	28	4	6	48	7.7
9	Buffalo Creek near Glencoe, Minn.	500	288–742	426	22	22	8	8	40	4.2
10	South Fork Crow River at Delano, Minn.	2,360	1,300–4,740	2,880	142	140	8	24	199	86
11	Pomme De Terre River at Appleton, Minn.	550	297–694	440	2.9	3.0	16	0.9	4.6	0.8
12	Le Sueur River near Rapidan, Minn.	3,100	2,270–2,950	2,500	276	276	4	54	446	100
13	Minnesota River at Mankato, Minn.	12,300	6,980–23,000	11,100	364	368	8	65	522	0.0
14	Minnesota River near Jordan, Minn.	14,600	7,980–18,300	13,400	3.9	4.0	8	1.1	6.5	1.5
15	Minnesota River at Fort Snelling State Park, Minn.	28,500	14,800–20,500	18,600	70	70	4	15	116	26
16	Cascade Creek at 45th Ave. SW in Rochester, Minn.	150	75–202	126	9	10	4	2.7	19	1.6
17	Cascade Creek at 35th Ave. NW in Rochester, Minn.	155	80–214	133	2.2	2.3	4	0.7	4.7	0.0
18	Zumbro River at Kellogg, Minn.	5,300	2,720–7,040	4,400	791	787	5	81	1,000	560
19	North Fork Whitewater River near Elba, Minn.	670	338–797	515	85	88	3	12	140	37
20	Whitewater River near Beaver, Minn.	1,600	844–1,730	1,360	--	--	6	480	3,000	480

Table 10. Sites in Minnesota used to develop dimensionless sediment rating curves.

[USGS, U.S. Geological Survey; Tau, measure of the strength of nonlinear relations. The measure of strength is scaled to be in the range of -1 to 1, and a value close to 0 indicates that no relation exists between two variables. Tau correlation values approaching values of 1 or -1 indicate a strong monotonic relation between two variables; *p*-value, statistical probability level; DSRC, dimensionless sediment rating curve; Minn., Minnesota; <, less than; SSC, suspended-sediment concentration; NGVD 29, National Geodetic Vertical Datum of 1929; NAVD 88, North American Vertical Datum of 1988; Ave., avenue; NW, northwest]

Site[a] number (figs. 1–4)	USGS station number	Station name	Pfankuch[b] stability rating	Rosgen[c] stream classification	Tau	*p*-value
Suspended-sediment concentration DSRC: sites with good/fair stability rating						
1[d]	04015330	Knife River near Two Harbors, Minn.	Fair	B2	0.79	<0.01
3[e]	04020000	Swan River near Toivola, Minn.	Good	C6	0.69	<0.01
4[d]	05062500	Wild Rice River at Twin Valley, Minn.	Fair	C5	0.70	<0.01
6[d]	05131500	Little Fork River at Littlefork, Minn.	Fair	F3	0.58	<0.01
7[e]	05131870	Big Fork River near Craigsville, Minn.	Good	C6	0.64	<0.01
19[f]	05376000	North Fork Whitewater River near Elba, Minn.	Fair	C4	0.60	<0.01

[a]Sites 8, 9, 11, and 15 not selected because of nonsignificant relation between SSC and streamflow (table 8).

[b]From Pfankuch, 1975.

[c]From Rosgen, 1994.

[d]U.S. Geological Survey streamgage.

[e]Minnesota Department of Natural Resources streamgage.

[f]Vertical datum is assumed, NGVD 1929 or NAVD 1988 datum elevation not established.

Site number (figs. 1–4)	USGS station number	Station name	Pfankuch[a] stability rating	Rosgen[b] stream classification	Tau	*p*-value
Suspended-sediment concentration DSRC: sites with poor stability rating						
2[c]	04015340	Sucker River near Palmers, Minn.	Poor	B2	0.55	<0.01
5[c]	05063000	Wild Rice River near Ada, Minn.	Poor	F5	0.66	<0.01
10[d]	05279400	South Fork Crow River at Delano, Minn.	Poor	C5	0.44	<0.01
12[d]	05320500	Le Sueur River near Rapidan, Minn.	Poor	F4	0.79	<0.01
13[d]	05325000	Minnesota River at Mankato, Minn.	Poor	F5	0.52	<0.01
14[d]	05330000	Minnesota River near Jordan, Minn.	Poor	F4	0.74	<0.01
16[e]	05372983	Cascade Creek at 45th Ave. SW in Rochester, Minn.	Poor	F5	0.57	<0.01
17[e]	0537298550	Cascade Creek at 35th Ave. NW in Rochester, Minn.	Poor	C4	0.48	<0.01
18[c]	05374900	Zumbro River at Kellogg, Minn.	Poor	F5	0.57	<0.01
20[c]	05376800	Whitewater River near Beaver, Minn.	Poor	C5	0.85	<0.01

[a]From Pfankuch, 1975.

[b]From Rosgen, 1994.

[c]Minnesota Department of Natural Resources streamgage.

[d]U.S. Geological Survey streamgage.

[e]Vertical datum is assumed, NGVD 1929 or NAVD 1988 datum elevation not established.

Table 10. Sites in Minnesota used to develop dimensionless sediment rating curves.—Continued

[USGS, U.S. Geological Survey; Tau, measure of the strength of nonlinear relations. The measure of strength is scaled to be in the range of -1 to 1, and a value close to 0 indicates that no relation exists between two variables. Tau correlation values approaching values of 1 or -1 indicate a strong monotonic relation between two variables; *p*-value, statistical probability level; DSRC, dimensionless sediment rating curve; Minn., Minnesota; <, less than; SSC, suspended-sediment concentration; NGVD 29, National Geodetic Vertical Datum of 1929; NAVD 88, North American Vertical Datum of 1988; Ave., avenue; NW, northwest]

Site[a] number (figs. 1–4)	USGS station number	Station name	Pfankuch[b] stability rating	Rosgen[c] stream classification	Tau	*p*-value
Bedload DSRC: Sites with good/fair stability rating						
1[d]	04015330	Knife River near Two Harbors, Minn.	Fair	B2	0.83	<0.01
8[d]	05245100	Long Prairie River at Long Prairie, Minn.	Fair	E5	0.31	0.046
9[e]	05278930	Buffalo Creek near Glencoe, Minn.	Fair	C4	0.79	<0.01
11[d]	05294000	Pomme De Terre River at Appleton, Minn.	Good	C4	0.37	0.025
19[f]	05376000	North Fork Whitewater Rivernear Elba, Minn.	Fair	C4	0.67	<0.01

[a]Sites 3, 4, 6, and 7 not selected because of nonsignificant relation between bedload and streamflow (see table 8).

[b]From Pfankuch, 1975.

[c]From Rosgen, 1994.

[d]U.S. Geological Survey streamgage.

[e]Minnesota Department of Natural Resources streamgage.

[f]Vertical datum is assumed, NGVD 1929 or NAVD 1988 datum elevation not established.

Site[ab] number (figs. 1–4)	USGS station number	Station name	Pfankuch[c] stability rating	Rosgen[d] stream classification	Tau	*p*-value
Bedload DSRC: Sites with poor stability rating						
5[e]	05063000	Wild Rice River near Ada, Minn.	Poor	F5	0.79	<0.01
10[e]	05279400	South Fork Crow River at Delano, Minn.	Poor	C5	0.69	<0.01
12[f]	05320500	Le Sueur River near Rapidan, Minn.	Poor	F4	0.56	<0.01
13[f]	05325000	Minnesota River at Mankato, Minn.	Poor	F5	0.67	<0.01
14[f]	05330000	Minnesota River near Jordan, Minn.	Poor	F4	0.54	0.01
16[g]	05372983	Cascade Creek at 45th Ave. SW in Rochester, MN	Poor	F5	0.78	<0.01
17[g]	0537298550	Cascade Creek at 35th Ave. NW in Rochester, MN	Poor	C4	0.71	<0.01
18[e]	05374900	Zumbro River at Kellogg, Minn.	Poor	F5	0.68	<0.01

[a]Site 2 not selected because of nonsignificant relation between bedload and streamflow (table 8).

[b]Site 20 not selected because sampler (BL-84) bag inoperable (mesh clogging) at flows greater than 500–700 ft^3/s.

[c]From Pfankuch, 1975.

[d]From Rosgen, 1994.

[e]Minnesota Department of Natural Resources streamgage.

[f]U.S. Geological Survey streamgage.

[g]Vertical datum is assumed, NGVD 1929 or NAVD 1988 datum elevation not established.

Errors in site-specific regression models associated with variability in measured SSC and bedload are quantified using the 95-percent confidence intervals. Thus, it is important to report the values of SSC and bedload at any given streamflow by using a range of values as opposed to a single SSC or bedload value. The effectiveness of the Pagosa Springs and Minnesota DSRC models in predicting SSC and bedload is based in part on the proximity of the model(s) fitted trendline of the DSRC models to the 95-percent confidence interval of the site-specific regression model trendline.

Table 11. Determination of dimensionless and corresponding dimensional values of streamflow and suspended-sediment concentration using Minnesota dimensionless sediment rating curves for the North Fork Whitewater River near Elba, Minnesota (site 19; U.S. Geological Survey station number 05376000).

[*Q*, streamflow; ft³/s, cubic foot per second; SSC, suspended-sediment concentration; mg/L, milligram per liter]

		Bankfull Q = 670 ft³/s	Bankfull SSC = 582 mg/L	Stability = Good/fair
Equation		Parameter		
$SSC = B_0 + B_1 Q^{B2}$		B_0	B_1	B_2
		0.026	0.974	0.951
Dimensionless ratio value		Dimensional value		Measured value
Q, ft³/s	SSC, (mg/L)	Streamflow, (ft³/s)	SSC, (mg/L)	SSC (mg/L)
Suspended-sediment concentration rating curve model prediction				
0.07	0.10	47	60	39
0.077	0.11	52	65	48
0.082	0.12	55	68	35
0.105	0.14	70	82	58
0.1205	0.16	81	91	38
0.135	0.17	90	100	34
0.159	0.2	107	114	20
0.17	0.21	114	120	79
0.196	0.23	131	136	36
0.202	0.24	135	139	59
0.226	0.26	151	153	37
0.25	0.29	168	167	81
0.5	0.53	335	308	299
0.575	0.6	385	350	343
1	1	670	582	582
1.118	1.11	749	645	640

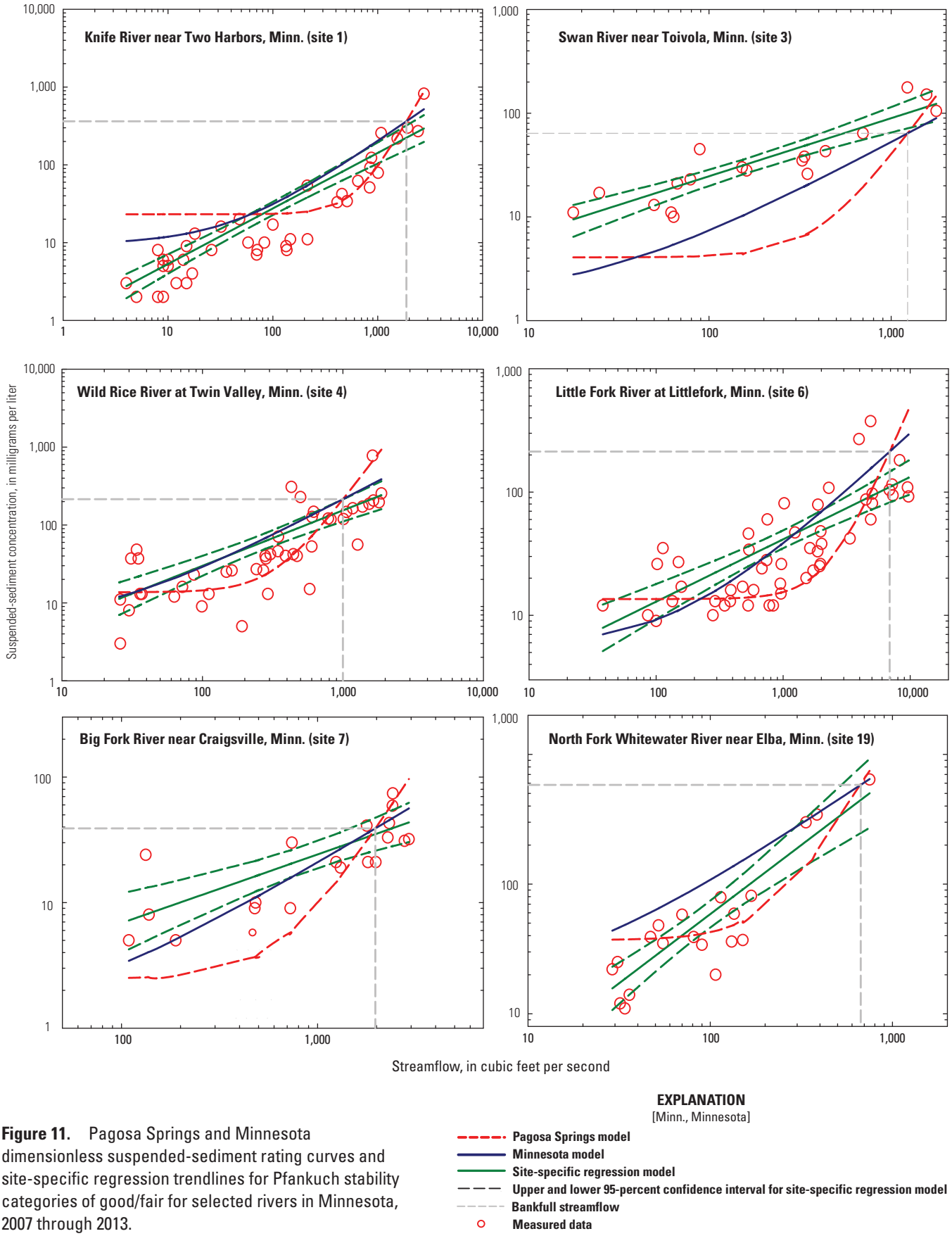

Figure 11. Pagosa Springs and Minnesota dimensionless suspended-sediment rating curves and site-specific regression trendlines for Pfankuch stability categories of good/fair for selected rivers in Minnesota, 2007 through 2013.

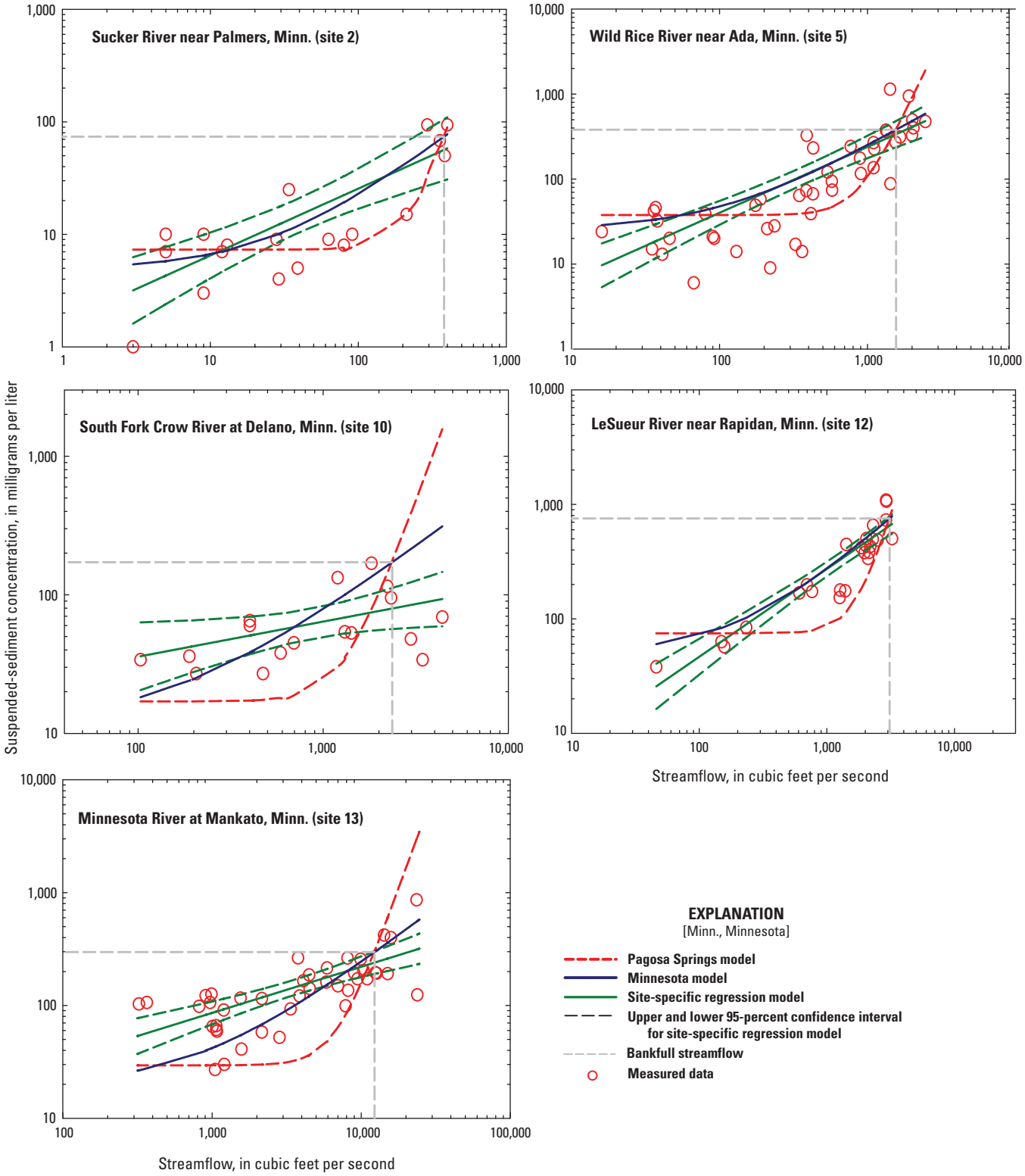

Figure 12. Pagosa Springs and Minnesota dimensionless suspended-sediment rating curves and site-specific regression trendlines for Pfankuch stability categories of poor for selected rivers in Minnesota, 2007 through 2013.

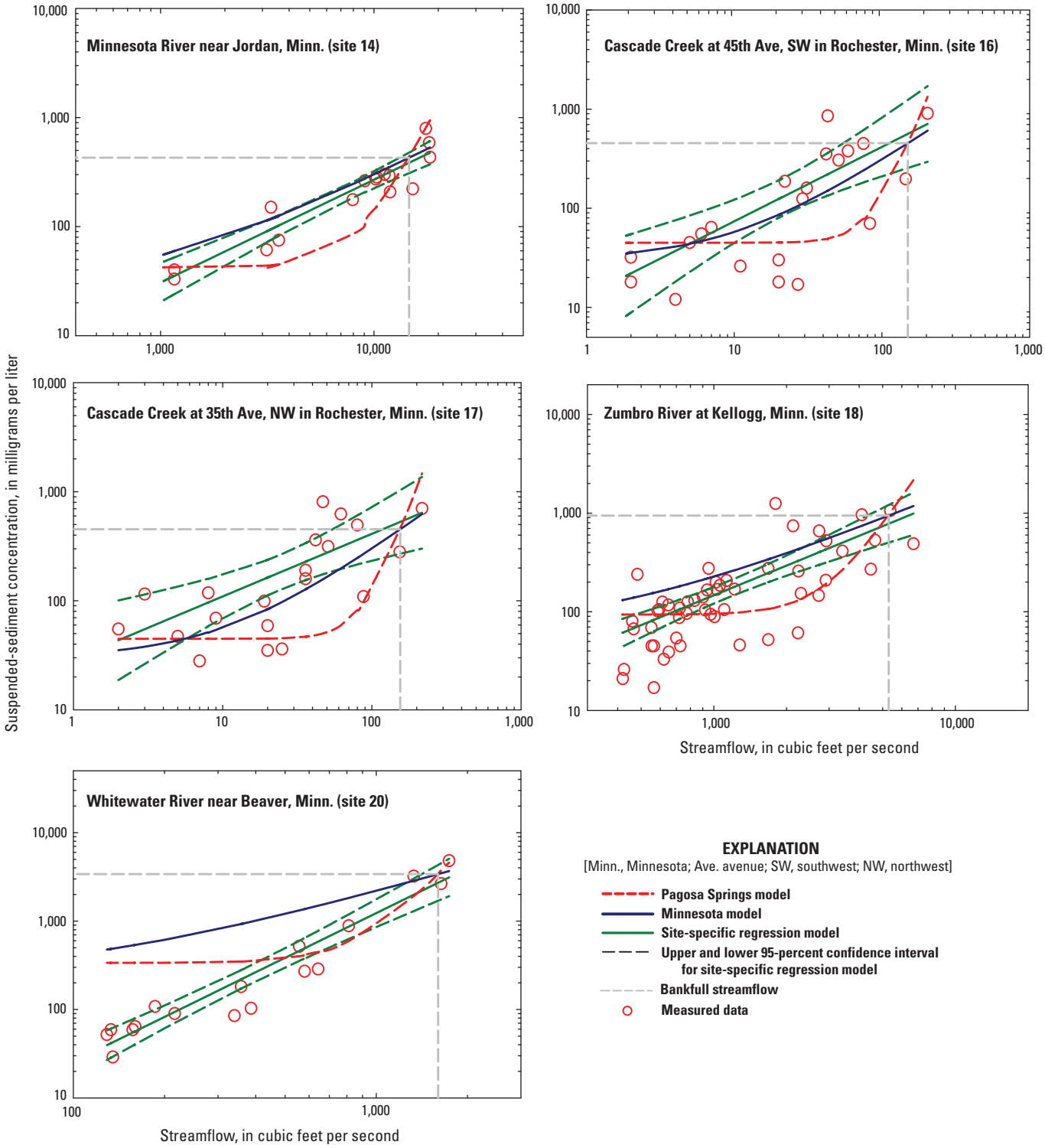

Figure 12. Pagosa Springs and Minnesota dimensionless suspended-sediment rating curves and site-specific regression trendlines for Pfankuch stability categories of poor for selected rivers in Minnesota, 2007 through 2013.—Continued

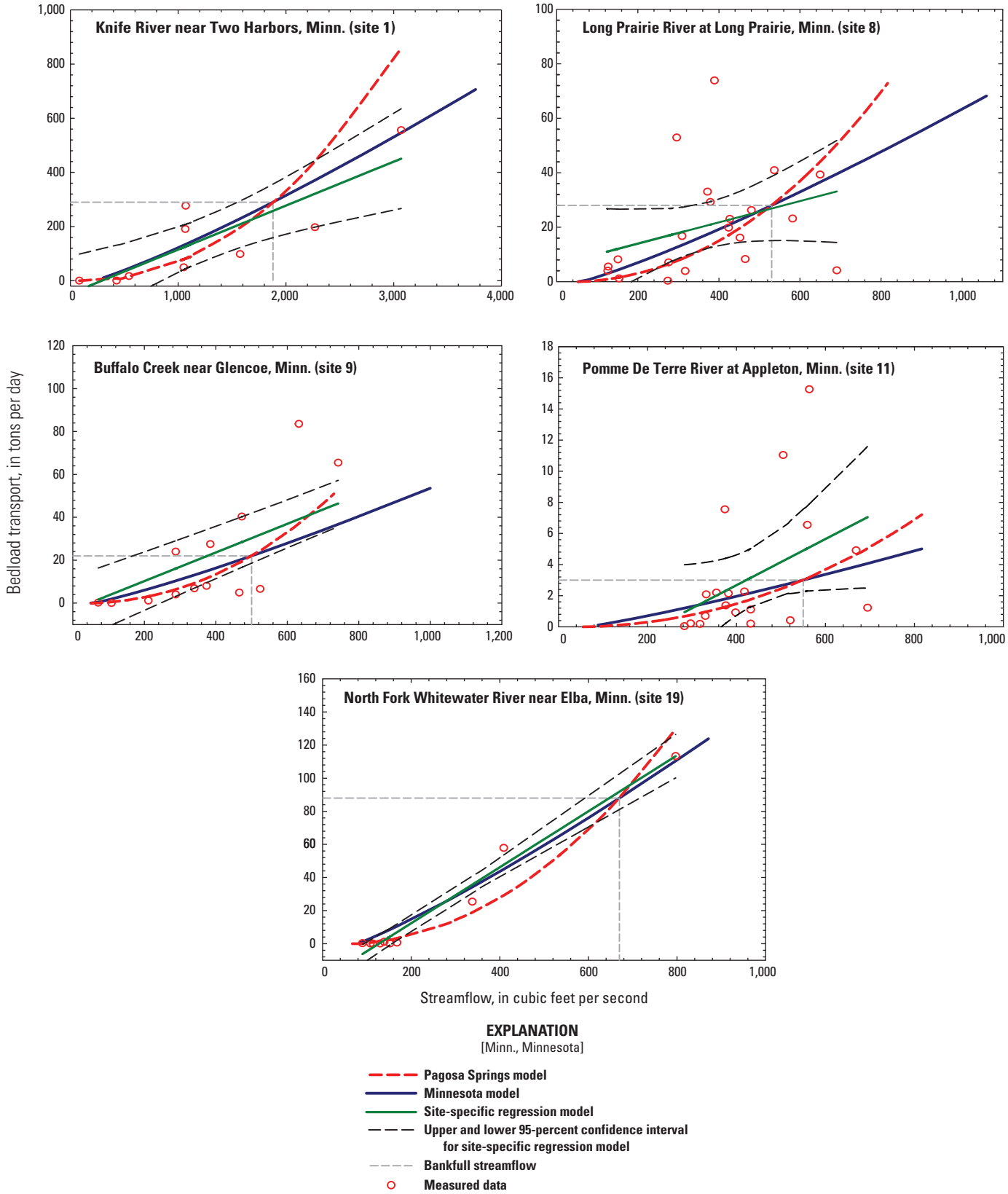

Figure 13. Pagosa Springs and Minnesota dimensionless bedload rating curves and site-specific regression trendlines for Pfankuch stability categories of good/fair for selected rivers in Minnesota, 2007 through 2013.

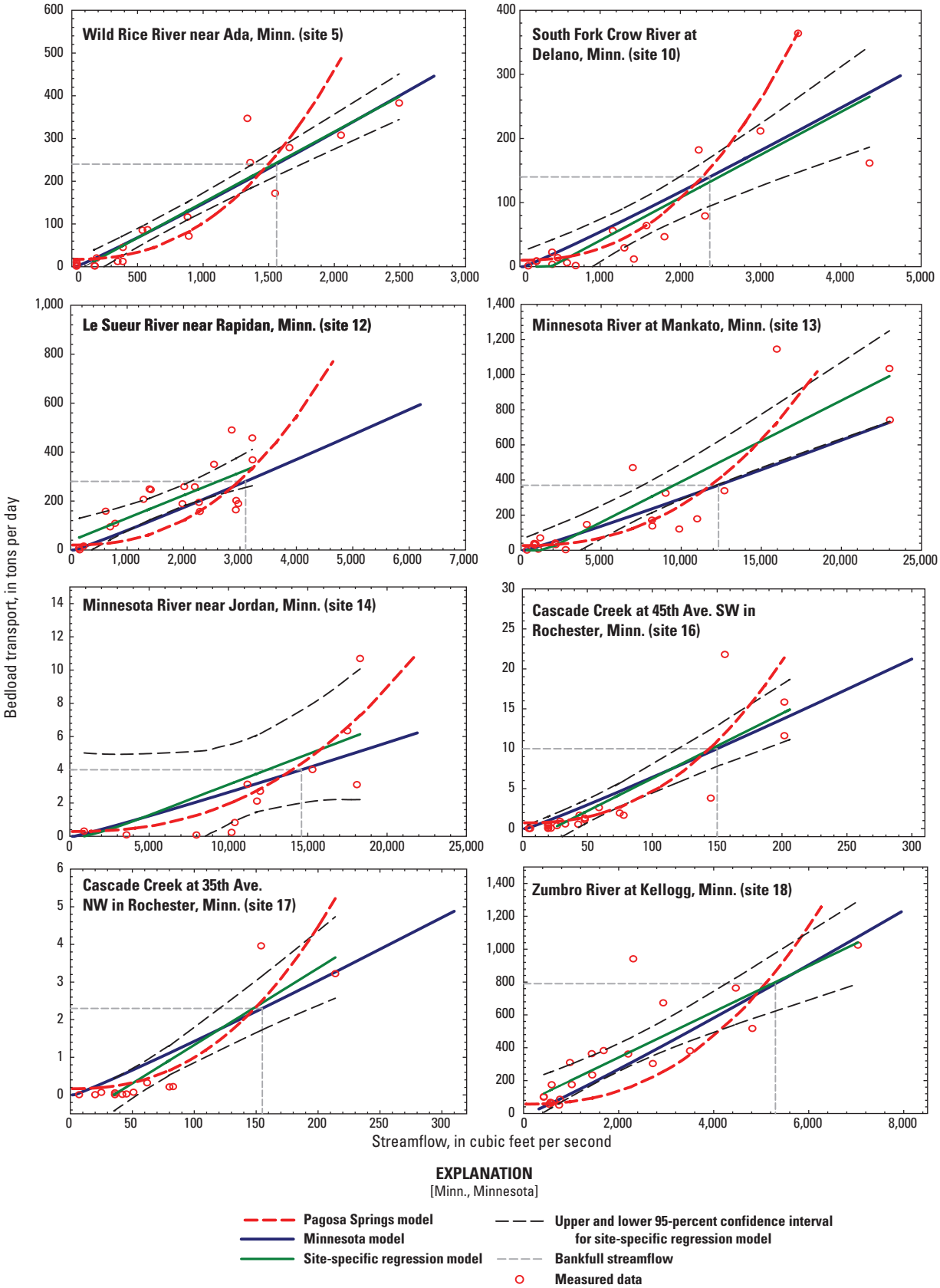

Figure 14. Pagosa Springs and Minnesota dimensionless bedload rating curves and site-specific regression trendlines for Pfankuch stability categories of poor for selected rivers in Minnesota, 2007 through 2013.

Suspended-Sediment Concentrations

Unique characteristics were observed among sites for the Pagosa Springs DSRC models developed to approximate SSC. Specifically, low sensitivity (little change in slope) at lower streamflows coupled with an identifiable inflection point associated with a marked increase in slope of the fitted trendline was observed for the Pagosa Springs DSRC models (figs. 11 and 12). Low sensitivity at low streamflows may not substantially affect estimates of annual sediment loads because higher streamflows typically contribute the bulk of sediment loads. Initially, there was concern that Pagosa Springs DSRC models did not represent SSC at zero flows because the intercept parameter forces a positive value for SSC at zero streamflow (equations 1 and 3). This concern was discounted because zero streamflow conditions do not necessarily infer a dry channel, and fine sediments may remain suspended during stagnant streamflow.

A notable concern is the disparity in values between regression exponents (slopes) from the Pagosa Springs DSRCs and site-specific regression exponents for rivers in Minnesota. Inspecting each site-specific regression model trendline alongside the regression trendlines for the Pagosa Springs DSRC models at flows near bankfull indicated that Pagosa Springs DSRC models resulted in distinctly larger slopes than the site-specific regression models for SSC (figs. 11 and 12). For good/fair stability sites, the mean slope of the Pagosa Springs DSRC models for estimating SSC was 3.5 times larger than the mean slope of the site-specific regression models. The largest difference in slope was at site 3 in northeastern Minnesota, which had a slope of 0.56 for the site-specific regression model compared to a slope of 2.41 for the Pagosa Springs model. The smallest difference was at site 19 in southeastern Minnesota, which had a slope of 1.07 for the site-specific regression model and slope of 2.41 for the Pagosa Springs DSRC model. For poor stability sites, the mean slope of the Pagosa Springs DSRC models (3.66) was 4.7 times larger than the mean slope of the site-specific regression models (0.78). The largest difference was at site 10, which had a slope of 0.25 for the site-specific regression model and a slope of 3.66 for the Pagosa Springs DSRC model. The smallest difference was at site 20, which had a slope of 1.68 for the site-specific regression model and a slope of 3.66 for the Pagosa Springs DSRC model. A consequence of this is that predictions of SSC from Pagosa Springs DSRC models will overestimate SSC and suspended-sediment loads at streamflows exceeding bankfull compared to the site-specific regression models.

Compared to Pagosa Springs DSRC models, Minnesota DSRC models for SSC more closely approximated the site-specific regression models developed from the measured data (figs. 11 and 12). Inspection of the regression trendlines for the Minnesota and Pagosa Springs DSRC models and the site-specific regression models indicate that the regional Minnesota DSRCs are more applicable to rivers in Minnesota. For example, Minnesota DSRC models were more sensitive to variability in streamflow during lower streamflows for SSC, unlike the Pagosa Springs DSRC models, which indicated little response to changes in streamflow at low streamflows. Also, the regression exponents for the Minnesota DSRC models more closely matched the site-specific regression exponents and were markedly lower than regression exponents from the Pagosa Springs DSRC models. For example, the mean slopes of 0.951 and 1.006 for SSC for the Minnesota DSRC models for good/fair and poor stability streams, respectively, were markedly lower than mean slopes of 2.41 and 3.66, respectively, for the Pagosa Springs DSRC models. Large differences in model slopes indicate that the individual river sediment signatures for Minnesota's rivers were not as well represented in the Pagosa Springs DSRC models as compared to the Minnesota DSRC models.

Although Minnesota DSRC models were better than Pagosa Springs DSRC models at approximating site-specific regression models, the effects of regional variation were evident in the model results. For rivers in southeastern Minnesota (sites 18 through 20), the Minnesota DSRC model regression lines were offset substantially (greater than) compared to the site-specific regression lines (figs. 11 and 12). Similar differences between regression trendlines for the Minnesota DSRC and site-specific regression models also were observed at site 10 in south-central Minnesota (fig. 12). Overall, the Minnesota DSRC models approximated the site-specific regression models more closely than the Pagosa Springs DSRC models for 14 out of the 16 sites.

Bedload

Regression trendlines for bedload for the Pagosa Springs and Minnesota DSRC models and site-specific regression models for good/fair and poor stability categories are shown in figures 13 and 14, respectively. For bedload, Pagosa Springs DSRC models had characteristics similar to those demonstrated by the SSC DSRC models. Similar to the SSC DSRC models, the slopes of the regression trendlines for bedload at streamflows exceeding bankfull were larger for the Pagosa Springs DSRC models than for the Minnesota DSRC and site-specific regression models for most sites. For example, mean slopes for the Minnesota DSRC models were 1.316 and 1.306 for good/fair and poor stability streams, respectively, compared to mean slopes of 2.19 and 2.38, respectively, for the Pagosa Springs DSRC models. In contrast to SSC models, all bedload models nearly intercepted the y-axis at 0 during periods of no streamflow, which corresponds to the expected response of little bedload transport during low streamflows (Bagnold, 1973; Leopold and Emmett, 1976). Bedload data are known to demonstrate wide variability at similar or identical flows (Edwards and Glysson, 1999) and the samples collected for this study had considerable variability across the range of streamflows (figs. 13 and 14).

In general, the predicted values of bedload from the Pagosa Springs and Minnesota DSRC models are contained within the 95-percent confidence intervals of site-specific regression models; however, the Minnesota models more closely approximated the site-specific regression models

than did the Pagosa Springs DSRC models for most sites during streamflows near and exceeding bankfull streamflow (figs. 13 and 14). At lower streamflows, the Minnesota and Pagosa Springs DSRC models indicate similar fits to the measured data.

Nash-Sutcliffe Model Efficiencies

Nash-Sutcliffe Efficiency values were determined for the Pagosa Springs DSRC models, Minnesota DSRC models, and site-specific regression models for each of the study sites. The NSE values are presented in figure 15 for SSC and in figure 16 for bedload.

Suspended-Sediment Concentrations

Among models for SSC, the site-specific regression models provided the overall best fits for 10 out of 16 sites (fig. 15) based on the NSE values. The exceptions were sites 1, 2, 5, 12, and 13 (figs. 15*A* and 15*B*), for which the NSE values indicated that the Minnesota DSRC model had a slightly better fit than the site-specific regression model, and site 20, for which NSE values indicated that the Pagosa Springs DSRC model had a better fit than the other two models but the site-specific regression model had a better fit than the Minnesota DSRC model.

For SSC at the good/fair stability sites, the NSE values associated with the Pagosa Springs DSRC model indicated that fits were better than using the mean value of the measured data for only 3 out of 6 sites (sites 1, 3, and 19) and worse fits than using the mean value for the remaining 3 sites (sites 4, 6, and 7; fig. 15*A*). Conversely, the Minnesota DSRC models provided a better fit for good/fair stability sites than using the mean value of the measured data for 5 out of 6 sites with the exception of site 6 in northern Minnesota, which had an NSE value near 0, indicating that the model prediction was no more accurate than the mean of the measured data at predicting values of SSC. Also, the Minnesota DSRC models predicted measured data substantially better than the Pagosa Springs DSRC model at sites 4 and 7. For these two sites (sites 4 and 7), NSE values for the Pagosa Springs DSRC models were -1.18 and -0.56, whereas NSE values for the Minnesota models were 0.37 and 0.44, respectively.

Nash-Sutcliffe Efficiency values for poor stability sites for SSC models were similar to those for the good/fair stability sites (fig. 15*B*). The Pagosa Springs DSRC models provided fits that were better than the mean value of the measured data for only 3 of 10 sites (sites 2, 12, and 20), a slightly better fit than the mean value of the measured data for 2 sites (sites 14 and 16), and worse fits than the mean value for the measured data for the remaining 5 sites. The Minnesota DSRC models provided fits that were better than the mean value of the measured data for 9 of 10 poor stability sites and a worse fit than the mean for one site (site 10).

Considering all good/fair and poor stability sites, one of the largest differences in NSE values between the Pagosa Springs and Minnesota DSRC models was observed at site 13 in the Minnesota River Basin, where the Pagosa Springs model NSE value was -16.4 compared with the Minnesota model NSE value of 0.43 (fig. 15*B*). For the 8 sites with negative NSE values using the Pagosa Springs DSRC model, the Minnesota DSRC model provided positive NSE values for 6 of these 8 sites. Moreover, the Minnesota DSRC model closely approximated site-specific model NSE values for 14 of 15 sites, and had slightly better NSE values than site-specific regression model for 4 sites (sites 1, 2, 5, and 12). For sites 6 and 10, the Minnesota DSRC model NSE values indicated that the model was no better than using the mean value of the measured data.

Bedload

For bedload, the NSE values for the Pagosa Springs DSRC models indicated that these models were a better or slightly better predictor of the measured values compared to using the mean value of the measured data for 11 of 13 study sites (fig. 16). The exceptions were sites 8 and 10, which had negative NSE values of -0.26 and -1.14, respectively. For the 11 sites with positive NSE values using the Pagosa Springs DSRC models, 5 sites (sites 5, 14, 16, 17, and 19) had NSE values that exceeded 0.6, 4 sites had NSE values that ranged between 0.2 and 0.6, and 2 sites (sites 11 and 18), had NSE values (0.05 and 0.12, respectively) that were only slightly better than using the measured samples mean value. The Minnesota bedload DSRC models indicated markedly better NSE values than the Pagosa Springs DSRC models for nearly every site. For the Minnesota DSRC models, all 13 sites had positive NSE values and closely approximated the site-specific regression model results. The largest differences in NSE values between Pagosa Springs and Minnesota DSRC models were observed at sites 10, 1, and 18. At these three sites, the NSE values for the Pagosa Springs DSRC models were -1.14, 0.19, and 0.12, respectively, compared to NSE values of 0.67, 0.64, and 0.54, respectively, for the Minnesota DSRC models.

Model Biases and Limitations

Model biases can affect calculation and subsequent interpretations of the NSE values if the presence and magnitude of systematic errors are not identified and accounted for (McCuen and others, 2006). Relative model bias (R_b) (equations 11 and 12) is a measure of the model's prediction error (residual error) relative to the mean value of the measured data points. An R_b value greater than 5 percent is considered substantial; positive values indicate that models overestimate measured values, whereas negative values indicate underestimation of measured values. Model biases are presented in table 12. For Pagosa Springs and Minnesota SSC and bedload

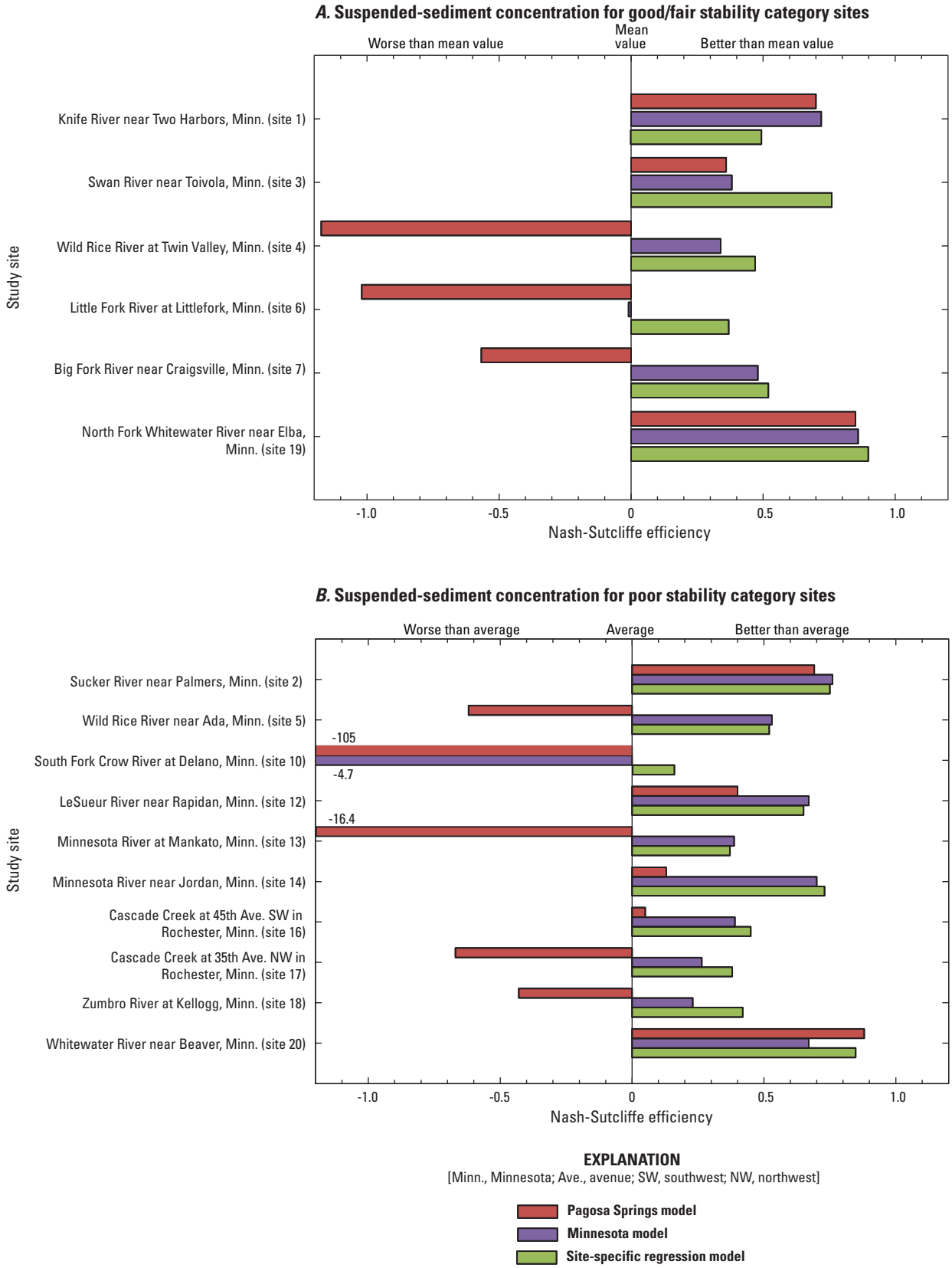

Figure 15. Nash-Sutcliffe Efficiency values for Pagosa Springs and Minnesota dimensionless rating curves and site-specific models for suspended-sediment concentrations for Pfankuch stability categories of good/fair and poor for selected rivers in Minnesota.

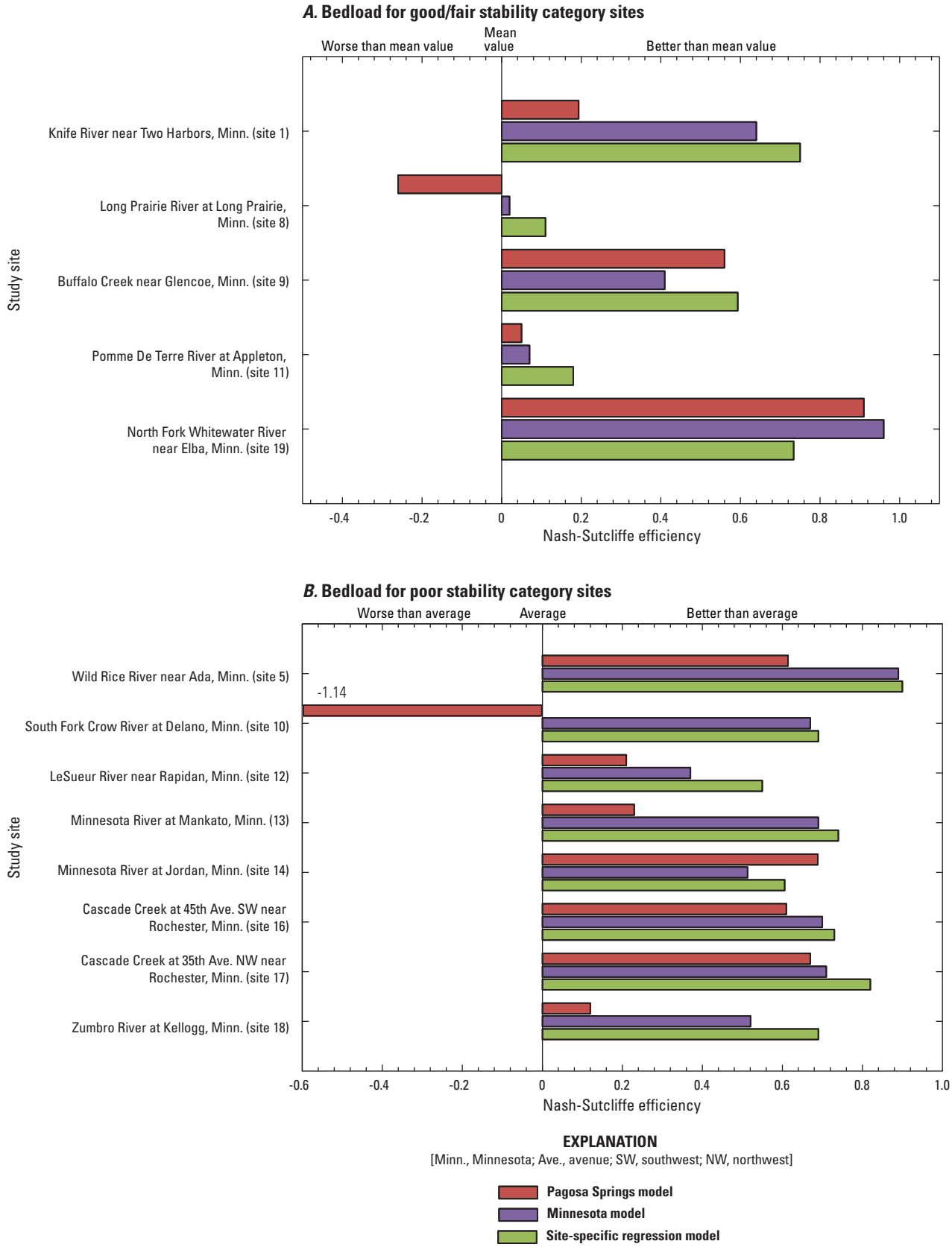

Figure 16. Nash-Sutcliffe Efficiency values for Pagosa Springs and Minnesota dimensionless rating curves and site-specific models for bedload for Pfankuch stability categories of good/fair and poor for selected rivers in Minnesota.

DSRC models, model biases were substantial for nearly every site (table 12). Biases ranged from 1 percent for the Minnesota DSRC bedload model at site 5 in northwestern Minnesota to 193 percent for the Pagosa Springs DSRC SSC model at site 10 in south-central Minnesota. Model biases negatively affect the ability of the models to accurately predict SSC, bedload, and total sediment loads.

The R_b value provides important information from which site-specific models predictive ability can be improved, but is limited as a corrective index for DSRC models because the purpose of DSRC models is to estimate SSC and bedload across multiple sites. Positive and negative model biases (table 12) require corrections to be applied to site-specific models to improve model predictive abilities; therefore, the magnitude of model biases should be examined before application of DSRC models. The application of a corrective index for bias in DSRC models depends on myriad factors beyond the scope of this study. Overall, the analysis indicates smaller model biases for the Minnesota DSRC model for SSC (29.9 percent) and bedload (19.6 percent) as compared to Pagosa Springs DSRC models of 37.4 and 29.2 percent, respectively (table 12).

Annual Sediment Loads

The R-LOADEST statistical package (Runkel and others, 2004; Cohn and others, 1989; R Development Core Team, 2011) was used to compute annual suspended-sediment loads, annual bedload, and 95-percent prediction intervals based on measured data from collected samples; these are referred to as “measured annual SSL” or “measured annual bedload”. Annual SSL and annual bedload for selected sites also were calculated from the predicted daily loads using equation 13 and the Pagosa Springs and Minnesota DSRC models; these are referred to as “estimated annual SSL” or “estimated annual bedload”. The measured and estimated sediment loads were compared for years 2012 and 2013.

Suspended-Sediment Loads

The R-LOADEST statistical package was used to compute (measured) annual SSL along with 95-percent prediction intervals for measured SSC data using the R statistical environment (R Development Core Team, 2011). Calculation of measured annual SSL was limited to four good/fair stability sites and eight poor stream stability sites because estimates require daily mean streamflows from streamgages (Cohn and others, 1989). Annual estimated SSL for the same four good/fair stream stability sites and eight poor stability sites were computed using predicted data from Pagosa Springs and Minnesota DSRC models for years 2012 and 2013. The measured annual SSL with 95-percent prediction intervals along with estimated annual SSL based on the Pagosa Springs and Minnesota DSRC models are presented in figures 17 through 19. The estimated annual SSL based on the Pagosa Springs and Minnesota DSRC models that are within the range of the 95-percent prediction intervals of the measured annual SSL using the R-LOADEST models are not considered to be significantly different from each other.

For the four good/fair stream stability sites (sites 1, 4, 6, and 7), the estimated annual SSL based on the Minnesota DSRC model were not significantly different than the measured annual SSL based on the R-LOADEST regression models for 2012 and 2013 (fig. 17). In contrast, the estimated annual SSL based on the Pagosa Springs DSRC model for the good/fair stream stability sites were significantly different than measured annual SSL for three sites (sites 1, 4, and 7) in 2012, and for three sites (4, 6, and 7) in 2013 (fig. 17). The Pagosa Springs DSRC model tended to underestimate measured annual SSL for 2012, and overestimate annual SSL in 2013 (fig. 17). Underestimation of annual SSL in 2012 by the Pagosa Springs model (sites 4 and 7) is attributed to a combination of factors that include variability among model parameters (that is, model constants, coefficients, and exponents) and low streamflow in 2012. For example, in 2012, site 4 had maximum daily mean streamflows that were less than the bankfull streamflow (table 2; table 6; fig. 7).

For poor stream stability sites, estimated annual SSL based on the Minnesota DSRC model were not significantly different from the measured annual SSL for 5 of 8 study sites (sites 2, 5, 12, 13, and 14) in 2012 (fig. 18) and not significantly different for 4 of 8 study sites (sites 2, 5, 13, and 14) in 2013 (fig. 19). For poor stability sites with significantly different SSL between the Minnesota DSRC model and measured annual SSL (figs. 18 and 19), the Minnesota DSRC model overestimated SSL for each site. In comparison, estimated annual SSL based on the Pagosa Springs DSRC model for poor stability sites were significantly different than measured annual SSL for 6 of 8 study sites (sites 2, 5, 10, 12, 14, and 20) in 2012 (fig. 18), and significantly different for all 8 sites (fig. 19) in 2013. The estimated annual SSL based on the Pagosa Springs model were significantly larger than measured annual SSL for sites in 2013, and also were substantially larger than estimated annual SSL based on the Minnesota DSRC model. The larger annual SSL estimated by the Pagosa Springs DSRC models are expected for sites with streamflows that exceed bankfull because Pagosa Springs DSRC models have substantially larger regression exponents (slopes) compared to the Minnesota DSRC models and site-specific regression models.

Table 12. Model biases for suspended-sediment concentration and bedload transport for Pagosa Springs and Minnesota dimensionless sediment rating curve models and site-specific models.

[USGS, U.S. Geological Survey; SSC, suspended-sediment concentration; DSRC, dimensionless sediment rating curve; Minn., Minnesota; --, model bias not computed; Ave., avenue; NW, north west]

Site number figs. 1–4	USGS station number	Site name	Pagosa Springs DSRC SSC model bias (percent)	Minnesota DRSC SSC model bias (percent)	Site-specific SSC model bias (percent)	Pagosa Springs bedload model bias (percent)	Minnesota DSRC bedload model bias (percent)	Site-specific bedload model bias (percent)
1	04015330	Knife River near Two Harbors, Minn.	28	38	-8	27	18	2
2	04015340	Sucker River near Palmers, Minn.	-13	7	-5	--	--	--
3	04020000	Swan River near Toivola, Minn.	-51	-51	-3	--	--	--
4	05062500	Wild Rice River at Twin Valley, Minn.	58	30	-3	--	--	--
5	05063000	Wild Rice River near Ada, Minn.	15	5	-5	19	1	2
6	05131500	Little Fork River at Littlefork, Minn.	13	35	-5	--	--	--
7	05131870	Big Fork River near Craigsville, Minn.	17	7	2	--	--	--
8	05245100	Long Prairie River at Long Prairie, Minn.	--	--	--	-23	-14	0
9	05278930	Buffalo Creek near Glencoe, Minn.	--	--	--	-26	-25	7
10	05279400	South Fork Crow River at Delano, Minn.	193	67	-0.4	71	17	2
11	05294000	Pomme De Terre River at Appleton, Minn.	--	--	--	-39	-32	0
12	05320500	Le Sueur River near Rapidan, Minn.	-35	6	-4	-32	-27	0
13	05325000	Minnesota River at Mankato, Minn.	54	-3	-2	21	-14	1
14	05330000	Minnesota River near Jordan, Minn.	8	11	-2	19	9	-7
16	05372983	Cascade Creek at 45th Ave. SW in Rochester, Minn.	-37	-27	-5	29	19	5
17	0537298550	Cascade Creek at 35th Ave. NW in Rochester, Minn.	-39	-33	-2	40	38	13
18	05374900	Zumbro River at Kellogg, Minn.	-15	42	1	-28	-25	0
19	05376000	North Fork Whitewater River near Elba, Minn.	-8	47	-9	-5	16	6
20	05376800	Whitewater River near Beaver, Minn.	15	70	9	--	--	--
		Mean absolute model basis	**37.4**	**29.9**	**4.1**	**29.2**	**19.6**	**3.5**

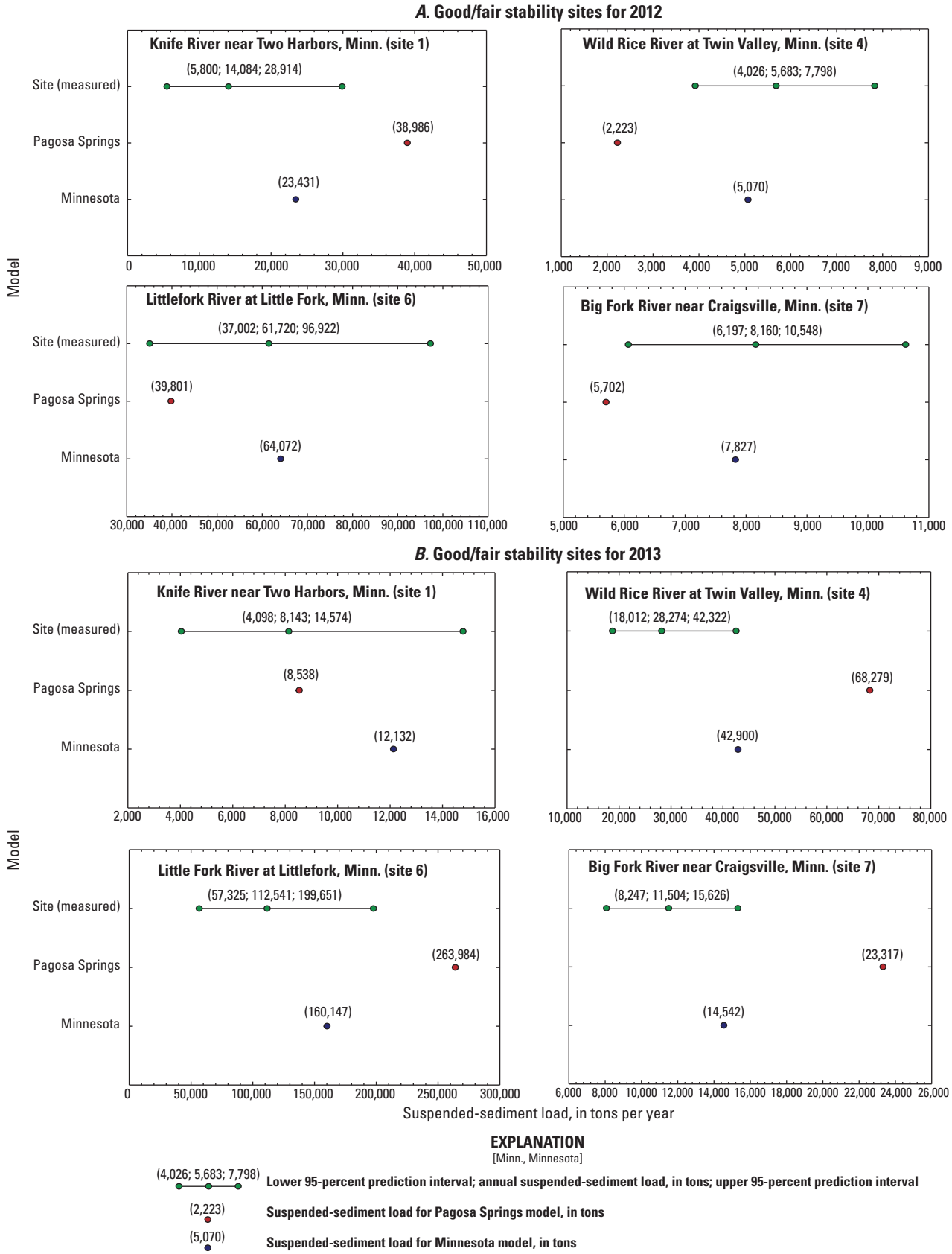

Figure 17. Measured annual suspended-sediment loads based on R-LOADEST models (site [measured]) with 95-percent prediction intervals, and estimated loads based on the Pagosa Springs and Minnesota dimensionless sediment rating curve models for good/fair stability sites. *A*, year 2012 and *B*, year 2013.

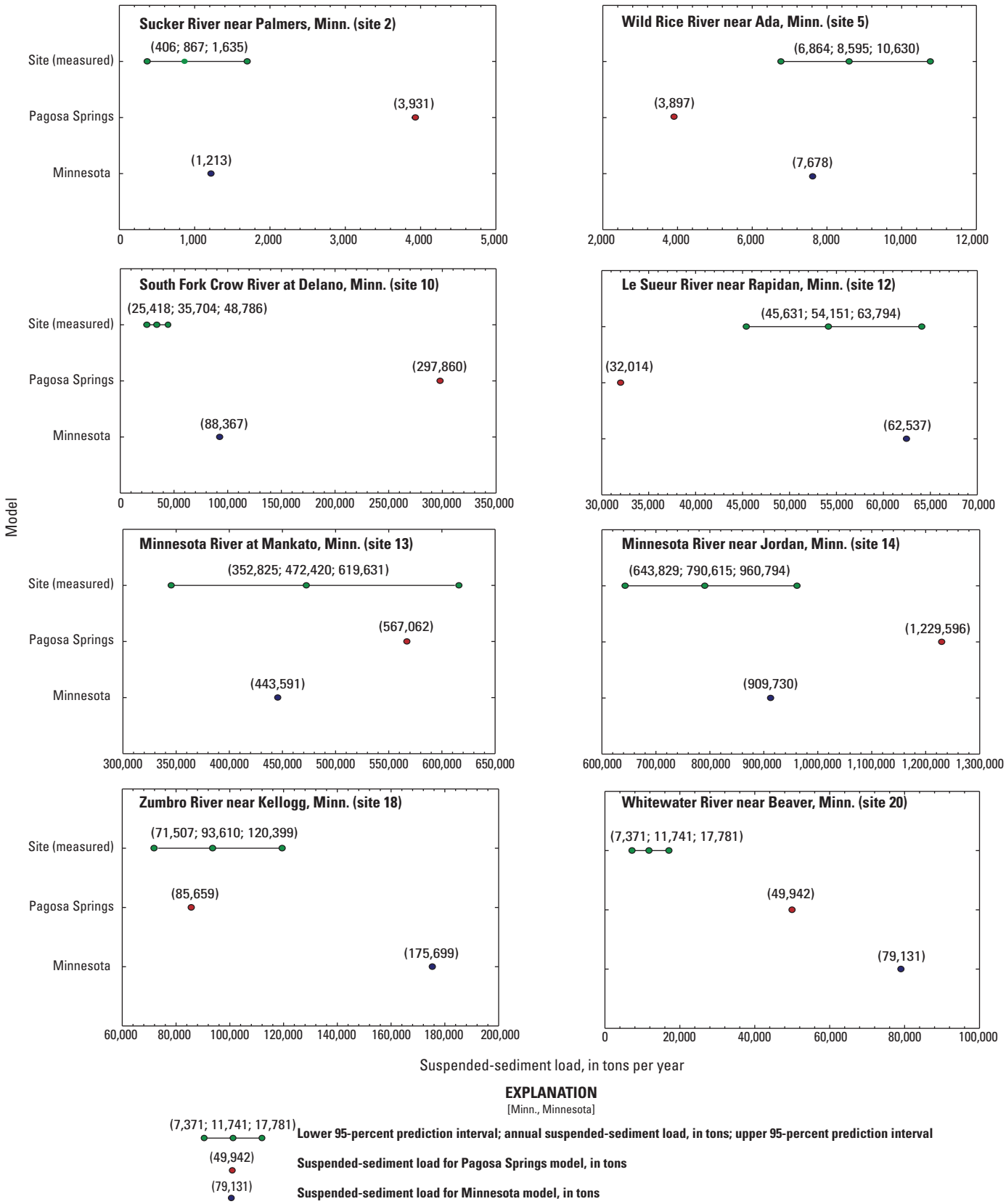

Figure 18. Measured annual suspended-sediment loads based on R-LOADEST models (site [measured]) with 95-percent prediction intervals, and estimated loads based on the Pagosa Springs and Minnesota dimensionless sediment rating curve models for poor stability sites for 2012.

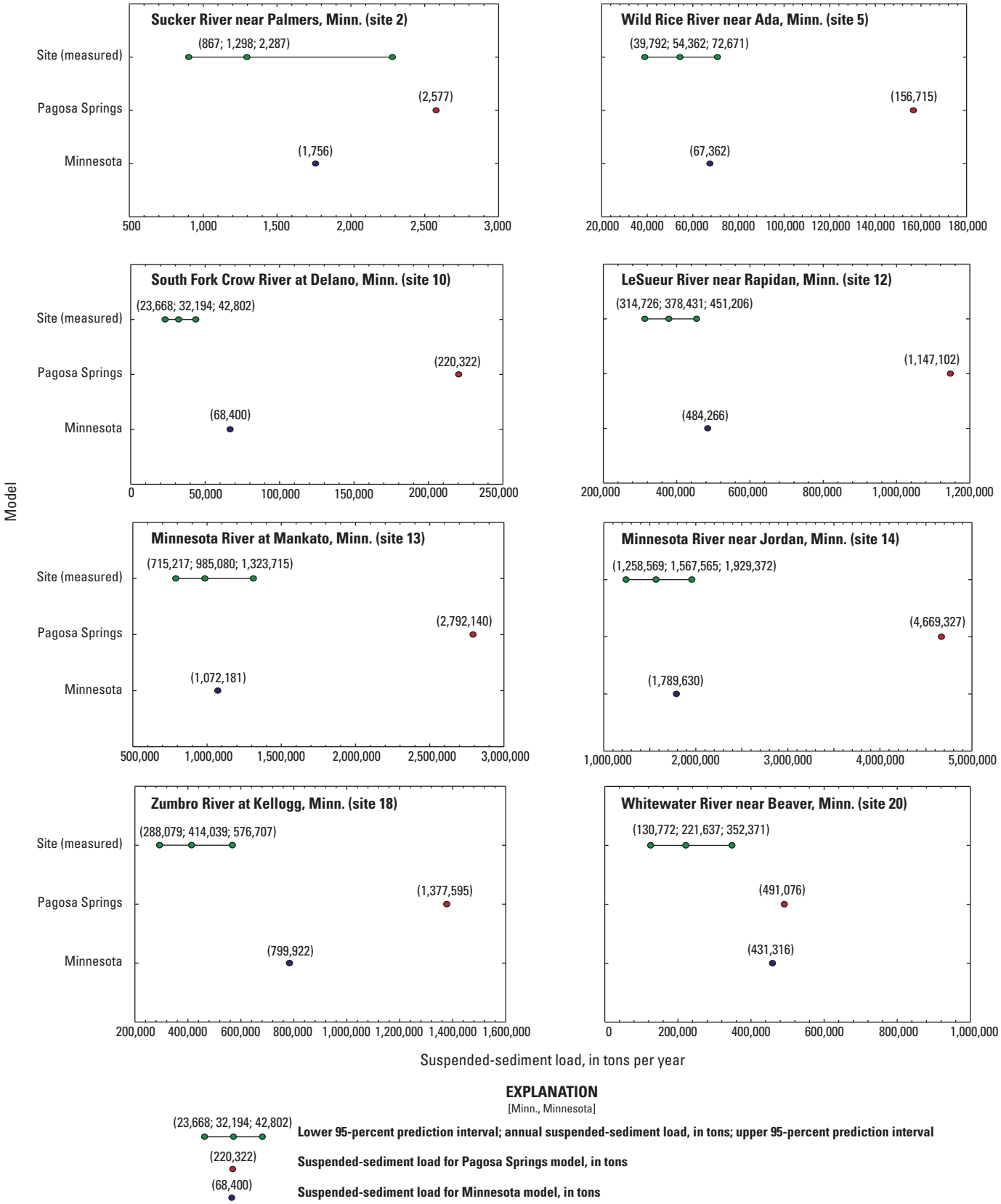

Figure 19. Measured annual suspended-sediment loads based on R-LOADEST models (site [measured]) with 95-percent prediction intervals, and estimated suspended-sediment loads based on the Pagosa Springs and Minnesota dimensionless sediment rating curve models for poor stability sites for 2013.

Bedload

The R-LOADEST statistical package was used to compute (measured) annual bedload along with 95-percent prediction intervals for measured bedload data. Calculation of annual bedload was limited to two good/fair stability sites and five poor stream stability sites. Estimated annual bedload for two good/fair stream stability sites and five poor stability sites using predicted data from the Pagosa Springs and Minnesota DSRC models were compared to measured annual bedload for 2012 (fig. 20) and 2013 (fig. 21).

For the two good/fair stream stability sites (sites 8 and 11), estimated annual bedload based on the Minnesota DSRC model were not significantly different than the measured annual bedload for 2012 (fig. 20) and 2013 (fig. 21). Estimated annual bedload based on the Pagosa Springs DSRC model for the same 2 good/fair stream stability sites were not significantly different than measured annual bedload for 1 out of the 2 sites in 2012, and were not significantly different for either of the 2 sites in 2013. The exception in 2012 was for site 8 in central Minnesota (fig. 20).

For poor stream stability sites, estimated annual bedload based on the Minnesota DSRC model were not significantly different from the measured annual bedload for 4 of 5 study sites (sites 5, 10, 12, and 13) in 2012 (fig. 20) and not significantly different for 3 of 5 study sites (sites 5, 10, and 13) in 2013 (fig. 21). For the two poor stability sites (sites 12 and 18) with significantly different annual bedload between the Minnesota DSRC model and measured annual bedload, the Minnesota DSRC model underestimated loads for each site. In comparison, the estimated annual bedload based on the Pagosa Springs model were significantly different than measured annual bedload for 2 of 5 study sites (sites 10 and 18) in 2012 (fig. 20), and significantly different for one site (site 18 in southeastern Minnesota) (fig. 21) in 2013. These results indicate that regression exponents (slopes) for Minnesota and Pagosa Springs DSRC models for bedload were markedly different than site-specific model slopes for sites 12 and 18, which are located in the Minnesota River Basin and southeastern Minnesota, respectively.

Implications of the Model Assessments

Results of data analyses indicate that DSRC models developed using data collected in Minnesota were more effective at compensating for differences in individual stream characteristics across a variety of basin sizes and flow regimes than DSRC models developed using data collected near Pagosa Springs, Colorado. Minnesota DSRC models retained a substantial portion of the unique sediment signatures for most rivers, although deviations were observed for streams with limited sediment supply and for rivers in southeastern Minnesota, which had markedly larger regression exponents. Compared to Pagosa Springs DSRC models, Minnesota DSRC models had regression slopes that more closely matched the slopes of site-specific regression models, had greater Nash-Sutcliffe Efficiency values, had lower model biases, and approximated measured annual loads more closely.

The results presented in this report indicate that regionally based DSRCs can be used to estimate reasonably accurate values of SSC and bedload. Practitioners are cautioned that DSRC reliability is dependent on representative measures of bankfull streamflow, SSCs, and bedload. It is, therefore, important that samples of SSC and bedload, which will be used for estimating SSC and bedload at the bankfull streamflow, are collected over a range of conditions that includes the ascending and descending limbs of the event hydrograph. Applicability of DSRC models may have substantial limitations under certain conditions. For example, DSRC models should not be used to predict SSC and loads for extreme streamflows, such as those that exceed twice the bankfull streamflow value because this constitutes conditions beyond the realm of current (2016) empirical modeling capability. Also, if relations between SSC and streamflow and between bedload and streamflow are not statistically significant, DSRCs should not be used to predict SSC or bedload, as this could result in large errors. For streams that do not violate these conditions, DSRC estimates of SSC and bedload can be used for stream restoration planning and design, and for estimating annual sediment loads for streams where little or no sediment data are available.

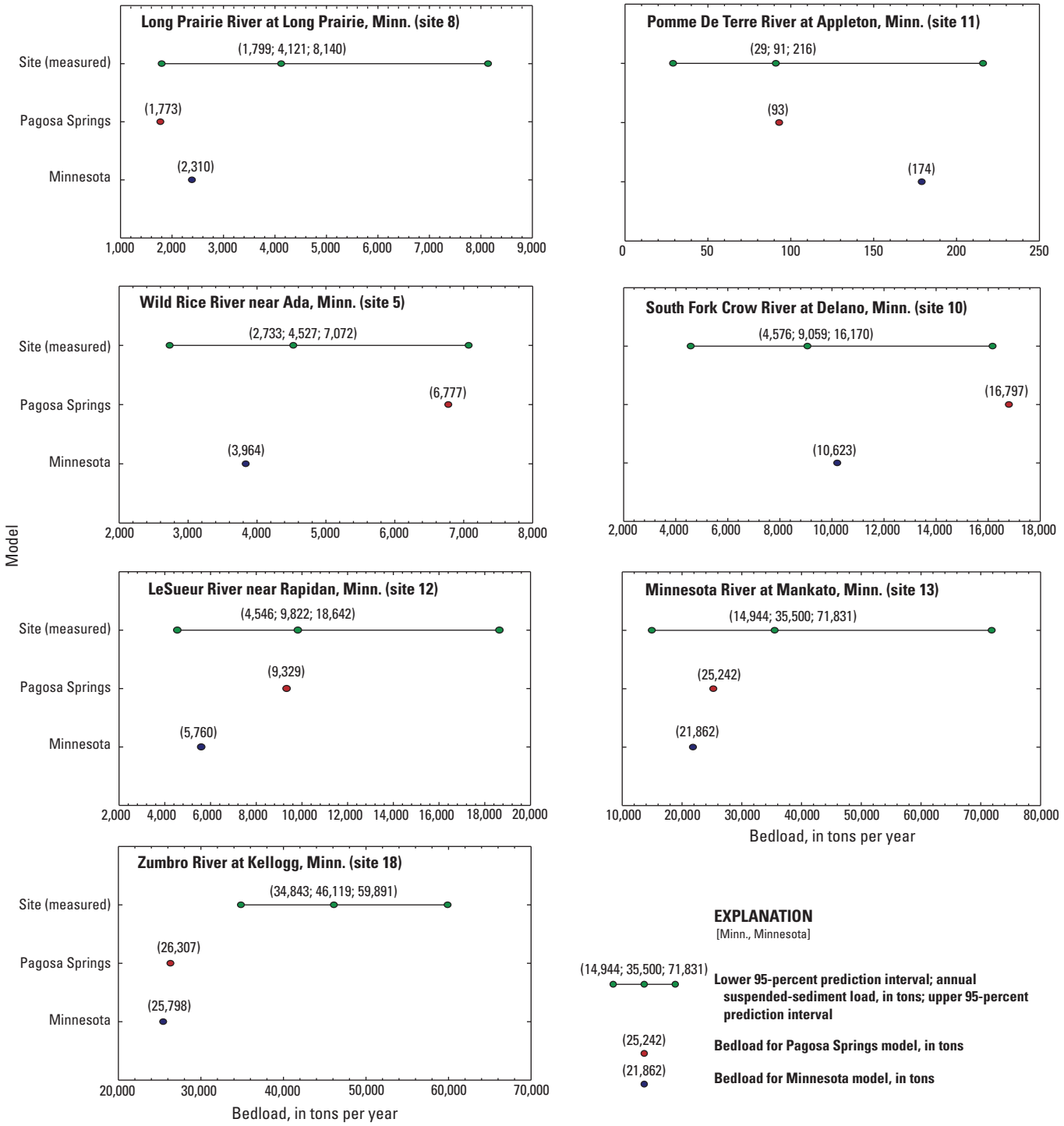

Figure 20. Measured annual bedload based on R-LOADEST models (site [measured]) with 95-percent prediction intervals and estimated bedload based on the Pagosa Springs and Minnesota dimensionless sediment rating curve models for good/fair stability sites (sites 8, 11) and poor stability sites (sites 5, 10, 12, 13, 18) for 2012.

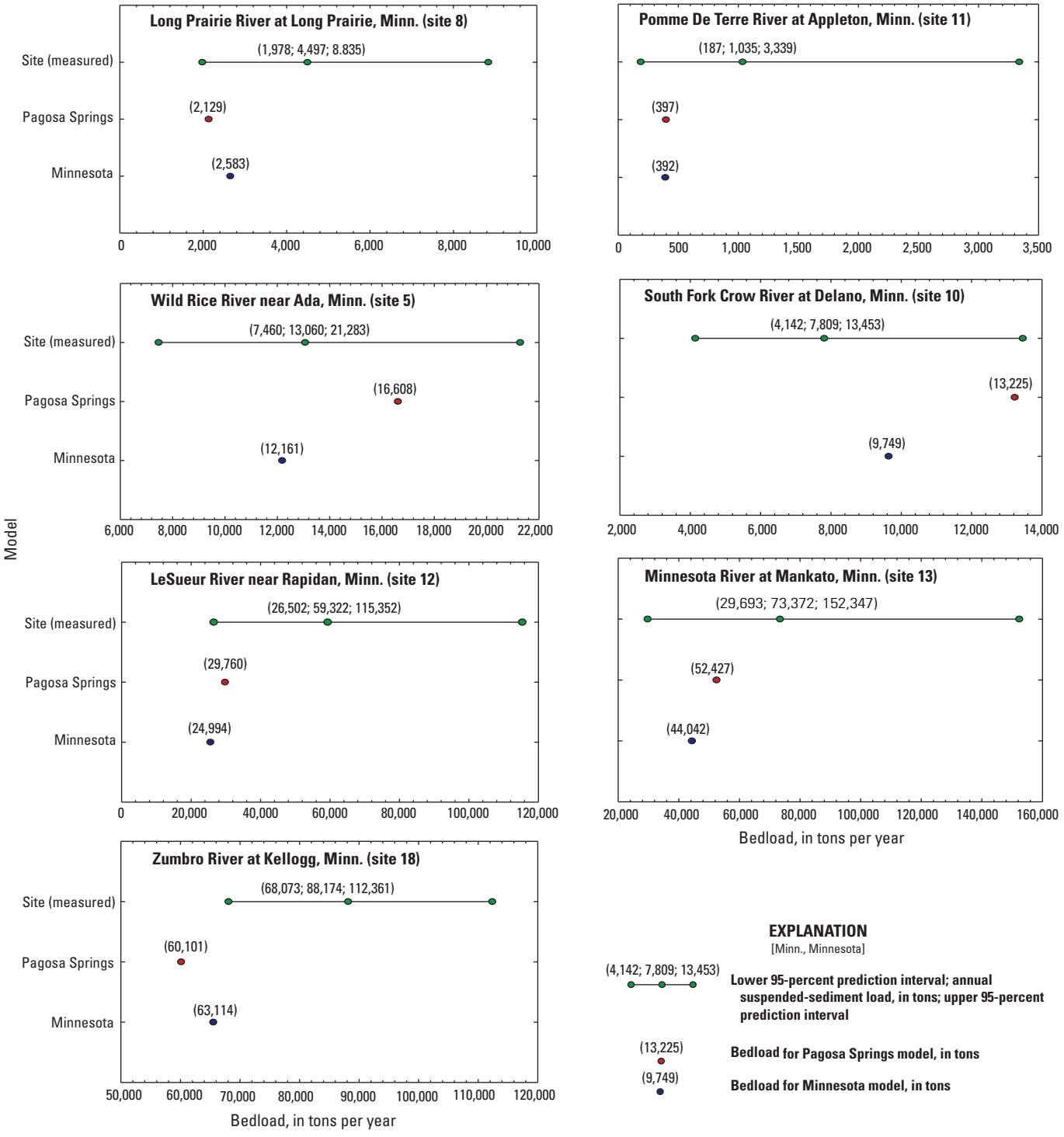

Figure 21. Measured annual bedload based on R-LOADEST models (site [measured]) with 95-percent prediction intervals and estimated bedload based on the Pagosa Springs and Minnesota dimensionless sediment rating curve models for good/fair stability sites (sites 8, 11) and poor stability sites (sites 5, 10, 12, 13, 18) for 2013.

Summary and Conclusions

Consistent and reliable sediment data are needed by Federal, State, and local government agencies responsible for monitoring water quality, planning river restoration, quantifying sediment budgets, and evaluating the effectiveness of sediment reduction strategies. Simple and dependable data collection and estimation techniques are needed to generate hydraulic and water-quality information for areas where data are unavailable or difficult to collect.

This report documents findings based on sediment data collected by the U.S. Geological Survey from 2007 through 2013, in cooperation with the Minnesota Pollution Control Agency and Minnesota Department of Natural Resources, on selected rivers in Minnesota. This study evaluated the use of dimensionless sediment rating curves (DSRCs) in reducing costs and improving the accuracy of predicting suspended-sediment concentrations (SSCs), bedload, and annual sediment loads. This entailed the application of DSRCs developed from a small group of streams located in the San Juan River Basin near Pagosa Springs in southwestern Colorado to rivers in Minnesota. Regionally based DSRC models for Minnesota also were developed and compared to DSRC models from Pagosa Springs, Colorado, to evaluate which model provided more accurate predictions of SSCs and bedload in Minnesota.

Multiple measures of goodness-of-fit were developed to assess the effectiveness of DSRC models in predicting SSC and bedload. More than 600 dimensionless ratio values of SSC, bedload, and streamflow were evaluated and delineated according to Pfankuch stability categories of good/fair and poor to develop four regionally based (Minnesota) DSRC models. The basis for the effectiveness of Pagosa Springs and Minnesota DSRC models was founded on measures of goodness-of-fit that included proximity of the fitted line of the models to the 95-percent confidence intervals of the site-specific model, Nash-Sutcliffe Efficiency (NSE) values, model biases, and deviation of annual sediment loads from each model to the annual sediment loads calculated from measured data. Following model development, NSE values were used to evaluate the ability of the Pagosa Springs and Minnesota DSRC models to predict measured SSC and bedload. Biases associated with the DSRC models were quantified to determine systematic errors of over- or under-estimations of SSC and bedload. Finally, estimated annual sediment loads based on predicted data from the Pagosa Springs and Minnesota DSRC models were compared to annual sediment loads calculated from measured data.

Composite plots comparing Pagosa Springs DSRCs, Minnesota DSRCs, site-specific regression models, and measured data indicated that regionally developed DSRCs (Minnesota DSRC models) more closely approximated measured data for nearly every site. These comparisons indicated that the fitted trendlines for the Pagosa Springs DSRC models had markedly larger slopes when compared to trendlines for the Minnesota DSRC models and the site-specific regression models, and over-represent SSC and bedload at streamflows exceeding bankfull. In contrast, the fitted trendlines for the Minnesota DSRC models indicated no significant difference from the site-specific models for 14 of 16 sites.

The NSE values indicated that the site-specific model for SSC provided the best fit for 10 out of 16 sites with the Minnesota DSRC model providing a slightly better fit for 5 sites, whereas the Pagosa Springs DSRC model provided the best fit for 1 site. The Minnesota DSRC model for SSC closely approximated NSE values of the site-specific regression models for 12 of 16 sites and had greater NSE values than the Pagosa Springs DSRC models for every site except the Whitewater River near Beaver site. The NSE values for Pagosa Springs DSRC models indicated that these models were a poor predictor for 3 of 6 good/fair stability sites and a poor predictor for 5 of 10 poor stability sites. In contrast, the Minnesota DSRC models for SSC indicated good fits for 5 of 6 good/fair stability sites and good fits for 9 of 10 poor stability sites. For bedload, the Pagosa Springs DSRC models indicated that fits were only slightly better than using the mean value of the measured samples for 11 of 13 sites. The Minnesota DSRC model for bedload provided good fits for all 13 sites and had greater NSE values than those from the Pagosa Springs DSRC models for 12 out of 13 sites.

Relative model biases were determined to be substantial (greater than 5 percent) for the Pagosa Springs and Minnesota DSRC models, with varying negative and positive biases associated with each site. Of these two models, the largest mean bias was for the Pagosa Springs DSRC model for SSC (37 percent), and the smallest mean bias was for the Minnesota DSRC model for bedload (20 percent). Site-specific models had an overall mean model bias of 4 percent, which was not substantial.

The R-LOADEST statistical package was used to compute annual suspended-sediment loads, annual bedload, and 95-percent prediction intervals based on measured data from collected samples (measured annual suspended-sediment loads and measured annual bedload). Annual suspended-sediment loads and annual bedload also were calculated using the R statistical package from predicted daily loads calculated from the Pagosa Springs and Minnesota DSRC models; these are referred to as “estimated annual suspended-sediment loads” and “estimated annual bedload”. The measured and estimated annual sediment loads were compared for years 2012 and 2013. The estimated annual sediment loads from the Pagosa Springs and Minnesota DSRC models that fell within the range of the 95-percent prediction intervals of the measured annual sediment loads were not considered to be significantly different. For good/fair stream stability sites, the estimated annual suspended-sediment loads from the Minnesota DSRC model for all comparable sites were not significantly different than the measured annual sediment loads for 2012 and 2013. In contrast, estimated annual suspended-sediment loads from the Pagosa Springs DSRC models for comparable good/fair stream stability sites were significantly different than measured annual suspended-sediment loads for 3 of the 4 sites in 2012, and for 3 of the 4 sites in 2013. The Pagosa Springs DSRC models tended to underestimate measured annual

sediment loads in 2012, and overestimate measured annual sediment loads in 2013. For poor stream stability sites, the estimated annual suspended-sediment loads from the Pagosa Springs DSRC models were significantly different than measured annual suspended-sediment loads for 6 of 8 study sites in 2012, and significantly different for all 8 sites in 2013.

The estimated annual bedload from the Minnesota DSRC models for two comparable good/fair stability sites were not significantly different than measured annual bedload for 2012 and 2013. The estimated annual bedload from the Pagosa Springs DSRC models for the same two good/fair stream stability sites were not significantly different than measured annual bedload for one of the two sites in 2012, and was not significantly different for either of the two sites in 2013. For poor stream stability sites, the estimated annual bedload from the Minnesota DSRC models were not significantly different from the measured annual bedload for 4 of 5 sites in 2012 and not significantly different for 3 of 5 sites in 2013. In comparison, the estimated annual bedload from the Pagosa Springs DSRC models for poor stability sites were significantly different than measured annual bedload for 2 of 5 study sites in 2012, and significantly different for 1 of 5 sites in 2013.

This study provided data from which multiple measures of goodness-of-fit were developed to assess the effectiveness of DSRC models in predicting SSCs and bedload for rivers in Minnesota. The data analyses indicated that the Minnesota DSRC models were better able to compensate for differences in streams across a variety of basin sizes and flow regimes as compared to Pagosa Springs DSRC models, and retained a substantial portion of site-specific sediment signatures for most of the study sites, although deviations were present for streams with limited sediment supply and for rivers in southeastern Minnesota. Moreover, Minnesota DSRC models had greater NSE values, lower model biases, and approximated measured annual sediment loads more closely than Pagosa Springs DSRC models. The results presented in this report indicate that regionally based DSRCs can be used to estimate reasonably accurate values of SSC and bedload.

Practitioners are cautioned that DSRC reliability is dependent on representative measures of bankfull streamflow, SSC, and bedload. It is, therefore, important that samples of SSC and bedload, which will be used for estimating SSC and bedload at the bankfull streamflow, are collected over a range of conditions that includes the ascending and descending limbs of the event hydrograph. Applicability of DSRC models may have substantial limitations under certain conditions. For example, DSRC models should not be used to predict SSC and sediment loads for extreme streamflows, such as those that exceed twice the bankfull streamflow value because this constitutes conditions beyond the realm of current (2016) empirical modeling capability. Also, if relations between SSC and streamflow and between bedload and streamflow are not statistically significant, DSRCs should not be used to predict SSC or bedload, as this could result in large errors. For streams that do not violate these conditions, DSRC estimates of SSC and bedload can be used for stream restoration planning and design, and for estimating annual sediment loads for streams where little or no sediment data are available.

References Cited

Abdi, H., and Williams, L.J., 2010, Jackknife, *in* Neil Salkind, ed., Encyclopedia of research design: Thousand Oaks, California: Sage, 10 p.

Asmus, B.J., 2011, Testing the applicability of the Pfankuch stability index in characterizing the physical integrity of low-gradient alluvial streams in Minnesota, USA and exploring its utility for stressor identification of biological impairments: University of Minnesota, Master's Thesis, 261 p., accessed April 29, 2016, at http://conservancy.umn.edu/handle/11299//120531.

Bagnold, R.A., 1973, The nature of saltation and of bed-load transport in water: Proceedings of the Royal Society of London, Series A, Mathematical and Physical Sciences, v. 332, no. 1591, p. 473–505.

Baker, R.A., 1980, Contaminants and sediment, volume 1, Fate and transport, case studies, modeling, toxicity: Ann Arbor, Mich., Ann Arbor Science, 558 p.

Barry, J.J., Buffington, J.M., Goodwin, P., King, J.G., and Emmett, W.W., 2008, Performance of bed-load transport equations relative to geomorphic significance—Predicting effective discharge and its transport rate: Journal of Hydraulic Engineering, v. 134, no. 5, p. 601–615. [Also available at http://dx.doi.org/10.1061/(ASCE)0733-9429(2008)134:5(601).]

Barry, J.J., Buffington, J.M., and King, J.G., 2004, A general power equation for predicting bed load transport rates in gravel bed rivers: Water Resources Research, v. 40, W10401, 22 p. [Also available at http://dx.doi.org/10.1029/2004WR003190.]

Blanchard, R.A., Ellison, C.A., Galloway, J.M., and Evans, D.A., 2011, Sediment concentrations, loads, and particle-size distributions in the Red River of the North and selected tributaries near Fargo, North Dakota, during the 2010 spring high-flow event: U.S. Geological Survey Scientific Investigations Report 2011–5064, 27 p. [Also available at http://pubs.usgs.gov/sir/2011/5064/.]

Bureau of Reclamation, 2010, BORAMEP: Bureau of Reclamation Automated Modified Einstein Procedure (BORAMEP) program for computing total sediment discharge: 48 p. [Also available at https://www.usbr.gov/tsc/techreferences/computer%20software/models/boramep/index.html.]

Chaterjee, Samprit, Hadi, A.S., and Price, Bertram, 2000, Regression analysis by example, (3d ed.): John Wiley and Sons, Inc., New York, 359 p.

Cohn, T.A., Caulder, D.L., Gilroy, E.J., Zynjuk, L.D., and Summers, R.M., 1992, The validity of a simple statistical model for estimating fluvial constituent loads—An empirical study involving nutrient loads entering Chesapeake Bay: Water Resources Research, v. 28, no. 9, p. 2353–2363. [Also available at http://dx.doi.org/10.1029/92WR01008.]

Cohn, T.A., Delong, L.L, Gilroy, E.J., Hirsch, R.M., and Wells, D.K., 1989, Estimating constituent loads: Water Resources Research, v. 25, no. 5, p. 937–942. [Also available at http://dx.doi.org/10.1029/WR025i005p00937.]

Crawford, C.G., 1991, Estimation of suspended-sediment rating curves and mean suspended-sediment loads: Journal of Hydrology, v. 129, p. 331–348. [Also available at http://dx.doi.org/10.1016/0022-1694(91)90057-O.]

Cummins, K.W., and Lauff, G.H., 1969, The influence of substrate particle size on the microdistribution of stream macrobenthos: Hydrobiologia, v. 34, no. 2, p. 145–484. [Also available at http://dx.doi.org/10.1007/BF00141925.]

Czuba, C.R., Fallon, J.D., and Kessler, E.W., 2012, Floods of June 2012 in northeastern Minnesota: U.S. Geological Survey Scientific Investigations Report 2012–5283, 42 p. with 3 app. [Also available at http://pubs.usgs.gov/sir/2012/5283/.]

Davis, B.E., 2005, A guide to the proper selection and use of federally approved sediment and water-quality samplers: U.S. Geological Survey Open-File Report 2005–1087, 20 p. [Also available at http://pubs.usgs.gov/of/2005/1087/.]

Death, R.G., and Winterbourn, M.J., 1994, Environmental stability and community persistence—A multivariate perspective: Journal of the North American Benthological Society, v. 13, p. 125–139. [Also available at http://dx.doi.org/10.2307/1467232.]

Death, R.G., and Winterbourn, M.J., 1995, Diversity patterns in stream benthic invertebrate communities—the influence of habitat stability: Ecology, v. 76, no. 5, p. 1446–1460. [Also available at http://dx.doi.org/10.2307/1938147.]

Dietrich, W.E., Kirchner, J.W., Ikeda, H., and Iseya, F., 1989, Sediment supply and the development of the coarse surface layer in gravel-bedded rivers: Macmillan Magazines Limited, 3 p.

Duan, Naihua, 1983, Smearing estimate–A nonparametric retransformation method: Journal of the American Statistical Association, v. 78, no. 383, p. 606–610. [Also available at http://dx.doi.org/10.1080/01621459.1983.10478017.]

Duncan, M.J., Suren, A.M., and Brown, S.L.R., 1999, Assessment of streambed stability in steep bouldery streams—Development of a new analytical technique: Journal of the North American Benthological Society, v.18, no. 4., p. 445–456. [Also available at http://dx.doi.org/10.2307/1468377.]

Dunne, T., and Leopold, L., 1978, Water in environmental planning: San Francisco, California, W.H. Freeman, 818 p.

Edwards, T.K., and Glysson, G.D., 1999, Field methods for measurement of fluvial sediment: U.S. Geological Survey Techniques of Water-Resources Investigations, book 3, chap. C2, 89 p. [Also available at http://pubs.usgs.gov/twri/twri3-c2/.]

Ellison, C.A., Savage, B.E., and Johnson, G.D., 2014, Suspended-sediment concentrations, loads, total suspended solids, turbidity, and particle-size fractions for selected rivers in Minnesota, 2007 through 2011: U.S. Geological Survey Scientific Investigations Report 2013–5205, 43 p., accessed April 29, 2016, at http://dx.doi.org/10.3133/sir20135205.

Fitzpatrick, F.A., Peppler, M.C., DePhilip, M.M., and Lee, K.E., 2006, Geomorphic characteristics and classification of Duluth-area streams, Minnesota: U.S. Geological Survey Scientific Investigations Report 2006–5029, 54 p. [Also available at http://pubs.usgs.gov/sir/2006/5029/.]

Gesch, D.B., 2007, The National Elevation Dataset, chap. 4 of Maune, D., ed., Digital elevation model technologies and applications—the DEM users manual, 2nd ed.: Bethesda, Md., American Society for Photogrammetry and Remote Sensing, p. 99–118.

Guy, H.P., 1969, Laboratory theory and methods for sediment analysis: U.S. Geological Survey Techniques of Water-Resources Investigations, book 5, chap. C1, 58 p. [Also available at http://pubs.usgs.gov/twri/twri5c1/.]

Helsel, D.R., and Hirsch, R.M., 2002, Statistical methods in water resources: Techniques of Water-Resources Investigations of the United States Geological Survey, book 4, chap. A3, 510 p. [Also available at http://pubs.usgs.gov/twri/twri4a3/.]

Hinkley, D.V., 1983, Jackknife methods, *in* Johnson, N.L., Kotz, S., and Read, C.B. eds., Encyclopedia of statistical sciences (volume 4): New York, Wiley, p 280–287.

Hirsch, R.M., 1982, A comparison of four streamflow record extension techniques: Water Resources Research, v. 18, no. 4, p. 1081–1088. [Also available at http://dx.doi.org/10.1029/WR018i004p01081.]

Jenkins, E.P., 2015, Predicting suspended sediment in Illinois rivers using dimensionless rating curves: Illinois, Graduate College of the University of Illinois at Urbana-Champaign, Ph.D. dissertation, 268 p., accessed April 29, 2016, at http://hdl.handle.net/2142/88014.

Julien, P.Y., 2002, Introduction to river mechanics: Cambridge U.K., Cambridge, University, 427 p.

Kendall, M.G., 1938, A new measure of rank correlation: Biometrika, v. 30, 81–93. [Also available at http://dx.doi.org/10.2307/2332226.]

Kendall, M.G., 1975, Rank correlation methods (4th ed.): London, Charles Griffin, 202 p.

Knighton, David, 1998, Fluvial forms and processes, a new perspective (1st ed.): New York, Oxford University Press Inc., 383 p.

Lane, E.W., 1955, The importance of fluvial morphology in hydraulic engineering: American Society of Civil Engineers Proceedings, v. 81, p. 1–17.

Leopold, L.B., and Emmett, W.W., 1976, Bedload measurements, East Fork River, Wyoming: Proceedings of the National Academy of Sciences, v. 73, no. 4, p. 1000–1004.

Leopold, L.B., Wolman, M.G., and Miller, J.P., 1964, Fluvial processes in geomorphology: San Francisco, California, Freeman, 522 p.

Lopes, V.L., Osterkamp, W.R., and Espinosa, M.B., 2001, Evaluation of selected bedload equations under transport- and supply-limited conditions: Proceedings of the Seventh Interagency Sedimentation Conference, Reno, Nevada, v. 1, p I-192–I-198.

Lower Minnesota River Watershed District, 2009, Management plan, S4 Section 4, Assessment of Problems and Issues: accessed April 29, 2016, at http://www.watershed-district.org/pdf/S4.PDF.

Lusardi, B.A., 1997, Minnesota at a glance—Quaternary glacial geology: Minnesota Geological Survey, University of Minnesota, 4 p., accessed April 29, 2016, at http://web.archive.org/web/20070203130249/http://www.winona.edu/geology/MRW/MNglance/Mn_Quaternary.pdf.

McCuen, R.H., Knight, A., and Cutter, A.G., 2006, Evaluation of the Nash-Sutcliffe Efficiency Index: Journal of Hydrologic Engineering, v. 11, no. 6, p. 597–602.

Minnesota Department of Natural Resources, 2014, MNDNR/MPCA cooperative stream gaging: accessed March 3, 2016, at http://www.dnr.state.mn.us/waters/csg/index.html.

Minnesota Department of Natural Resources, 2016a, Land: accessed March 3, 2016, at http://www.dnr.state.mn.us/faq/mnfacts/land.html.

Minnesota Department of Natural Resources, 2016b, Climate of Minnesota: accessed March 3, 2016, at http://www.dnr.state.mn.us/climate/index.html.

Minnesota Department of Natural Resources, 2016c, Basins of Minnesota: accessed March 3, 2016, at http://www.dnr.state.mn.us/watersheds/basins.html.

Minnesota Department of Natural Resources, 2016d, Natural history—Minnesota's geology: accessed March 3, 2016, at http://www.dnr.state.mn.us/snas/naturalhistory.html.

Minnesota Department of Natural Resources, 2016e, Minnesota Climatology Working Group: accessed March 10, 2016, at http://files.dnr.state.mn.us/lands_minerals/geology-handbook.pdf.

Minnesota Department of Natural Resources, 2016f, Minnesota land cover classification system: accessed March 10, 2016, at http://www.dnr.state.mn.us/mlccs/index.html.

Minnesota Geospatial Information Office, 2016, Hydrography standard—watersheds: accessed April 22, 2016, at http://www.mngeo.state.mn.us/committee/hydro/HUC_Names_official.html.

Minnesota Pollution Control Agency, 2009, Minnesota's impaired waters and total maximum daily loads (TMDLs): accessed April 29, 2016, at http://www.pca.state.mn.us/water/tmdl/index.html.

Minshall, G.W., 1984, Aquatic insect-substratum relationships, *in* Resh, V.H. and Rosenberg, D.M., eds., The ecology of aquatic insects: New York, Praeger, p. 358–400.

Montgomery, D.R., and Buffington, J.M., 1998, Channel processes, classification, and response, *in* Naiman, R.J., and Bilby, R.E., eds., River ecology and management: New York, Springer-Verlag, Inc., p. 13–42.

Nash, J.E., and Sutcliffe, J.V., 1970, River flow forecasting through conceptual models part 1—A discussion of principles: Journal of Hydrology, v. 10, no. 3282–3290. [Also available at http://dx.doi.org/10.1016/0022-1694(70)90255-6.]

Natural Resources Conservation Service, 2012, List of soil surveys by State: accessed December 12, 2012, at http://soils.usda.gov/survey/printed_surveys/.

Ojakangas, R.W., and Matsch, C.L., 1982, Minnesota's geology: Minneapolis, University of Minnesota Press, 255 p.

Padmanabhan, G., and Johnson, B.H., 2010, Regional dimensionless rating curves to estimate design flows and stages: Journal of Spatial Hydrology, v. 10, no. 1, p. 41–75.

Pfankuch, D.J., 1975, Stream reach inventory and channel stability evaluation: Missoula, Montana, U.S. department of Agriculture Forest Service, no. R1-75-002, GPO no. 696-260/200, 26 p.

Porterfield, George, 1972, Computation of fluvial-sediment discharge: U.S. Geological Survey Techniques of Water-Resources Investigations, book 3, chap. C3, 65 p. [Also available at http://pubs.usgs.gov/twri/twri3-c3/.]

Quenouille, M.H., 1956, Notes on bias in estimation: Biometrika, v. 43, no. 3/4, p. 353–360. [Also available at http://dx.doi.org/10.2307/2332914.]

Rantz, S.E., and others, 1982, Measurement and computation of streamflow—Volume 1, Measurement of stage and discharge, and volume 2, Computation of discharge: U.S. Geological Survey Water-Supply Paper 2175, 631 p. [Also available at http://pubs.usgs.gov/wsp/wsp2175/.]

Rasmussen, P.P., Gray, J.R., Glysson, G.D., and Ziegler, A.C., 2009, Guidelines and procedures for computing time-series suspended-sediment concentration and loads from in-stream turbidity-sensor and streamflow data: U.S. Geological Survey Techniques and Methods, book 3, chap. C4, 54 p. [Also available at http://pubs.usgs.gov/tm/tm3c4/.]

R Development Core Team, 2011, R Installation and Administration, Version 2.14.1, 2011-12-22, accessed April 29, 2016, at http://streaming.stat.iastate.edu/CRAN/doc/manuals/R-admin.pdf.

Rickly Hydrological Co., Inc., 2015, Tacoma bank-operated cableway system, technical specifications document, 6 p., accessed April 29, 2016, at http://www.rickly.com/.

Robertson, A.L., and Milner, A.M., 1999, Meiobenthic arthropod communities in new streams in Glacier Bay National Park, Alaska: Hydrobiologia, v. 397, p. 197–209. [Also available at http://dx.doi.org/10.1023/A:1003782323718.]

Rose, W.J., 1992, Sediment transport, particle sizes, and loads in lower reaches of the Chippewa, Black, and Wisconsin rivers in western Wisconsin: U.S. Geological Survey Water-Resources Investigations Report 90–4124, 38 p. [Also available at https://pubs.er.usgs.gov/publication/wri904124.]

Rosgen, D.L., 1994, A classification of natural rivers: Catena, v. 22, p. 169–199. [Also available at http://dx.doi.org/10.1016/0341-8162(94)90001-9.]

Rosgen, D.L., 1996, Applied river morphology*:* Pagosa Springs, Colorado, Wildland Hydrology, 388 p.

Rosgen, D.L., 2001b, A stream channel stability assessment methodology: Proceedings of the Seventh Federal Interagency Sedimentation Conference, March 25 to 29, 2001, Reno, Nevada, 11 p. [Also available at http://www.u-s-c.org/html/documents/streamstability.pdf.]

Rosgen, D.L., 2006, Flowsed/Powersed—Prediction models for suspended and bedload transport: Proceedings of the Eighth Federal Interagency Sedimentation Conference (8th FISC), April 2–6, 2006, Reno, Nevada, p. 761–769.

Rosgen, D.L., 2007, Watershed Assessment of River Stability and Sediment Supply (WARSS), (2d ed.): Fort Collins, Colorado, Wildland Hydrology, 1933 p.

Rosgen, D.L., 2010, The application and validation of dimensionless sediment rating curves: 2nd Joint Federal Interagency Conference, Las Vegas, Nevada, June 27–July 1, 2010, 11 p.

Rounick, J.S., and Winterbourn, M.J., 1982, Benthic faunas of forested streams: New Zealand Journal of Ecology, v. 5, p. 140–150.

Rose, W.J., 1992, Sediment transport, particle sizes, and loads in lower reaches of the Chippewa, Black, and Wisconsin Rivers in Western Wisconsin: U.S. Geological Survey Water-Resources Investigations Report 90–4124, 38 p.

Runkel, R.L., Crawford, C.G., and Cohn, T.A., 2004, Load Estimator (LOADEST)—A FORTRAN program for estimating constituent loads in streams and rivers: U.S. Geological Survey Techniques and Methods, book 4, chap. A5, 69 p. [Also available at https://pubs.er.usgs.gov/publication/tm4A5.]

Sauer, V.B., and Turnipseed, D.P., 2010, Stage measurement at gaging stations: U.S. Geological Survey Techniques and Methods, book 3, chap. A7, 45 p. [Also available at http://pubs.usgs.gov/tm/tm3-a7/.]

Sims, P.K., and Morey, G.G., 1972, Geology of Minnesota—A centennial volume: Minneapolis, Minnesota Geological Survey, University of Minnesota, 632 p.

TIBCO Software Inc., 2010, TIBCO Spotfire S+: Somerville, Massachusetts, accessed November 9, 2012, at http://spotfire.tibco.com/products/s-plus/statistical-analysis-software.aspx.

Tornes, L.H., 1986, Suspended sediment in Minnesota streams: U.S. Geological Survey Water-Resources Investigations Report 85–4312, 33 p. [Also available at http://pubs.er.usgs.gov/publication/wri854312.]

Tornes, L.H., Brigham, M.E., and Lorenz, D.L., 1997, Nutrients, suspended sediment, and pesticides in streams in the Red River of the North Basin, Minnesota, North Dakota, and South Dakota, 1993–95: U.S. Geological Survey Water-Resources Investigations Report 97–4053, 77 p. [Also available at http://pubs.er.usgs.gov/publication/wri974053.]

Troendle, C.A., Rosgen, D.L., Ryan, S., Porth, L., and Nankervis, J., 2001, Developing a ‘reference’ sediment transport relationship: Proceedings of the Seventh Federal Interagency Sedimentation Conference, Reno, Nevada, March 25–29, p. 73–80.

Tukey, J.W., 1986, The future of processes of data analysis, *in* The collected works of John W. Tukey (Volume IV): New York, Wadsworth, p. 517–549.

U.S. Army Corps of Engineers, 2003, Bed material budget for the St. Paul District Reach of the Upper Mississippi River, Anoka, Minnesota to Guttenburg, Iowa: St. Paul, Minnesota, U.S. Army Corps of Engineers.

U.S. Environmental Protection Agency, 1990, National water quality inventory—1988 report to Congress: Washington, D.C., Office of Water, U.S. Environmental Protection Agency Report 440–4–90–003, 266 p.

U.S. Environmental Protection Agency, 1992, National water quality inventory—1990 report to Congress: Washington, D.C., Office of Water, U.S. Environmental Protection Agency Report 503/9–92/006, 248 p.

U.S. Environmental Protection Agency, 1995, National water quality inventory—1994 report to Congress: Washington, D.C., Office of Water, U.S. Environmental Protection Agency Report 841-R-95-005, 566 p.

U.S. Environmental Protection Agency, 1998, National water quality inventory—1996 report to Congress: Washington, D.C., Office of Water, U.S. Environmental Protection Agency Report 841-R-97-008, 202 p.

U.S. Environmental Protection Agency, 2000, National water quality inventory—1998 report to Congress: Washington, D.C., Office of Water, U.S. Environmental Protection Agency Report 841-F-00-006, 631 p.

U.S. Environmental Protection Agency, 2002, National Water Quality Inventory—2000 Report to Congress: Washington, D.C., Office of Water, U.S. Environmental Protection Agency Report 841-F-02-003, 224 p.

U.S. Environmental Protection Agency, 2007, National water quality inventory—2002 report to Congress: Washington, D.C., Office of Water, U.S. Environmental Protection Agency Report 841-R-07-001, 44 p.

U.S. Environmental Protection Agency, 2012, Minnesota water quality assessment report: U.S. Environmental Protection Agency Report, accessed October 31, 2015, at http://iaspub.epa.gov/waters10/attains_state.control?p_state=MN&p_cycle=2012.

U.S. Geological Survey, 2015, Welcome to StreamStats, Minnesota: Web page accessed August 7, 2014, at http://water.usgs.gov/osw/streamstats/minnesota.html.

U.S. Geological Survey, 2016, National Water Information System (NWISWeb)—USGS surface-water data for Minnesota: U.S. Geological Survey database, accessed March 25, 2016, at http://waterdata.usgs.gov/mn/nwis/sw/.

Watson, C.C., Biedenharn, D.S., and Bledsoe, B.P., 2002, Use of incised channel evolution models in understanding rehabilitation alternatives: Journal of the American Water Resources Association, v. 38, no. 1, p. 151–160. [Also available at http://dx.doi.org/10.1111/j.1752-1688.2002.tb01542.x.]

Wolman, M.G., and Miller, J.P., 1960, Magnitude and frequency of forces in geomorphic processes: Journal of Geology, v. 68, p. 54–74. [Also available at http://dx.doi.org/10.1086/626637.]

Wood, M.S., 2014, Estimating suspended sediment in rivers using acoustic Doppler meters: U.S. Geological Survey Fact Sheet 2014–3038, 4 p. [Also available at http://dx.doi.org/10.3133/fs20143038.]

Appendixes

Pfankuch stream channel stability surveys (Pfankuch, 1975) were completed at each of the 20 study sites by Minnesota Department of Natural Resources or U.S. Geological Survey (USGS) field staff using the Rosgen (2007) modified Pfankuch stability rating assessment form. Pfankuch stability ratings of good/fair and poor were used to delineate data for the development of dimensionless sediment rating curve models. The Pfankuch stability rating for each of the 20 study sites is presented in table 1–1 as a Microsoft® Excel spreadsheet. The first worksheet is named "Readme" and contains the abbreviations used in the other worksheets. A worksheet for each of the 20 study sites by USGS station number is included in table 1–1.

Streamflow, suspended-sediment concentrations, suspended particle-size fractions, bedload, and bedload particle-size distributions collected during 2007 through 2013 from study sites are presented in table 1–2.

Table 1–1. Pfankuch stream stability surveys for study sites in Minnesota. Available online at http://dx.doi.org/10.3133/sir20165146.

Table 1–2. Streamflow, suspended-sediment concentrations, bedload particle-size fractions, bedload, and suspended particle-size fractions collected from selected sites in Minnesota, 2007 through 2013. Available online at http://dx.doi.org/10.3133/sir20165146.

Table 1–3. Summary of site-specific simple linear regression models for suspended-sediment concentrations and bedload transport for selected sites in Minnesota, 2007 through 2013. Available online at http://dx.doi.org/10.3133/sir20165146.

Publishing support provided by:
Rolla Publishing Service Center

For more information concerning this publication, contact:
Director, USGS Minnesota Water Science Center
2280 Woodale Drive
Mounds View, Minnesota 55112
(763) 783–3100

Or visit the Minnesota Water Science Center Web site at:
http://mn.water.usgs.gov/

Ellison and others—**Application of Dimensionless Sediment Rating Curves for Rivers in Minnesota**—Scientific Investigations Report 2016–5146

ISSN 2328-0328 (online)
http://dx.doi.org/10.3133/sir20165146